THE UNIVERSITY OF ALBERTA

"Petrology and Tectonic Setting of the Satellitic Tertiary Coryell Intrusives of Southeastern British Columbia"

by

Kathleen A. Berndt

A THESIS

SUBMITTED TO THE FACULTY OF GRADUATE STUDIES AND RESEARCH

IN PARTIAL FULFILMENT OF THE REQUIREMENTS FOR THE DEGREE

OF Master of Science

Geology

EDMONTON, ALBERTA

Fall 1983

All Location Maps Have Been Adapted From The Original Source For Use ~~Of~~ In This Thesis

Kathy Bendt

THE UNIVERSITY OF ALBERTA

RELEASE FORM

NAME OF AUTHOR Kathleen A. Berndt

TITLE OF THESIS "Petrology and Tectonic Setting of the Satellitic Tertiary Coryell Intrusives of Southeastern British Columbia"

DEGREE FOR WHICH THESIS WAS PRESENTED Master of Science

YEAR THIS DEGREE GRANTED Fall 1983

Permission is hereby granted to THE UNIVERSITY OF ALBERTA LIBRARY to reproduce single copies of this thesis and to lend or sell such copies for private, scholarly or scientific research purposes only.

The author reserves other publication rights, and neither the thesis nor extensive extracts from it may be printed or otherwise reproduced without the author's written permission.

(SIGNED) Kathy Berndt

PERMANENT ADDRESS:

895 NORTHSHORE BLVD.N.

BURLINGTON, ONTARIO

CANADA

DATED OCTOBER 6 19 83

THE UNIVERSITY OF ALBERTA

FACULTY OF GRADUATE STUDIES AND RESEARCH

The undersigned certify that they have read, and recommend to the Faculty of Graduate Studies and Research, for acceptance, a thesis entitled "Petrology and Tectonic Setting of the Satellitic Tertiary Coryell Intrusives of Southeastern British Columbia" submitted by K. Berndt in partial fulfilment of the requirements for the degree of Master of Science.

R A Brummer

Supervisor

R. St. J. Lambert

E. R. Kanasewich

Date 5 October 1983

C M. Scrimgeour

Dedication

To my mother and father who have always offered me encouragement and help.

ABSTRACT

The Coryell intrusives form a group of lower-Eocene mafic, alkaline plutonic rocks located in southeastern British Columbia. Intrusion through the Hudsonian basement and emplacement into the Omineca Belt took place during the final phases of the Laramide Orogeny. A 9-point $^{87}Sr/^{86}Sr$ isochron prepared on a centrally located intrusion, north of Salmo, gives an age of 50.8 ± 0.6 Ma.

The main syenitic batholith is located just west of the town of Rossland and numerous satellitic plutons were intruded at distances extending 80 km to the east. Several groups of coeval, associated volcanic rocks (Kamloops and Midway Groups) occur westward as far as the Fraser River. The furthest eastern intrusions are believed to be remnants of shallow volcanic necks. Cross-cutting, related lamprophyric and aplitic dykes are common. The smaller eastern stocks are comprised of alkali melasyenites with porphyritic trachybasalts constituting large proportions of two volcanic plugs.

The mineralogy of this rock series is dominated by orthoclase feldspar with lesser amounts of highly poikilitic clinopyroxene, dark Ti-rich biotite and phlogopite, forsteritic olivine and minor andesine. Chemically, the intrusions belong to the continental potassic alkali basalt series.

High barium, strontium, rubidium and potassium contents are characteristic of the entire series. Two distinct groups can be delineated on the basis of mineralogy, chemistry and geography. The western group is characterized by enriched incompatible element values, a lower mafic content and more pervasive alteration relative to the eastern intrusions.

An initial $^{87}Sr/^{86}Sr$ ratio of 0.7070 has been obtained for these rocks, suggesting either a crustal influence or the incorporation of a Rb-rich mantle phase. To account for the enriched Rb, Sr, Ba and K contents as well as the elevated $^{87}Sr/^{86}Sr$ ratio, metasomatism of the upper mantle by a volatile-, alkali- and incompatible element-enriched fluid phase is proposed. This fluid phase

would produce a phlogopitic lherzolite zone in the upper mantle. Small amounts of partial melting of this contaminated mica peridotite could produce the chemical characteristics of these plutons. Evidence for the existence of the metasomatized parental magma is provided by the abundant lamprophyre dykes.

The Pacific–North America transform boundary came into existence during Lower Eocene (53 Ma) time and led to the formation of an extensional network of strike–slip and normal faults. The occurrence of a tensional tectonic regime provided the locus for thermal doming centralized beneath the main batholith. Either a localized mantle plume or the collapse of the underlying subducted plate may have been the dominant factor controlling Eocene magmatism in this area. Some degree of crustal influence, though difficult to prove conclusively, may be indicated by the elevated $^{87}Sr/^{86}Sr$ ratio and the U/Th characteristics.

Acknowledgements

I would like to express my gratitude to my supervisor, Dr. R. A. Burwash, for his guidance, suggestions and patience during the preparation of this thesis. Beth Burwash contributed her excellent humour and a lot of hard work towards the sampling and mapping in the field. Dr. H. Baadsgaard was an enormous help in carrying out the strontium isotope analyses.

I also wish to thank Jenni Blaxley for thin-section preparation and my good friend Amdahl for help with the typing, copying, drafting and calculating. Finally, thanks to the staff and students in the Department of Geology who were always there with their support.

Financial support for this project was supplied from NSERC and EMR grants to R. A. Burwash.

Table of Contents

Chapter		Page
I.	INTRODUCTION	1
	A. Purpose and Method of Study	1
	B. Location, Physiography and General Geology	2
	General Geology	4
	C. Previous Work	5
II.	TECTONIC SETTING	7
	A. Introduction	7
	B. Regional Geology and Tectonics	7
	C. Eocene Magmatism	9
III.	GEOGRAPHIC EXTENT AND MODE OF OCCURRENCE OF CORYELL PLUTONS	11
	A. Main Coryell Syenite Batholith	11
	B. Rossland Intrusions	11
	Railway Cut	12
	Highway Cut	13
	C. Jersey Intrusion	14
	D. Ymir Intrusion	16
	E. Eastern Intrusions	18
	Cultus Stock	18
	McGregor Intrusion	19
IV.	PETROGRAPHY	22
	A. Classification System	22
	B. Introduction	22
	C. Biotite Augite Melasyenites	25
	D. Biotite Olivine Augite Alkali-Feldspar Melasyenites	29
	E. Porphyritic Olivine Biotite Augite Trachybasalts	31
	F. Leucocratic Syenite-granite Core of the Ymir Pluton	34
	G. Lamprophyres	35
	H. Pyroxene Cumulates	36
	I. Miscellaneous Rock Types	37

V. GEOCHEMISTRY 38
A. Introduction 38
Method 38
Classification 38
B. Major Element Geochemistry 44
C. Trace Element Geochemistry 56
Residual Alkali Elements 57
Immobile Elements 64
Uranium and Thorium 69
Metallic Elements 71
Summary 74
Time of Intrusion 75
Strontium Initial Ratios 77
VI. PETROGENESIS 79
A. Initiation of Melting 79
B. Petrogenetic Models 79
C. Coryell Model 81
Source Composition and Partial Melting 81
Low Pressure Fractional Crystallization 83
VII. SUMMARY AND CONCLUSIONS 84
REFERENCES 87
APPENDIX I. GEOCHEMICAL ANALYSES 94
APPENDIX II. NORMATIVE CALCULATIONS 107
APPENDIX III. MODAL ANALYSES 117
APPENDIX IV. MICROPROBE ANALYSES 123

Tables

Table 1: Precision estimates of McMaster XRF data 39

Table 2: Mean major element values for each pluton 45

Table 3: Strontium isotope results 76

Figures

Figure 1: Location map 3

Figure 2: Generalized geology of the study area with pluton locations 4

Figure 3: Geology and sample location sites, Rossland Highway 13

Figure 4: Geology and sample location sites, Rossland Railway 14

Figure 5: Geology and sample location sites, Jersey 15

Figure 6: Geology and sample location sites, Ymir 17

Figure 7: Geology and sample location sites, Cultus 19

Figure 8: Geology and sample location sites, McGregor 20

Figure 9: Petrographic classification of modal mineralogical compositions 23

Figure 10: Modal mineralogy 24

Figure 11: AFM diagram 41

Figure 12: $Na_2O + K_2O$ versus SiO_2 plot 43

Figure 13: MgO versus Al_2O_3 plot 46

Figure 14: MgO versus Na_2O plot 47

Figure 15: MgO versus SiO_2 plot 48

Figure 16: MgO versus K_2O plot 49

Figure 17: MgO versus Fe_2O_3 plot 50

Figure 18: MgO versus CaO plot 51

Figure 19: MgO versus K_2O/Na_2O plot 53

Figure 20: CNK diagram 55

Figure 21: Distance versus differentiation index (Larsen factor) 56

Figure 22: Sr versus Ba plot 58

Figure 23: Sr versus Rb plot 61

Figure 24: MgO versus Nb plot 62

Figure 25: MgO versus TiO_2 plot 63

Figure 26: MgO versus P_2O_5 plot 65

Figure 27: MgO versus Y plot 67

Figure 28: K_2O versus Rb plot 68

Figure 29: CaO versus Y plot 69

Figure 30: U versus Th plot 71

Figure 31: MgO versus Ni plot 73

Figure 32: MgO versus Cr plot 74

Figure 33: Strontium isotope isochron plot 78

Plates

Plate 1A: clinopyroxene alteration – Rossland 26

Plate 1B: hypersthene – Mt. McGregor 26

Plate 2A: alkali–feldspar melasyenite – Ymir 28

Plate 2B: central core zone – Ymir 28

Plate 3A: resorbed biotite – McGregor 30

Plate 3B: calcite – Jersey 30

Plate 4A: porphyritic trachyte – Cultus 32

Plate 4B: zoned clinopyroxene – Cultus 32

Plate 5A: pyroxene cumulate – Jersey 36

Plate 5B: biotite – augite lamprophyre – Mt. McGregor 36

I. INTRODUCTION

A. Purpose and Method of Study

The main objective in undertaking this study was to devise a petrogenetic model for the events surrounding the intrusion of the Coryell alkaline plutons in southeastern British Columbia during the lower-Eocene. The entire area has been of significant economic interest since the late 1800's and mineralization can often be related to a Tertiary event (Fyles *et al.*, 1973).

Gold, silver, copper, lead, zinc and tungsten have been the most important metals produced from the various mining camps. Recent exploration has involved the delineation of porphyry molybdenum deposits.

Earlier studies on the Coryell intrusions have involved mainly descriptive and petrographic work with limited major element data. No trace element or strontium isotope work had been previously undertaken.

Before a model could be constructed, it was necessary to:

a. determine the total range of compositions, both mineralogical and chemical, of samples collected from the Coryell plutons,

b. determine the nature of the variations between the extremes, establishing and limiting the mechanisms causing the variation,

c. determine the time of intrusion of the Coryell stocks.

Field work was carried out during the summers of 1979 and 1980. The majority of the work was centred around six small plutons selected in order to obtain a wide geographic coverage. 103 samples were collected and 78 thin sections were prepared for petrographic examination.

The information from improved geophysical techniques, advances in experimental petrology and improved analytical techniques for measuring isotopes and trace elements have all been utilized in this study and interpretation.

B. Location, Physiography and General Geology

Sampling and mapping were conducted mainly within the boundaries of the west half of the Nelson map area (Little, 1960) (Figure 1). The area of concentration extends from the United States border, north to about 49°, 20' and covers an east to west range between 116°, 45' and 118°, 00' (Figure 2).

The study area is bounded geographically by Kootenay Lake to the east and the town of Rossland to the west.

Accessibility in this region varies considerably. Sampling in the western sections was accomplished using road and railway cuts whereas the rugged eastern terrain overlooking Kootenay Lake required the utilization of helicopter support. Outcrop exposure was excellent at all sampling locations.

The map area lies totally within the Nelson and Bonnington Ranges of the Selkirk Mountains. The highest peaks in the more subdued, rounded southern Selkirks range between 2000-2500 m (7000-8000 feet). Gentle, bush-covered slopes in the western section grade to steep, barren peaks in the east.

General Geology

Sedimentary and igneous rocks in this area range from Late Proterozoic to Eocene. The southeastern corner of the region is dominated by the Upper Proterozoic through early Paleozoic succession of conglomerates, schists, quartzites and limestones. These complexly folded, faulted and metamorphosed rocks form the western side of the north-trending Kootenay Arc.

Evidence for Silurian to Mississippian deposits is absent in this region, owing to the influence of the Caribooan Orogeny.

The middle to upper-Jurassic Nelson batholith dominates the structure of the central portion of the study area. It occurs west of the Kootenay Arc and was intruded during the first half of the Columbian Orogeny.

The latest rocks present in this area are represented by the alkaline Tertiary Coryell intrusives and associated dykes.

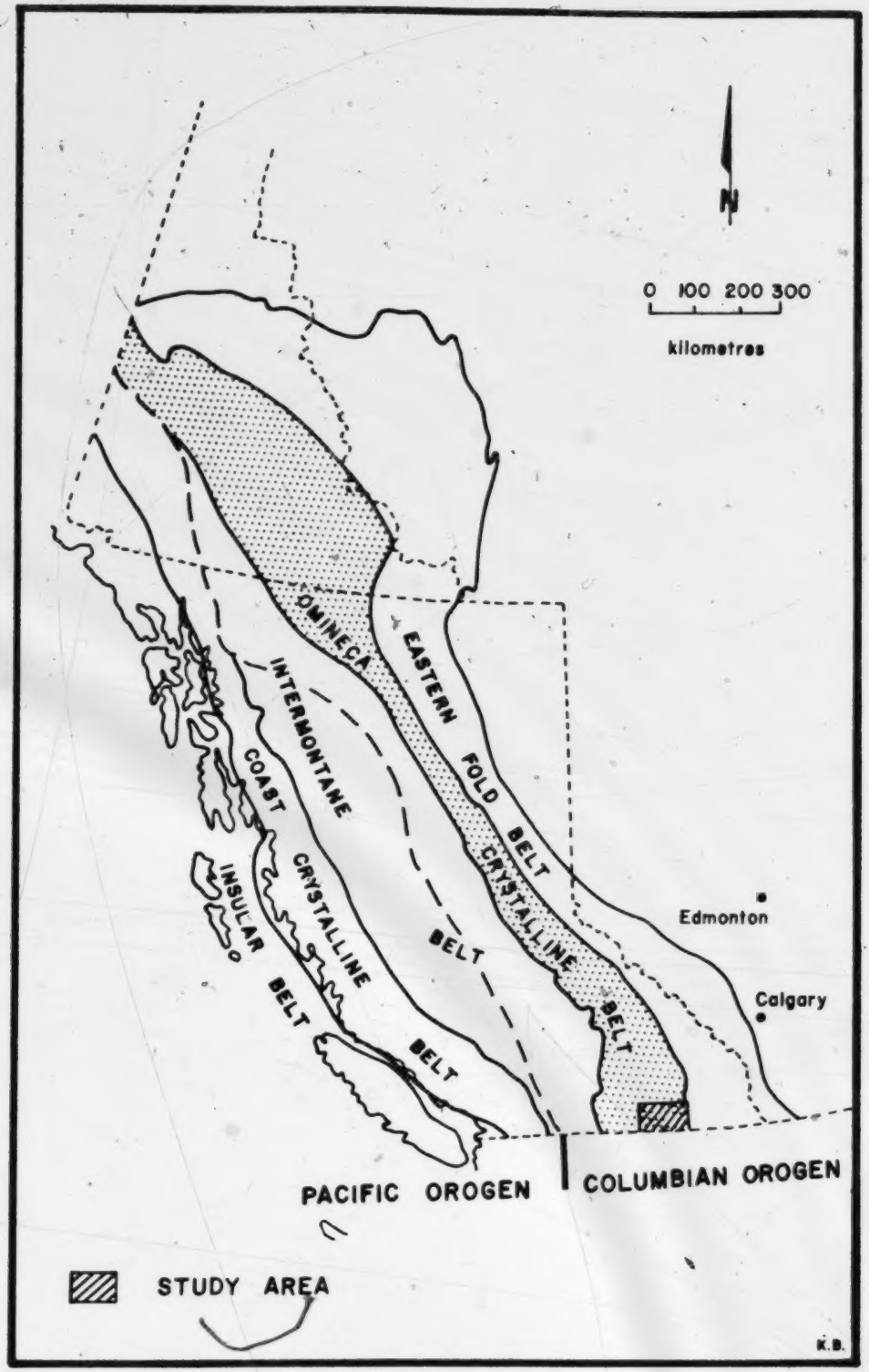

FIGURE 1. Location map (from Gabrielse and Reesor, 1974)

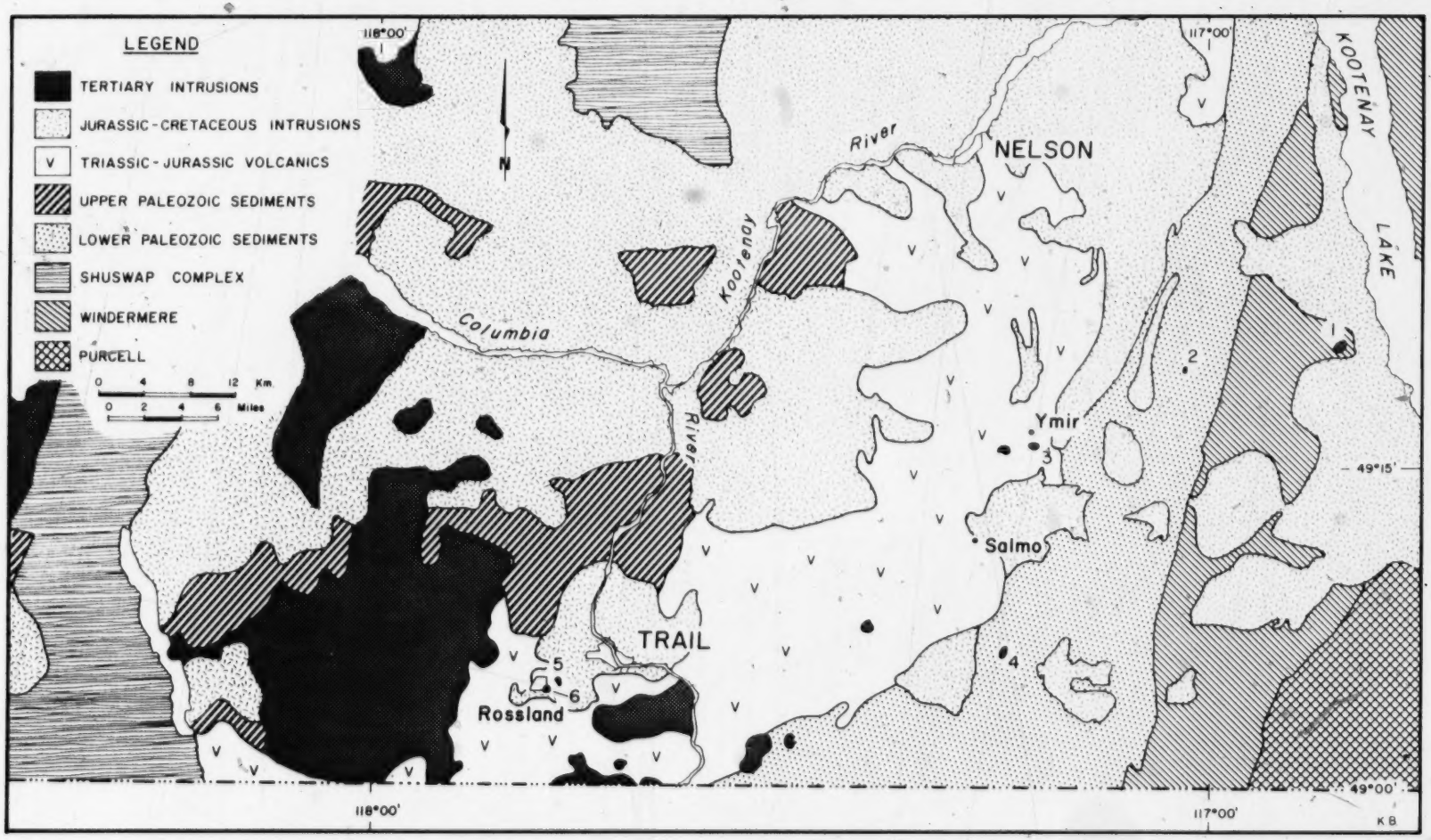

FIGURE 2. **Generalized geology of the study area with pluton locations.**
1. Mt. McGregor, 2. Cultus, 3. Ymir, 4. Jersey, 5. Rossland Highway Cut, 6. Rossland Railway Cut.

C. Previous Work

The Coryell intrusions were first noted by Dawson in 1890. In 1912, Daly gave them the name "Coryell syenite", named after a local railway station. He described the main batholith along with the associated Sheppard granite and related bodies (Little, 1960, p. 90). Other Tertiary intrusions in the Rossland area were summarized by Drysdale in 1915 (pp. 230-237).

It may be helpful here to point out and clarify some overlapping terminology. Daly (1912) named the intrusion located half way between Sheep Creek and Lost Creek, the "Salmon River monzonite" and McAllister (1950) has called the stock one mile south of Ymir the "Salmo River plug". To eliminate any confusion, I have given different names to these two plutons. Respectively, the first is called the Jersey intrusion owing to its proximity to the Jersey Zn-Pb mine and the second has been designated the Ymir pluton.

The Ymir stock, just south of the town of Ymir, was initially recorded by Drysdale (1917, pp. 38-40). McAllister (1950) presented a thorough description of this intrusion (his "Salmo River plug"), discussing the field relations and petrography. His petrographic examination, however, was based on the examination of only 2 thin sections and no chemical analyses were performed.

McAllister pointed out the close similarity of the zoned Ymir pluton with the Shonkin Sag laccolith in Montana.

Drysdale (1917) suggested that the Ymir pluton represented the eroded core of an old volcanic conduit. He presented an east-west section passing through the pluton, showing the so-called "pulaskite" core zone. Although he classifies this intrusion as a monzonite, later examination has undoubtedly proven it to be a mafic syenite.

The Jersey stock ("Salmon River monzonite") was described by Daly (1912) and a small BASc. thesis was prepared by Padgham (1955). Padgham noted a zonation in this stock towards a less mafic interior. He also observed felsic and mafic inclusions and six lamprophyre dykes were examined on its eastern contact. Chemical analyses have been done by Daly as well as a norm calculation and a petrographic mode.

Petrographic and field descriptions were made by McAllister (1950) on the Cultus Creek stock (McAllister called it the "Labe Creek plug"). He noted a gradation in this pluton from an olivine-rich basaltic rim to a coarser olivine-poor, highly altered central zone, similar to the Ymir pluton.

Mt. McGregor was described by Rice (1941). He gave the name McGregor Intrusives to the 4 stocks on top of Mt. McGregor and the related sills and dykes in the east half of the Nelson map sheet. Based on their chemical and mineralogical similarity to the Coryell intrusions to the west, they have been considered part of this same event. Rice (1941) believed that the Mt. McGregor intrusions were volcanic necks and points out the abundant lamprophyres associated with them.

Another pluton of interest, not visited by the author, is located about 1.6 kilometres to the west of the Ymir stock. It is called the May Blossom chonolith and was described thoroughly by McAllister (1950) and Drysdale (1917). Its mineralogy is similar to that of the Ymir pluton and Drysdale reports that it is cut by ore-bearing fissures.

Numerous biotite- and biotite-olivine lamprophyres (Mathews, 1953) are found throughout the entire area possessing chemical similarities to the satellitic Coryell plutons. Mathews (1953) has observed granitic inclusions in the lamprophyre dykes found in the Sheep Creek area and notes their chemical and mineralogical affinities with kimberlites. He considered these Tertiary lamprophyres to be derived from a similar magma to that of the Jersey pluton ("Salmon River monzonite") and emphasized their contemporaneity with Sheep Creek ores.

The last major review of the Coryell plutons was compiled in a Geological Survey of Canada Memoir by Little in 1960 and a reassessment was made in Little's 1982 paper.

The previous work has indicated that the rock types within the Coryell suite range from potassic shonkinites to leucocratic syenites. It has also been established that the Coryell's were later than any other intrusives except for the basic (basaltic and lamprophyric) and acid (rhyolitic) dykes which cut the plutons.

II. TECTONIC SETTING

A. Introduction

The Coryell intrusions examined in this study lie on the eastern edge of the Omineca Crystalline Belt in the core of the Columbian Orogen (Wheeler and Gabrielse, 1972). The main Coryell batholith was emplaced into the Shuswap Metamorphic Complex and the eastern intrusions occur within the Nelson Plutonic Complex and the Kootenay Arc (See Figure 2).

B. Regional Geology and Tectonics

The initiation of Cordilleran tectonics began with the formation of a rift zone in the craton sometime in the late Proterozoic (Monger *et al.*, 1972). Proterozoic and lower Paleozoic sediments and volcanics were deposited into the area now known as the Omineca Crystalline Belt or Omineca Geanticline. This belt has been the site of medium to high-grade metamorphism, intense deformation and magmatic activity since mid-Jurassic time.

The collision of allochthonous terranes from the west caused tectonic overlap and compressional thickening in the eugeosyncline formed off the cratonic edge (Monger *et al.*, 1982). The Columbian Orogen, of which the Omineca Belt forms the core, consists of 2 main pulses (Price, 1981). The first late Jurassic-early Cretaceous pulse was caused by the collision with Stikinia and the second pulse, during the Late Cretaceous and Early Paleogene reflects the attachment of the allochthonous Wrangellia terrane.

This last pulse represents the Laramide Orogeny. The Coryell intrusions were emplaced during the waning phases of this period. The characteristically amagmatic style of the Laramide is associated with a shallowing in the angle of plate descent between 80 and 70 Ma (Dickinson and Snyder, 1978).

Although the Laramide period (85-45 Ma) was a time of abnormally high convergence rates (Keith, 1982), the low angle dip of the plate and corresponding lack of asthenospheric penetration severely curtailed magmatism in the western United States.

The exact cause of the late-Laramide magmatism may be attributed to several factors. Amalgamation of the Pacific, Kula and Northern Farallon Plates, occurring around 53 Ma, produced a transform boundary along the western edge of the craton. Based on extensive measurements of dyke swarms in this area, Price (1981) postulates the existence of a rotational force, linked to the transform faulting off the coast. This caused ductile stretching of the intervening lithosphere between the Fraser River fault zone and the Rocky Mountains. The relaxing, extensional regime may have helped to initiate a localized mantle plume. Alternatively, a subducted slab may have been present beneath British Columbia at this time, and magmatism could be attributed to the collapse of this plate.

The nature of the underlying crust and mantle is a significant influence on the prevailing orogenic activity of this region. The western edge of the Precambrian craton or miogeosyncline most likely follows the western boundary of the Omineca Crystalline Belt, corresponding to the $^{87}Sr/^{86}Sr$ 0.704-0.706 transition (Monger *et al.*, 1982). Geophysical measurements below the Omineca Belt suggest a crustal thickness of 30 km with a lower density than the thicker crust occurring to the east (Stacey, 1973). Electrical measurements show the lower portion of the crust to be conductive and hydrated, possibly inferring a zone of partial melting.

It should be pointed out that considerable north-eastward movement of the overlying eugeosynclinal and miogeosynclinal rocks has occurred since the Late Jurassic. This movement was probably in the order of 200 km and has involved rocks within the Omineca Belt (Price and Mountjoy, 1970; Brown, 1978) as well as those in the Eastern Fold Belt. Therefore, it is quite probable that rock units formed to the west of the craton during the Jurassic (eg.-Rossland Volcanics : $^{87}Sr/^{86}Sr$ = 0.704) may presently lie above the cratonic basement. All the Coryell plutonics have most likely penetrated the cratonic edge.

C. Eocene Magmatism

Price and Mountjoy (1970) suggest that the hiatus separating the Paleocene clastic wedges of the Interior Plains from the Upper Eocene sediments represents the termination of Laramide thrusting, followed shortly thereafter by intrusion of the Coryell plutons and the extrusion of the associated lower-Eocene volcanics to the west and north-west.

The Coryell intrusions represent the largest bodies of Eocene age in the southern Canadian Cordillera. They are shallow, epizonal intrusives and are probably related to associated volcanics. Their emplacement represents a geothermal event of considerable magnitude resulting in the resetting of K/Ar dates over large areas, to the 50 Ma age representing the time of their intrusion (Medford, 1975; Mathews, 1981).

The effects of this resetting event are delineated to the west by the Okanagan Valley and to the east by the Kootenay Arc. Resetting has also affected rocks within the Arc itself (personal communication, Burwash, 1983). The possibility exists that a much larger extent of still covered, shallow Coryell underlies this entire area, continuing into the Northwestern United States as well.

Eocene radiometric dates have also been obtained for alkaline suites of rocks east of the Coryell trend. The intrusions in the Sweetgrass Arch have K-Ar dates of 48 Ma (Baadsgaard *et al.*, 1961) and those located in the Shonkin Sag laccolith are also Tertiary in age.

It is well-documented that the existence of neutral or tensional stress systems appear to aid in the production of alkaline magmas (eg.- East African Rift system, Bailey, 1964). Many Tertiary volcanics occur along well-defined northerly-trending tensional fracture zones in southern British Columbia. Although extensive block-faulting and evidence for extension is associated with the related Eocene extrusives in the Greenwood area (Monger, 1967), the relationship between faulting and the intrusions east of the main batholith is not obvious. Mulligan (1951) points out the emplacement of one of the Coryell intrusions into the nose of a major drag fold in the Rossland Volcanics just west of Ymir. The Coryell intrusives examined in this study show no linearity of

emplacement, although faulting at depth may certainly be obscured by later events therefore this possibility can not be eliminated.

Early-Eocene volcanism is a very widespread event north and west of the main Coryell batholith (Mathews, 1964), extending as far as the Okanagan Valley. The Kamloops Group, Kettle River Formation, Midway Group and Marron Formation are all part of this event. The relationship between these volcanics and the Coryell suite is still uncertain although considerable chemical and mineralogical similarities exist with the younger formations, particularily the Marron Formation (Monger, 1967).

III. GEOGRAPHIC EXTENT AND MODE OF OCCURRENCE OF CORYELL PLUTONS

The Coryell rocks extend from Kootenay Lake in the east to the Okanagan Valley in the west. They occur 100 km to the north of the 49th parallel and Coryell equivalents can be identified in the northwestern United States.

Examination of the intrusives in the field distinguishes a continuous range of rock types, ranging from leucocratic syenite in the west to more mafic syenites and porphyritic alkali basalts in the east.

A. Main Coryell Syenite Batholith

The large Coryell batholith is the centre of the Tertiary alkaline plutonism in the southern interior of British Columbia. The total area covered is approximately 1,850 km² (720 square miles) (Gabrielse *et al.*, 1974). The batholith is dominantly composed of coarse to mediumgrained syenite that is pink to pale buff in colour (Little, 1960). Orthoclase, microperthite and andesine are the major minerals. Smaller amounts of quartz, hornblende and biotite are also present. In the buff phase of the syenite, augite percentages increase and quartz tends to be rare.

Satellitic stocks are spatially related to the batholith possessing a far less differentiated character, becoming increasingly more mafic with distance from the batholith. These smaller, possibly cogenetic plutons are typically steep-sided, elliptical intrusions that stand out as positive topographic features. Their contact with the surrounding country rock is generally sharp and they weather to smooth, rounded outcrops through extensive exfoliation.

B. Rossland Intrusions

Samples collected from two intrusions located about 6 kilometres to the east of the central batholith are chiefly coarse-grained syenites with 35% mafics, mainly biotite and augite with some minor olivine. The groundmass consists of perthite. Augite occurs as large euhedral crystals, often reaching 7

mm in length.

Railway Cut

The westernmost of the two intrusions, called the Rossland Railway Cut, is bisected by an abandoned railway bed in the centre of Rossland. This pluton intrudes the middle to upper-Jurassic Nelson batholith (Figure 3). Discrete, thin felsic bands run vertically through the pluton, caused by flow-banding in the magma chamber. Dilation fractures are common and contain felsic, late stage magmatic or hydrothermal differentiates.

Highway Cut

The more easterly of these two intrusions, called the Rossland Highway Cut, is cut by the road from Trail to Rossland. It forms an elliptical plug approximately 1/2 km by 3/4 km in diameter and intrudes the Nelson batholith (Figure 4). The mineralogy of this intrusion is similar to that of the Rossland Railway Cut and it is dissected by numerous fine grained mafic dykes and aplites.

C. Jersey Intrusion

A third plug, located 50 kilometres east of the main batholith, has been named the Jersey pluton. This 1 km wide stock intrudes Lower Cambrian sediments (Figure 6). Mineralogically it is almost identical to the two intrusions at Rossland. Very basic, coarse-grained patches of shonkinite occur within the Jersey pluton. The mafic constituents of the shonkinites are similar to those in the pluton itself but the percentage of these is significantly increased (to over 60%), suggesting a cumulate nature. Felsic pods, similar in nature to those found in the Rossland Railway Cut, are common.

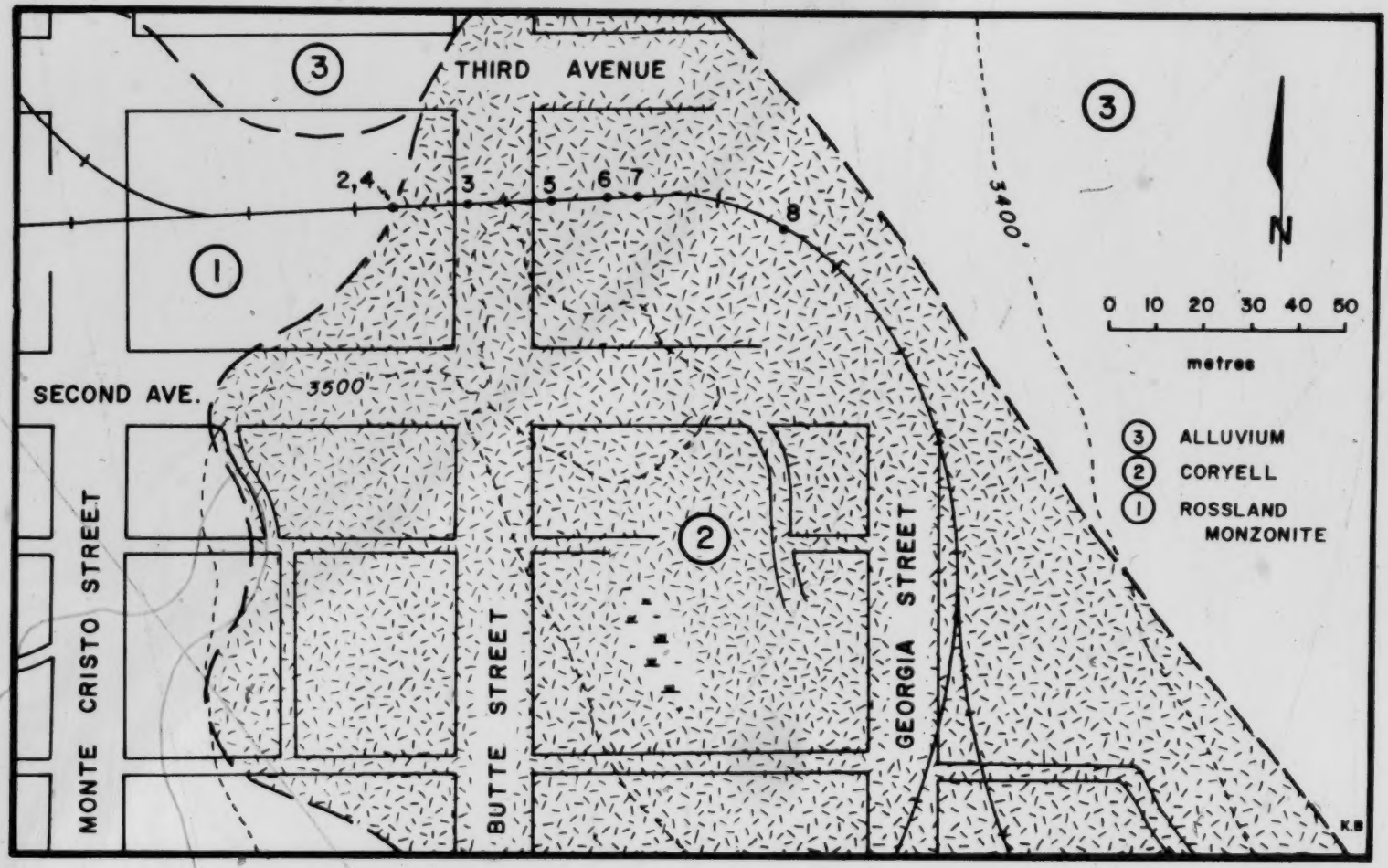

FIGURE 3. Geology and sample collection sites, Rossland railway locality.
Geological boundaries, topography and cultural features from Map. No. 1002 (Drysdale, 1909).
Sample suite - U of A No. 10617.

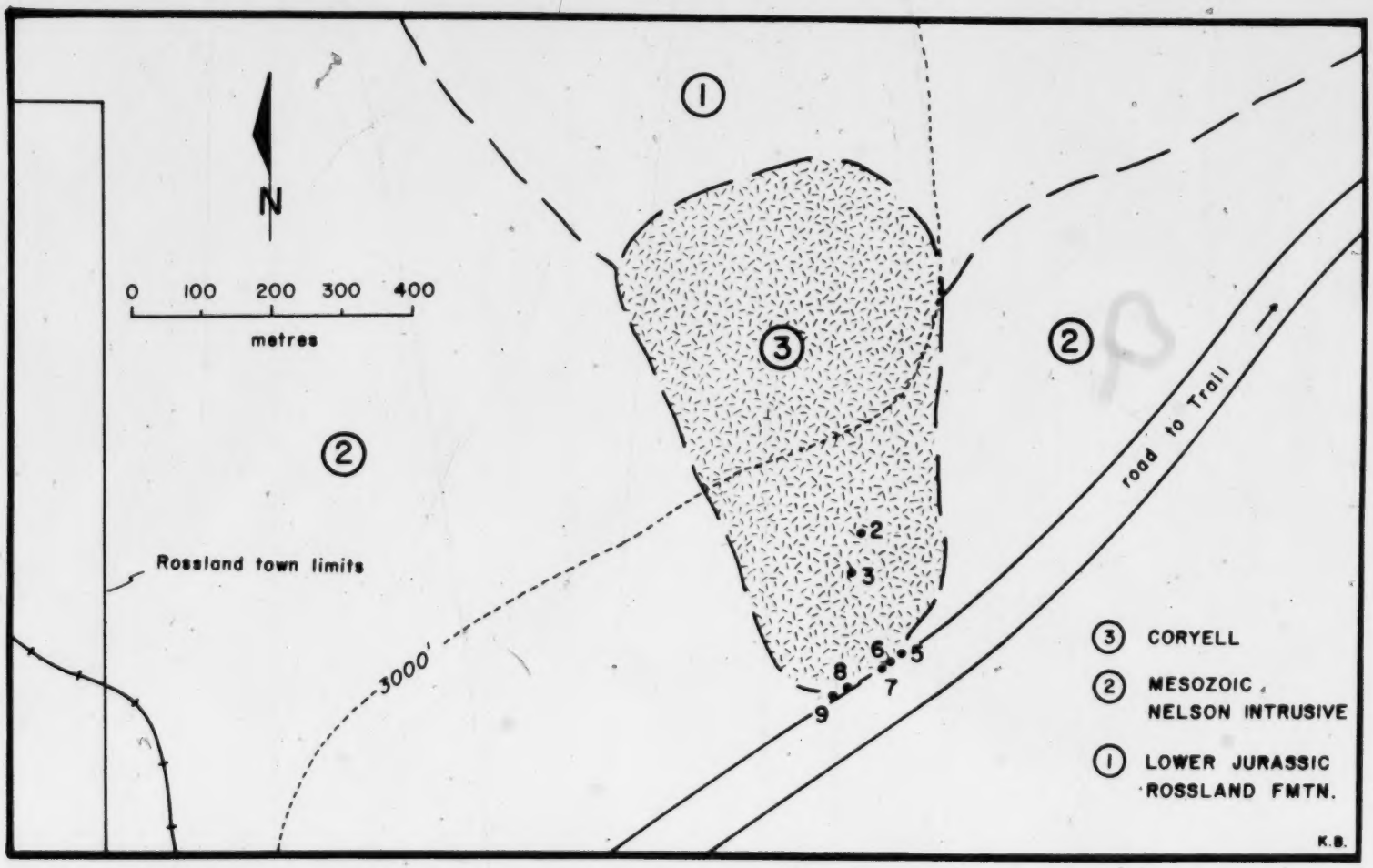

FIGURE 4. Geology and sample collection sites, Rossland highway locality.
Geological boundaries, topography and cultural features from Map 108A, Nelson West Half (Little, 1960).
Sample suite - U of A No. 10621.

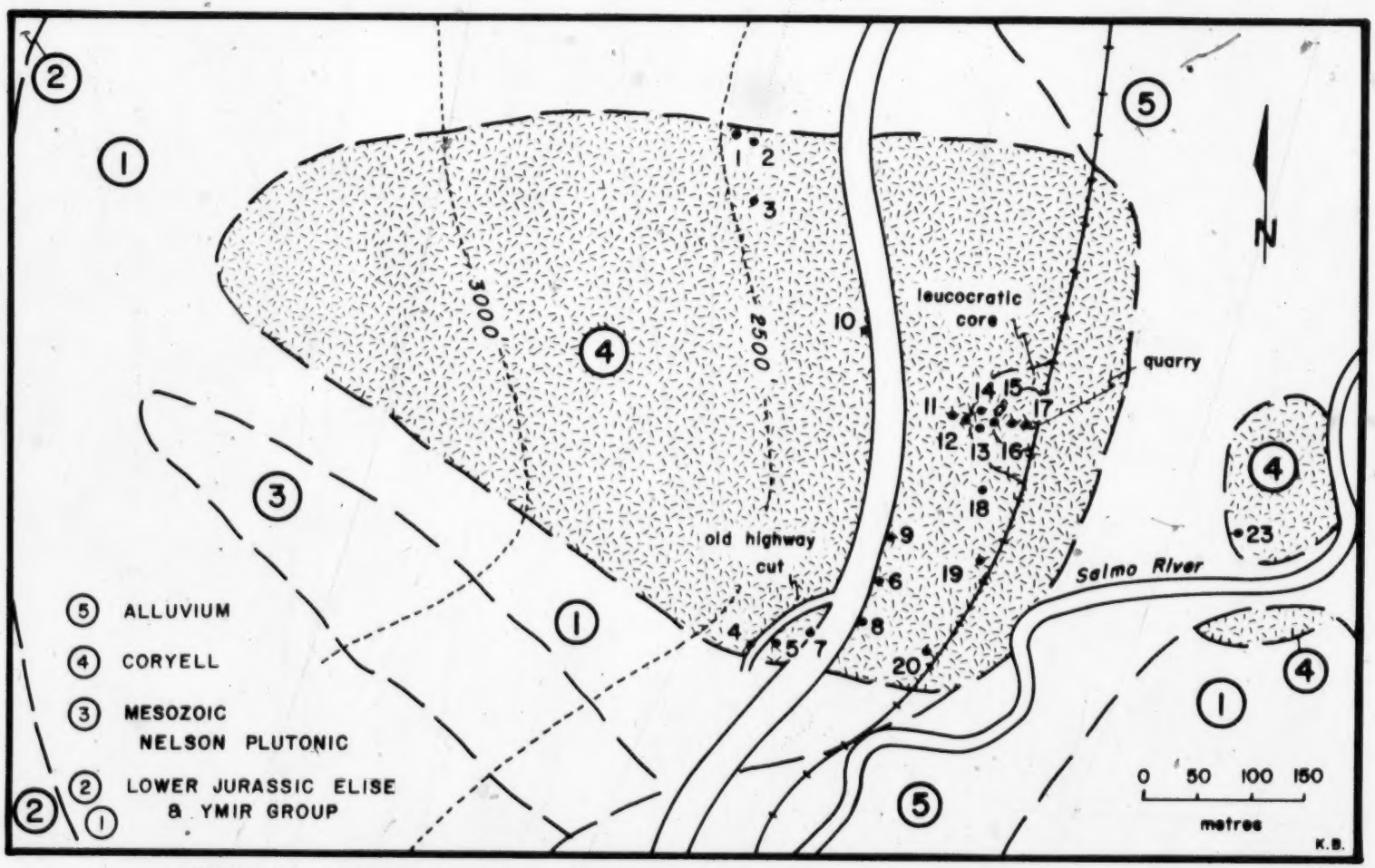

FIGURE 5. Geology and sample collection sites, Ymir pluton.
Geological boundaries, topography and cultural features from GSC Map 1144A, Geology Ymir (1963).
Sample suite - U of A No. 10563.

D. Ymir Intrusion

Twenty kilometres to the north of the Jersey pluton (also at a distance of 50 kilometres from the main batholith) lies the most intensively studied intrusion. The Ymir pluton forms a 1 kilometre by 1/2 kilometre wide elliptical body that intrudes the lower Jurassic Ymir Group sediments (Figure 5). The contact has been baked to a pyroxene hornfels for up to 100 metres away. The Ymir pluton consists of two separate intrusive episodes. The outer rim (constituting 90% of the pluton) is a basic syenite and represents the initial intrusion. A second magma was intruded into the centre of the first mass while it was still warm. In contrast to the three previously described plutons, the main body of the Ymir plug is more mafic, with a significantly higher proportion of olivine (up to 20%). Total mafics exceed 45% of the rock, with a tendency to become less mafic towards the centre.

Coarse-grained euhedral augites, olivines and biotites are embedded in a medium-grained groundmass consisting of orthoclase with extremely minor andesine.

The core of the Ymir pluton is a more highly differentiated material, exposed in a small quarry blasted into the centre of the intrusion. This leucocratic core consists of coarse-grained, mauve coloured rock with a distinct trachytoid texture. Its contact with the main body is gradational over 2 metres. McAllister (1950) found fragments of the outer basic syenite embedded in the central leucocratic core, suggesting a semi-consolidated state before intrusion of the second magma pulse. An attractive blue iridescence (schiller structure) is seen on the large potassium feldspar laths. Augite and olivine contents drop considerably (to 5% each), so that mafics constitute only 20% of this central phase, the remainder being coarse-grained orthoclase.

At the very centre of the core zone a single sample was collected containing abundant quartz.

Marked flow-banding, segregating mafic and felsic constituents is characteristic of the Ymir pluton. Late leucocratic dykes emplaced into shrinkage fractures occur within the stock, and may be offshoots from the central core

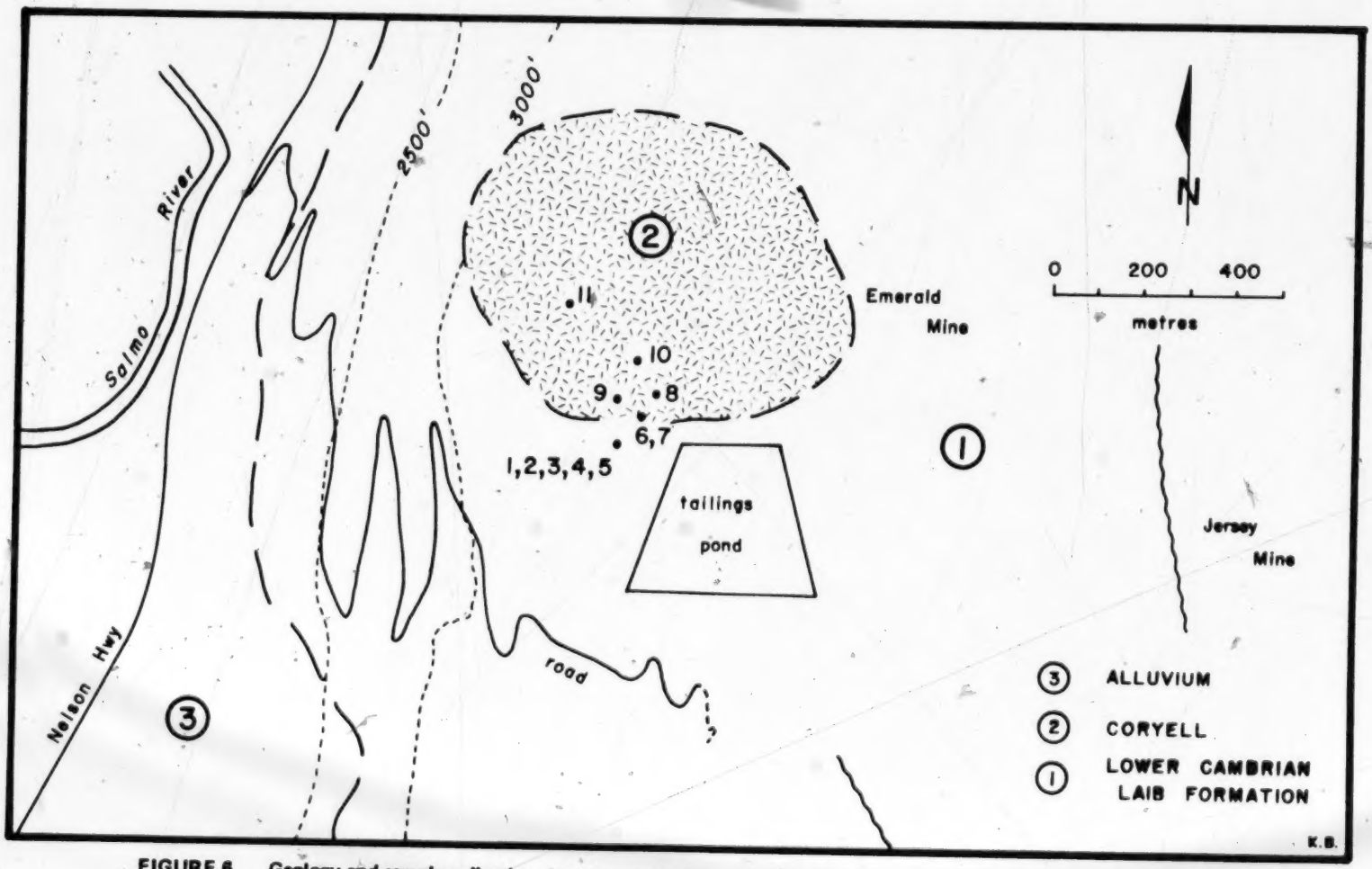

FIGURE 6. Geology and sample collection sites, Jersey pluton.
Geological boundaries, topography and cultural features from Map C (Fyles + Hewlett, 1959)
Sample suite - U of A No. 10564.

zone.

E. Eastern Intrusions

The two most easterly plutons, the Cultus Creek and Mt. McGregor intrusions are emplaced 65 and 80 kilometres, respectively, from the main Coryell batholith west of Rossland. They both appear to be remnants of old volcanic necks. These two plutons constitute the most mafic members of the series.

The dominant mineralogy of these intrusions is that of a fine-grained, porphyritic alkali basalt although coarser phases occur as well. Phenocrysts of olivine and augite are embedded in an aphanitic groundmass, consisting of feldspars and biotite.

Cultus Stock

The Cultus Creek stock (also known as the "Labe Creek plug") appears as a black, solitary intrusion with steep, blocky cliffs forming the outer walls. This volcanic plug is approximately 1 kilometre by 1.5 kilometres in diameter and intrudes the Lower Cambrian Laib formation (Figure 7). The outer rim of this pluton is very fine-grained and a gradation to a coarser central area occurs. The pyroxenes of the inner zone are highly altered to amphibole and the rocks are essentially olivine free.

Extremely acid dykes, up to a metre wide, cross-cut the intrusion and abundant felsic pods and xenoliths were observed.

McGregor Intrusion

The most easterly intrusion of the entire Coryell suite is found at the top of Mt. McGregor at an elevation of 2241 m (7352 feet). Intruding the Horsethief Creek series of the Windermere Group, is the 1.5 by 1.2 kilometre wide McGregor stock (Figure 8).

Rice (1941) outlined four discrete bodies on this mountain top overlooking Kootenay Lake. We sampled the largest of these bodies on the

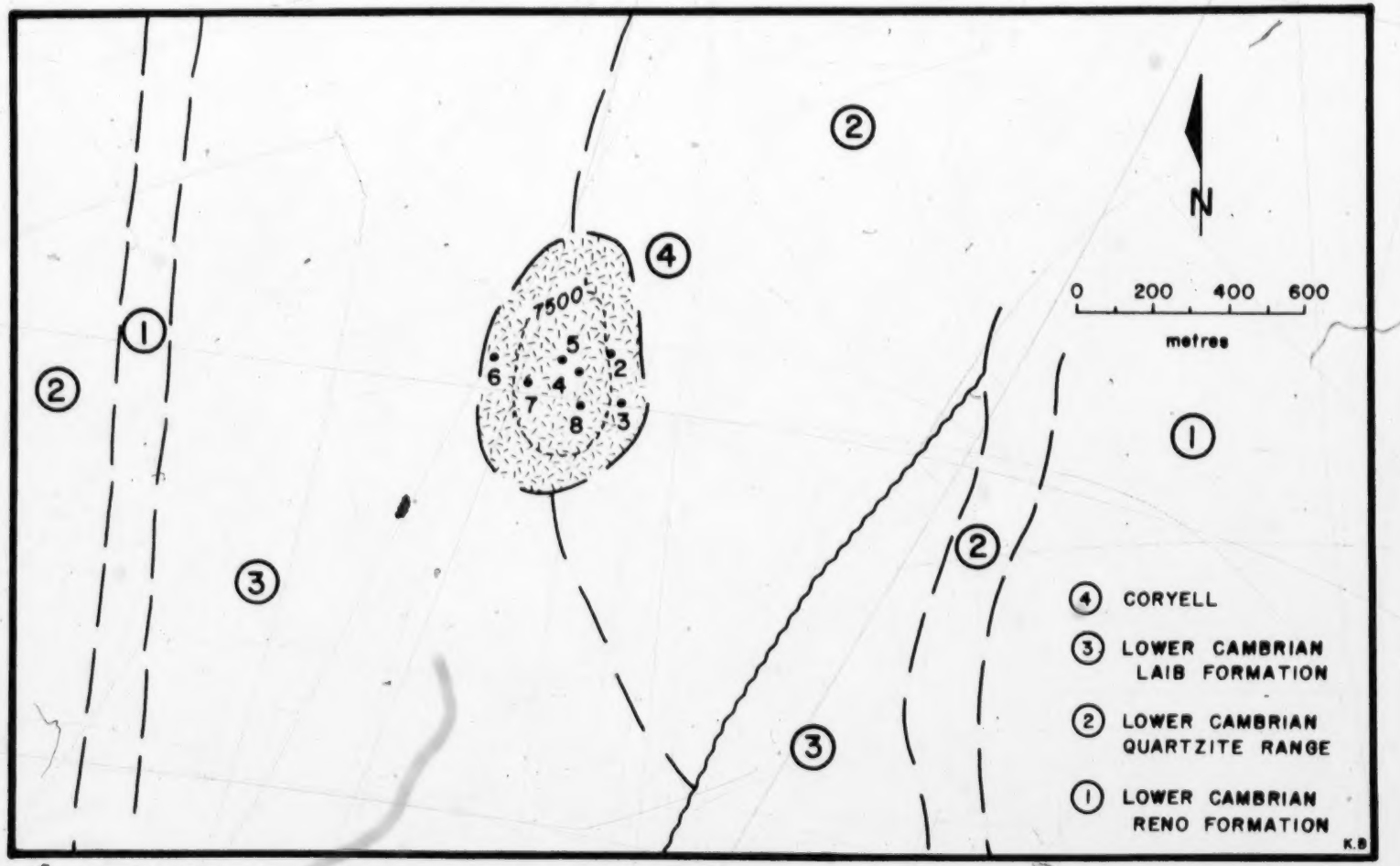

FIGURE 7. Geology and sample collection sites, Cultus stock.
Geological boundaries from Map 1109A, Nelson West Half (Little, 1960).
Sample suite - U of A No. 10620.

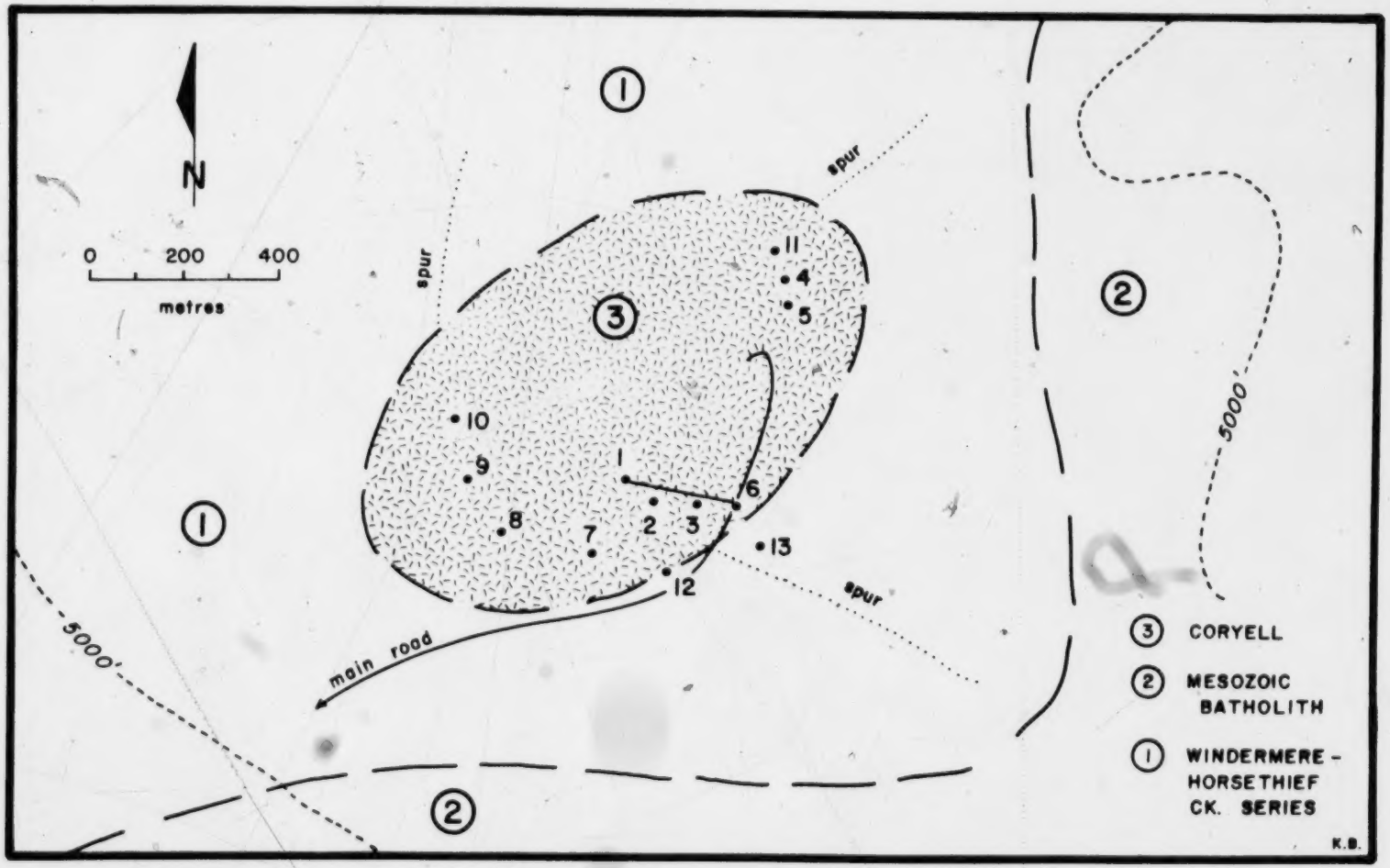

FIGURE 8. Geology and sample collection sites, Mt. McGregor locality.
Geological boundaries from Map 603A, Nelson East Half (Rice, 1941)
Sample suite - U of A No. 10619.

crest of the peak. Grain size, appearance and composition vary greatly throughout this stock with no apparent relationship to the pluton boundary. The coarser grained phases are shonkinitic (melasyenitic) in nature, with the finer varieties more appropriately called trachybasalts. Some samples contained up to 70% mafic minerals, mainly biotite (up to 35%) with lesser augite and olivine. Augite phenocrysts are up to 5 mm long and are ubiquitous in all samples. The groundmass is mainly feldspars and orthoclase was identified in phaneritic samples.

The coarsest grained varieties are lamprophyres and are extremely altered, friable rocks. Partially resorbed felsic xenoliths are abundant, and are most probably remnants of the underlying granitic Mesozoic batholith.

IV. PETROGRAPHY

A. Classification System

Realizing that no uniquely superior method of classifying rocks exists, I have adopted the recommendations of the IUGS Subcommission on the Systematics of Igneous Rocks (Streckeisen, 1973, 1979).

All igneous rocks, whether they are plutonic or volcanic will be classified and named according to their modal mineral content (measured in volume percent) (Figure 9).

Alternative classification systems utilizing geochemical analyses will be discussed in the section on geochemistry.

B. Introduction

This petrographic review is based on the examination of 67 thin sections and general microprobe observation of 3 polished sections. The modal mineralogy of each sample was tabulated using between 500-1000 point counts (depending on sample homogeneity and grain size) (Figure 10). Modal analyses are contained within Appendix III.

The volumetrically predominant rock types constituting the satellitic Coryell intrusions are mafic syenites and trachybasalts. Three major subdivisions can be delineated:

1) the biotite augite melasyenites, characteristic of the Rossland and Jersey intrusions,

2) the biotite olivine augite alkali-feldspar melasyenites of the Ymir pluton, and

3) the fine-grained porphyritic olivine biotite augite trachytes found in both the Cultus Creek and Mt. McGregor stocks.

Mafic shonkinites, lamprophyric pegmatites, late dykes and the differentiated leucocratic granite core of the Ymir intrusion are minor in relative volume, though nevertheless important in the interpretation of these plutons.

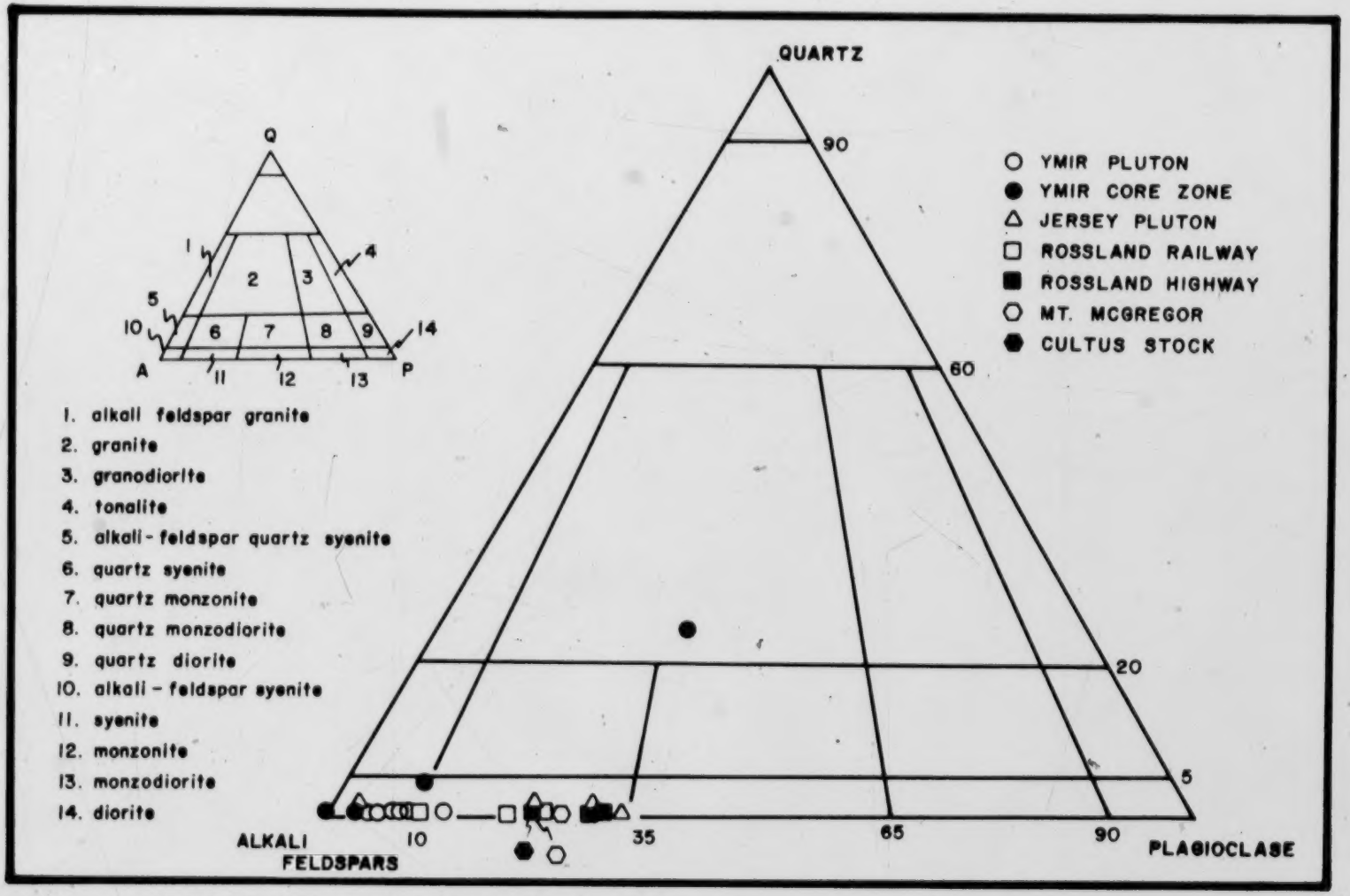

FIGURE 9. Petrographic classification of modal mineralogical compositions - Coryell plutons. (from Streckeisen, 1973).

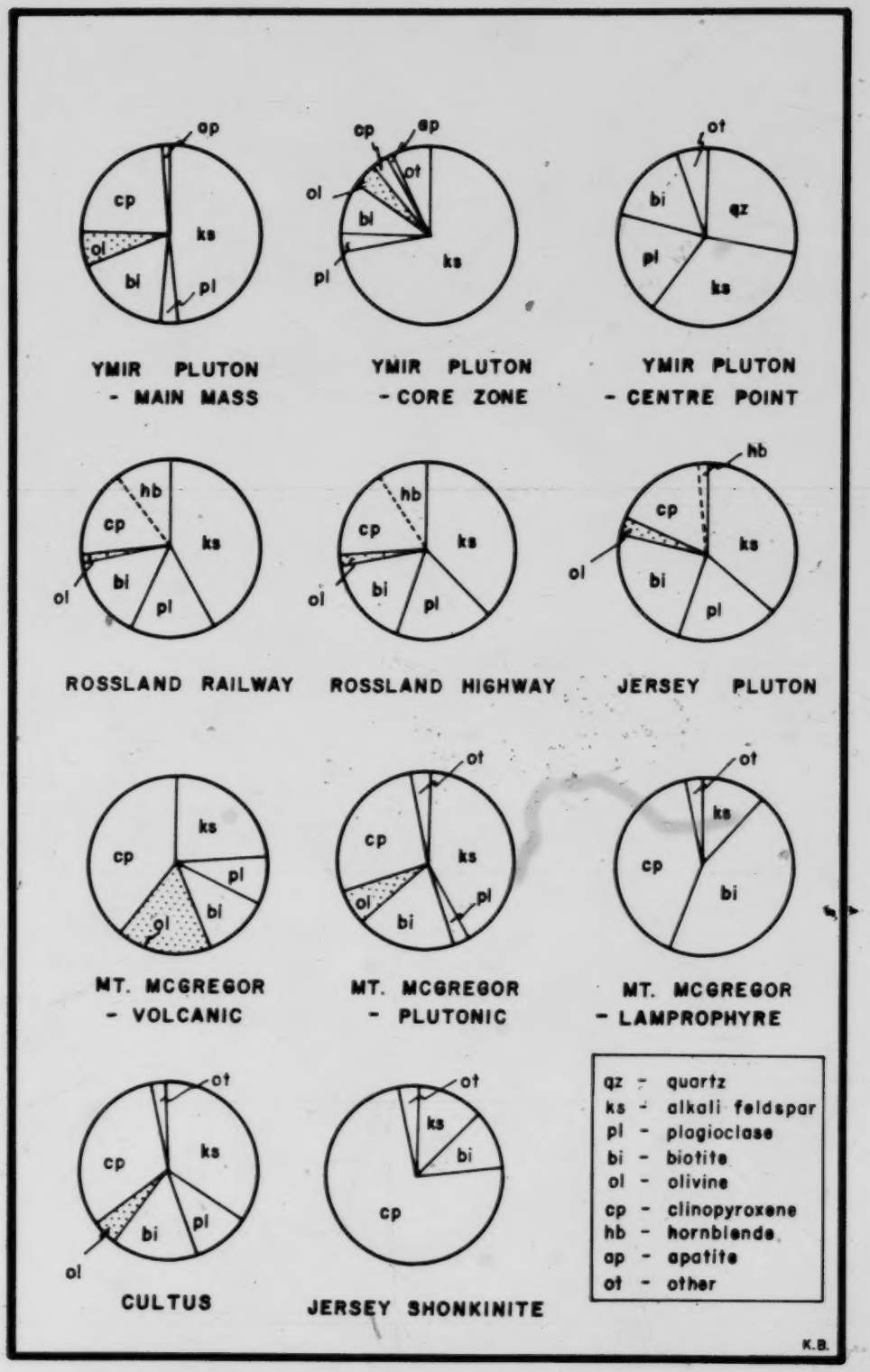

FIGURE 10. Modal mineralogy (based on 500 - 1000 point counts)

C. Biotite Augite Melasyenites

The biotite augite melasyenites, composing the Rossland and Jersey plutons are typically medium to coarse-grained rocks. Early formed euhedral augite and biotite crystals compose from 30 to 40% of the sample. They are surrounded by anhedral alkali feldspars containing abundant plagioclase laths.

These rocks distinguish themselves from the other Coryell samples by the pervasive replacement of the augite grains by a bright green hornblende (Plate 1A). This replacement can constitute up to 50% of the clinopyroxene in the Rossland intrusions, but is normally around 30%. The other unique features include slightly higher amounts of plagioclase and a severely reduced olivine content with total alteration of the olivine which is present.

Augite crystals, constituting between 20 and 30% of the rock, are strongly poikilitic with abundant inclusions of biotite, magnetite, plagioclase, alkali feldspar, apatite and some completely replaced olivine. Although normally forming as clean euhedral, stumpy prisms, the clinopyroxenes found in the Jersey pluton possess a peculiar habit. They are often composed of numerous, randomly-oriented grains, creating a patchwork texture unknown in other Coryell intrusions. Light zoning and twinning are standard features of the augites in this category. Microprobe analysis indicates a more magnesium-rich core, as expected. The augites in these rocks are iron-rich when compared with those in the alkali-feldspar syenites of the Ymir intrusion.

The dark brown biotites (20-30%) show strong pleochroism and occur both as inclusions in the augite and as discrete euhedral laths within the alkali feldspars. From microprobe analysis, the inclusions are slightly more magnesium-rich.

Several different forms of biotite occur, ranging from stubby laths to elongated prisms. Grain-size averages 2 mm in the stubby varieties and 5 mm in the elongated crystals. It is generally riddled with apatite inclusions and grains of magnetite. A change along the edges to green biotite is commonly observed, notably when the biotite is in contact with an altered olivine crystal. The breakdown to chlorite, although rarely seen, starts from the centre of the

Plate 1A

Replacement of clinopyroxene by secondary amphibole - Rossland railway cut

Photomicrograph. Characteristic of the Group I intrusions is the more pervasive alteration of the augite crystals (up to 50%). Light kaolinitic coating on the alkali feldspars.
Plane polarized light. Magnification = 50x

Plate 1B

Alteration products of forsteritic olivine - Mt. McGregor

Photomicrograph. Biotite, magnetite and yellow bowlingite replacing olivine.
First order yellow-beige mineral at lower left-hand side of the olivine is an orthopyroxene.
Crossed polars. Magnification = 50x.

1A

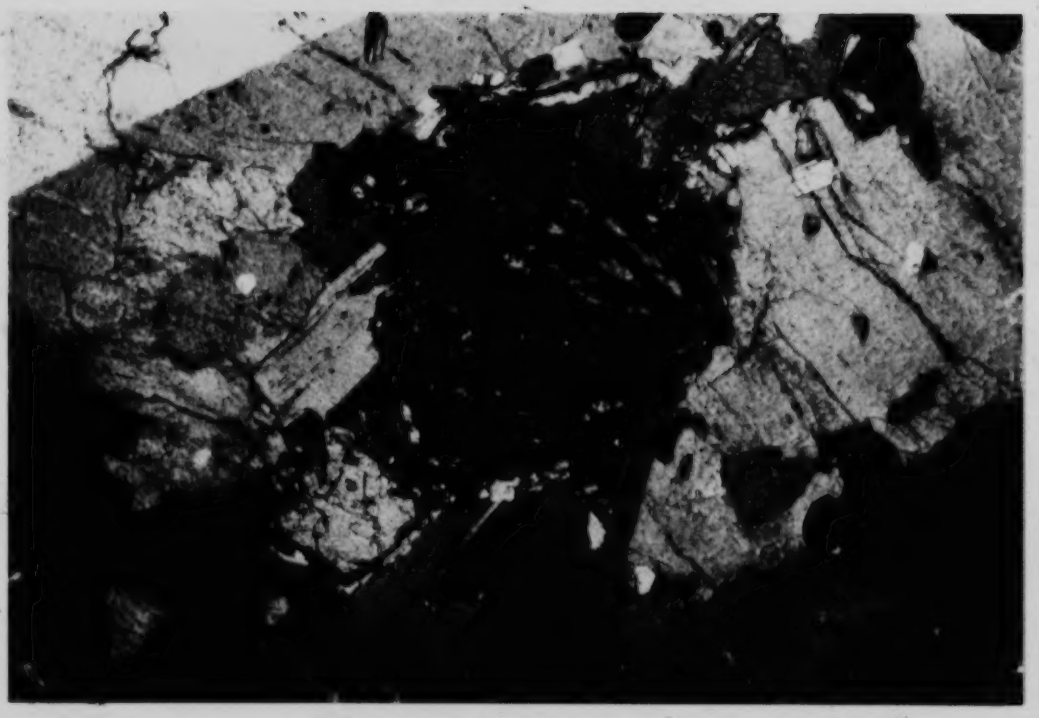

1B

crystal and is often accompanied by minute particles of sphene and epidote.

Olivine forms less than 5% of these syenites and is almost completely replaced by magnetite, talc and yellow bowlingite. It occurs sometimes as inclusions within the augite crystals. Chemical composition of the olivine, as discerned from 2V measurements of nearly 90 degrees (biaxial positive), indicates a forsterite content of 85%.

Anhedral alkali feldspar is the major component in these samples, making up 30 to 40%. A light dusting of kaolinite is present in all sections and simple twinning (Carlsbad) is common. Fine-grained, randomly-oriented plagioclase laths (20%) with hazy, indistinct outlines, appear to be resorbing into the alkali feldspar. They are lightly saussuritized and sericitized. Measurements of extinction angles on sharp twins showing perpendicular cleavage give An contents between An_{24} (oligoclase) and An_{37} (andesine). Distinguishing between the hazy, indistinct plagioclases and alkali feldspars is a problem with these rocks and modal estimates must be considered tentative.

The incidence of calcite, amounting to as much as 5% in the Jersey pluton is an important feature to note. It appears only in trace quantities in the Rossland intrusions, seemingly related to an increased amount of alteration of the pyroxenes. The presence of calcite in the Jersey pluton may be a strong indication of contamination by country rocks at shallow depths (Plate 3B). The Jersey stock intrudes the Lower Cambrian Laib formation which consists of interlayered limestones, argillites and schists.

In the absence of lime-rich country rocks, the occurrence of CO_2 in large quantities has important implications for the generation of alkaline magmas.

Apatite and magnetite (or more accurately, an opaque iron oxide) are abundant accessory minerals. The magnetite appears as inclusions both within the augite and biotite and forms part of the alteration from earlier olivines. In the group of more highly altered samples, the magnetite takes on a more skeletal nature, greatly increasing in size.

Plate 2A

Biotite olivine melasyenite - Ymir pluton

Photomicrograph. This rock constitutes 90% of the Ymir pluton. It consists of 25% strongly poikilitic augite crystals, 15% olivine (upper right) with a forsterite content of 85. 15% euhedral biotites with up to 7% TiO_2 inclusions within the clinopyroxenes include phlogopite, olivine and apatite. Anorthoclase groundmass with minor (5%) andesine. Crossed polars. Magnification = 50x.

Plate 2B

Leucocratic syenite - granite core - Ymir pluton

Photomicrograph. 25% quartz occurs in the central area of this intrusion. Alkali feldspars form 70% (including minor microcline - lower left). Biotite content - 15%. Augite and olivine are absent except for small remnants now represented by chloritic alteration. Crossed polars. Magnification = 50x.

2A

2B

D. Biotite Olivine Augite Alkali-Feldspar Melasyenites

The Ymir pluton is composed almost entirely of a medium-grained mafic alkali-feldspar melasyenite (Plate 2A). Mafic content often exceeds 50% of the rock. The olivine and alkali feldspar contents are much enriched over those in the biotite augite melasyenites, at the expense of plagioclase. Alteration in these rocks is comparatively minor, the original minerals being readily identifiable.

The typically poikilitic, often euhedral, well-twinned augite crystals (20-25%) show almost no alteration effects. They have the usual inclusions of biotite, olivine, apatite and feldspars.

The dark brown pleochroic biotites (15-20%) contain apatite inclusions and some magnetite. A change to greenish biotite can be observed in a few samples.

Microprobe analyses on both an inclusion of biotite and a later-formed euhedral crystal of biotite, show a large variation in magnesium content. The inclusion is technically a phlogopite (Mg/Fe greater than 2) and although the later crystal is a true biotite, it also contains more magnesium than iron. Titanium content of the later-formed biotite was over 7% versus less than 1% for the inclusion.

In contrast to the biotite augite melasyenites at Rossland and Jersey, the olivine (10-20%) here is virtually unaltered. The crystals are universally covered with fine magnetite dust exsolving mainly from the fractures. A yellowish bowlingite replacement is sometimes present. The total replacement of the olivine by a thick talc-magnetite mass often seen in the other plutons is not as common here, although in certain isolated cases, it can become extremely prominent. A strongly magnesium-rich (Fo_{85}) composition is inferred from 2V measurements. The olivine occurs as discrete subhedral crystals and is also poikilitically included within the augites.

A fairly clean alkali felspar is the predominant mineral (40-50%) of the Ymir stock. Perthitic intergrowths are not common, although minute plagioclase crystals are embedded within the large alkali feldspars. Some minor exsolution of small spindles and patches occurs but is less apparent here than in any

Plate 3A

Magmatically corroded biotites - Mt. McGregor

Photomicrograph. Patchy stringers of biotite forming 2% of the groundmass.
Crossed polars. Magnification = 50x.

Plate 3B

Interstitial calcite - Jersey intrusion

Photomicrograph. Forms up to 5% of samples in the Jersey pluton.
Crossed polars. Magnification = 50x.

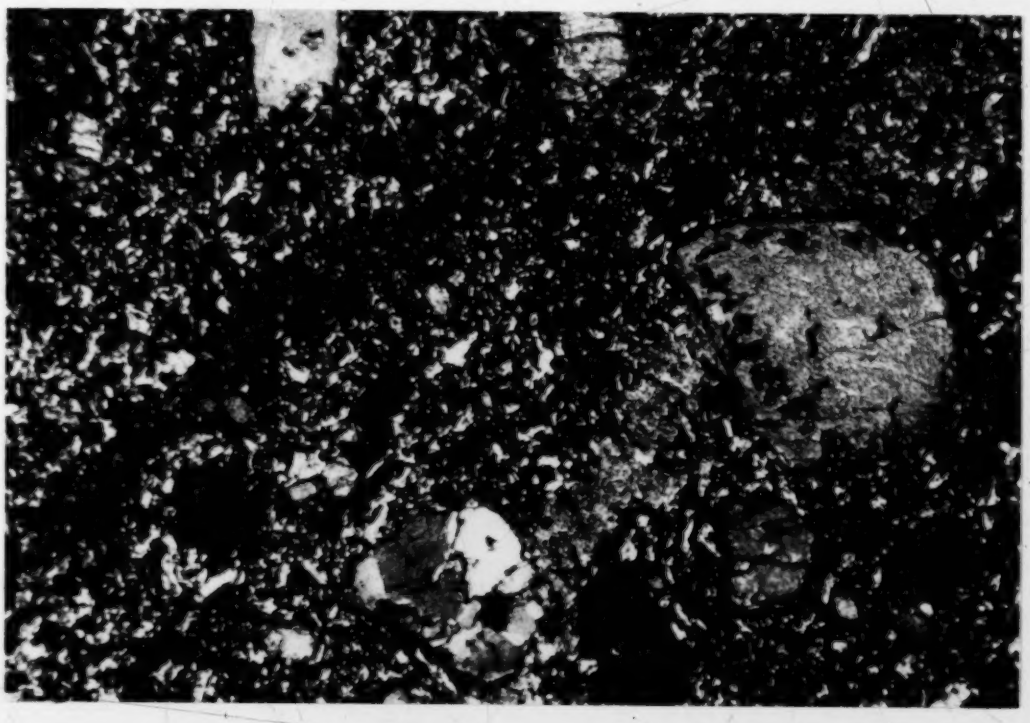

3A

3B

other Coryell intrusion. 2V measurements of approximately 60 degrees on the alkali feldspars place them into the range given for an orthoclase cryptoperthite. Microprobe analysis of these orthoclases attest to their high sodium contents, Na/K ratios average 1:2.

The main mass of the Ymir pluton usually contains less than 5% visible plagioclase. This is the lowest amount of plagioclase present in all the sampled plutons. Anorthite determinations range between 30 and 50 (andesine). Alteration of the plagioclases is almost non-existent and microprobe analysis suggests a composition falling more into the labradorite range (from Deer *et al.*, 1962).

Apatite is the main accessory mineral in these rocks.

E. Porphyritic Olivine Biotite Augite Trachybasalts

The Cultus Creek and Mt. McGregor stocks, the furthest eastern occurrences of Coryell intrusions, are composed mainly of fine-grained porphyritic trachybasalts (Plate 4A). Medium-grained (3-5 mm) phenocrysts of augite and olivine, constituting 20 to 40% of the rock are enclosed in a matrix containing biotite with varying percentages of feldspars. These trachybasalts contain the least amount of felsic components of all the Coryell rocks, confirming the increasingly mafic trend going eastwards. Augite has surpassed the alkali feldspars in volume. The groundmass displays a large grain-size variation from fine-grained to microcrystalline. Alteration in these hypabyssal rocks is almost totally lacking.

The euhedral augite phenocrysts show remarkably prominent zoning. Poikilitic inclusions are also concentrically zoned, usually with the central portion being full of inclusions and the band at the rim being clearer (Plate 4B). In the Cultus stock, up to 4 cyclic repetitions of these poikilitic to non-poikilitic pairs can be observed. The usual inclusions of biotite, olivine and feldspar are contained within the augites and complex twinning is common. It is interesting to note that the sample with the finest matrix contained no biotite inclusions in the augite. The degree of alteration can be directly related to the grain-size of the matrix. The finest-grained samples are almost totally unaltered whereas the

Plate 4A

Porphyritic trachyte - Cultus stock

Photomicrograph. Augite and minor olivine phenocrysts (20-40%) embedded in a fine-grained matrix of feldspars, biotite and some clinopyroxene.
Note the apparent lack of inclusions within the augite phenocrysts. Alteration is almost non-existent.
Crossed polars. Magnification = 50x.

Plate 4B

Zoning of a poikilitic augite - Cultus stock

Photomicrograph. Clear bands alternate with bands containing abundant inclusions. Up to 4 cycles of these bands.
Rim is clear of inclusions.
Crossed polars. Magnification = 50x.

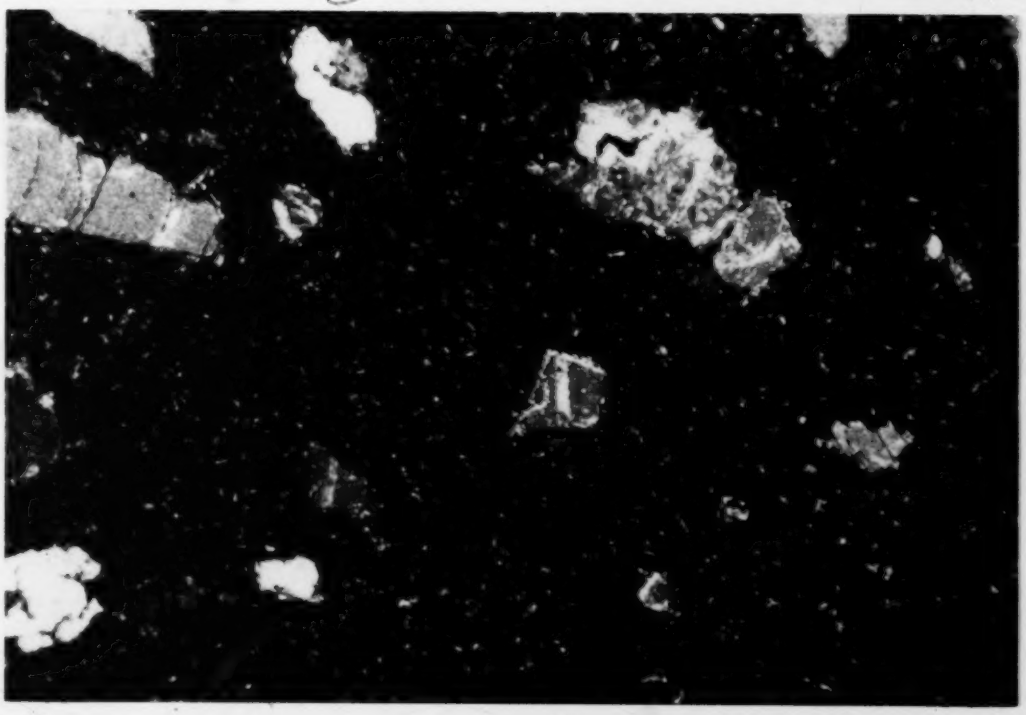

4A

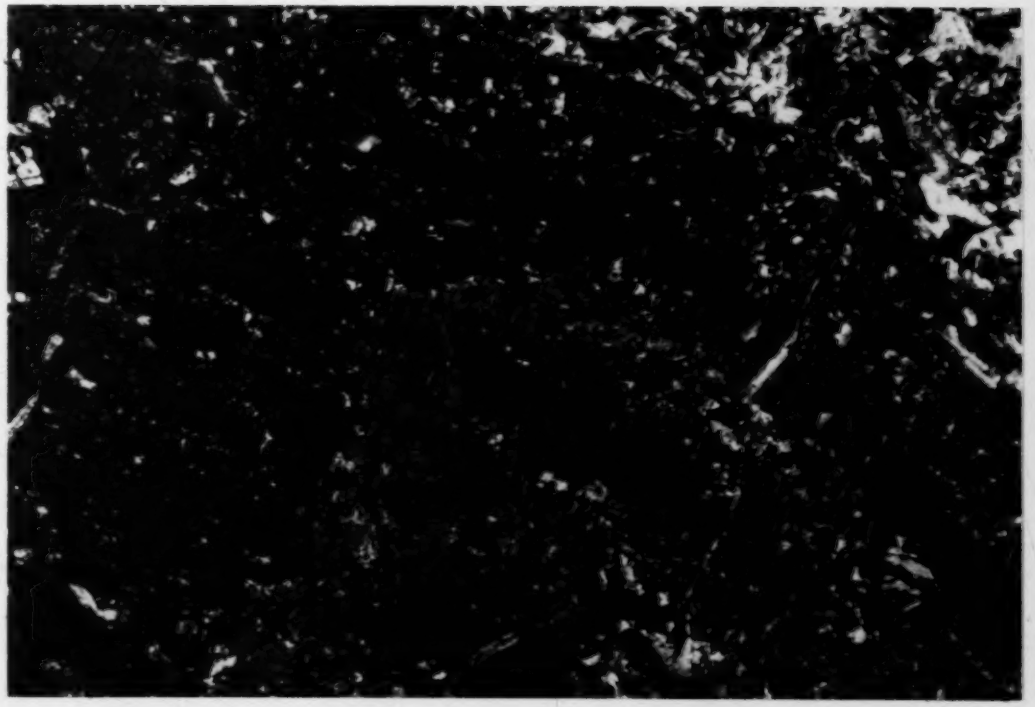

4B

coarser samples show a slight uralitization of the augite rims. A slightly higher volatile content, coupled with the possibility of slower cooling is inferred from this observation. Augite also occurs as very fine-grained blebs within the groundmass.

Olivine phenocrysts constitute 10% of these trachybasalts and forsterite contents are in the order of 85%. The olivines are crossed with irregular fractures filled with copius magnetite dust. As alteration and groundmass grain-size increase, yellow bowlingite forms and in the coarsest samples, on Cultus, up to 70% of the olivine can be altered to talc, magnetite and bowlingite. Alteration of the olivine inclusions within the augites is always more advanced.

Biotite crystals (10-20%) form as part of the groundmass. Their form is unique in that they occur as tiny equant flakes forming long, broken up, patchy stringers (Plate 3A). This suggests the occurrence of possible late magmatic resorption. The patchy stringers are best developed in the McGregor intrusion although the Cultus trachytes also show evidence for this.

Feldspars form the bulk of the groundmass and it is difficult in the finer-grained varieties to distinguish the plagioclases from the alkali feldspars. The minute plagioclase laths often form interlocking matts of crystals and pilotaxitic flow texture is common, the plagioclases wrapping themselves around the phenocrysts. The size variation of both the plagioclase laths and alkali feldspar grains can be quite marked, even within a particular thin section. Very tentative An determinations give values of around An_{30} (andesine).

The distribution of magnetite in the groundmass is also an important feature. It occurs sporadically throughout the groundmass of most of these porphyritic rocks. In one sample though, the finest-grained rock of the Cultus stock, it constitutes a far greater proportion of the groundmass, becoming a major component.

F. Leucocratic Syenite-granite Core of the Ymir Pluton

The central portion of the Ymir intrusion takes on a mineralogical character decidedly different from the main mass. The mafic content decreases from 50% in the rim to 20% in this core zone and extensive deuteric and hydrothermal alteration has permeated the entire core. Alkali feldspars are kaolinized, augites uralitized and olivine is 95 to 100% replaced by talc, bowlingite and magnetite. Total olivine and augite contents have dropped to less than 10%. Alkali feldspar has increased conspicuously to 60-70% of the rock.

Plagioclase amounts to approximately 5%. Optical determinations suggest a composition falling within the range for andesine although microprobe results infer a lower An content, probably oligoclase.

Biotite in this central zone is relatively undepleted and unaltered, still comprising 10-20%. Microprobe analysis indicates a relatively iron-rich biotite compared to the main mafic mass of this intrusion, with a titanium content approaching 7 percent.

Late fissure-filling dykes are obviously related to the core zone magma, showing an even more extreme mineralogy, being totally devoid of olivine. These rocks are full of large magnetite crystals and sphene, associated primarily with the biotites.

There is a very small area, centrally located in the core zone of the pluton, which exhibits the most highly differentiated composition. Abundant quartz (25%) is notable, considering the almost total absence of quartz in all other Coryell samples (Plate 2B). Comparatively large amounts (20%) of plagioclases with An_{45} are found. Olivine and augite are completely absent, although small amounts of chloritic alteration products can still be identified.

Biotite content remains essentially unchanged between the core zone and the main mass, indicating negligible fractionation of the biotite, even in the most extreme situations.

Saussuritization of the plagioclase approaches 80% in most grains and the kaolinized alkali feldspar is abundantly perthitic. This leucocratic, quartz-rich core zone proves the existence of strong low-pressure, shallow crystal fractionation

in these plutons.

G. Lamprophyres

Extremely coarse-grained lamprophyric dykes are found on the crest of the Mt. McGregor intrusion. They are composed of 3 main minerals: 45% diopsidic augite, 40% biotite and 10% alkali feldspar. Olivine is absent.

Grain sizes of the diopsidic clinopyroxenes reach up to 5 mm. The poikilitic texture so prominent in all the other samples of Coryell is absent, indicating a slower cooling rate. This mineral is pale green in hand specimen, unlike the darker amber brown colours of the augites found in other samples. Inclusions of biotite do occur within the pyroxene and alteration to a secondary amphibole is apparent.

Biotite crystals reach up to 1 cm in the thin section slab and laths reaching 2 cm have been measured in hand specimen. The phlogopitic biotite is strongly crenulated (Plate 5B).

Large anhedral alkali feldspars show almost no signs of alteration. Olivine is a standard mineral in all other rock types found on Mt. McGregor. Its total absence in these lamprophyres is an important observation, suggesting that olivine may never have been a liquidus phase in these late dykes.

Minor amounts of magnetite occur throughout the lamprophyres, though it is mainly in association with the biotite. Large apatite crystals appear liberally sprinkled through the orthoclases. Sphene can be easily identified throughout the sample as it forms relatively large crystals.

The mineralogy of these lamprophyres suggests a primitive origin.

H. Pyroxene Cumulates

The last important rock type that should be mentioned is the pyroxene-rich cumulate which is found in pods both at the Jersey pluton and the Rossland Railway cut. These rocks have been called shonkinites (Plate 5A).

The peculiar habit of the shonkinites is immediately noticable. The cumulates consist almost entirely of fine-grained, mostly euhedral crystals of

Plate 5A

Cumulate shonkinite - Jersey pluton

Photomicrograph. Idiomorphic clinopyroxene crystals (75%) containing abundant irregular masses of biotite. Groundmass is alkali feldspar (10-15%). Note large size variation of the euhedral clinopyroxenes.
Second generation biotite crystals formed after the clinopyroxene was accumulated.
Crossed polars. Magnification = 50x.

Plate 5B

Biotite - Augite lamprophyre - Mt. McGregor

Photomicrograph. Showing clear, highly crenulated biotite crystals (42%). Slightly altered but inclusion-free clinopyroxene crystals (45%) surround it. 10% alkali feldspar surrounds the euhedral biotite and clinopyroxene. Sphene and apatite form abundant accessory minerals.
Crossed polars. Magnification = 50x.

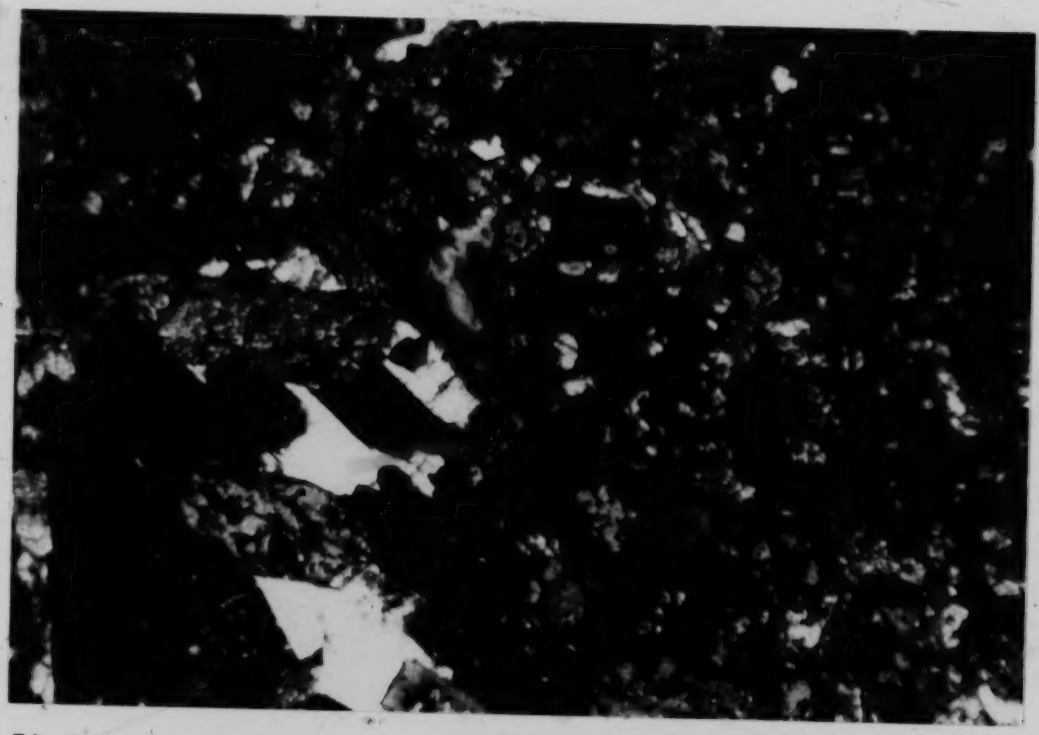

5A

5B

augite, packed together into a solid mass.

Large euhedral biotite phenocrysts appear to have grown around the clinopyroxenes, representing 2nd stage, late biotite.

A very large amount of biotite is included within the clinopyroxenes, not as euhedral crystals but more as irregular blebs. Many augite crystals form perfectly euhedral hexagonal crystals. There is essentially no magnetite in these cumulates, only a small amount associated with the biotites. Crystal sizes vary quite abruptly, reinforcing the theory that they are indeed cumulates.

Caution must be exercised when interpreting these mafic rocks, so as not to misinterpret them as being parental-type magmas.

I. Miscellaneous Rock Types

Aplite dykes cut the Rossland Highway cut and Cultus stock. Their genetic relationship to the Coryell intrusions is questionable and it is not known whether they are related to the same event.

Abundant evidence of xenoliths occurs in both the Cultus and McGregor intrusions. Indirect evidence of country rock involvement is suggested by the presence of abundant calcite in the Jersey pluton. These factors must be considered when interpreting the genesis and geochemistry of these small intrusions.

Worth noting is the singular appearance of hypersthene (low Ca-pyroxene) in one sample on Mt. McGregor (Plate 1B). It is apparently in a "reaction relationship" with the olivine, a feature supposedly uncharacteristic of alkaline rocks.

V. GEOCHEMISTRY

A. Introduction

Method

Whole rock major, minor and trace element analyses were performed on 74 selected samples. Major and minor elements, as well as Rb, Sr, Ba, Y, Zr and Nb were determined via X-ray fluorescence at McMaster University in Hamilton. In an effort to indicate the precision of the XRF analyses, a duplicate sample was sent with the initial batch of analyses. Table 1 shows the average deviation for each element. Samples were also sent to McMaster for uranium and thorium analyses using neutron activation. Trace metal determinations of Ni, Cu, Co, Cr, Mo, Pb, Zn, Hg and As were done by Chemex Labs in Vancouver using atomic absorption spectrophotometry. Results are presented in Appendix I.

Normative mineral calculations (Appendix II) are provided for the 6 plutons studied. The normative calculations were performed using a CIPW norm computer program with modifications based on suggestions by Irvine and Baragar (1971). On the basis of 10 ferrous iron determinations, performed at the University of Alberta, the least oxidized samples contained approximately 20-25% ferric iron. This ratio was implemented for the norm calculation.

Microprobe data obtained from 3 sections was used to augment the existing geochemical analyses (Appendix IV).

Classification

Various classification systems based on geochemistry have been proposed for igneous rocks.

Traditional Classification Schemes

A brief review of some of the older classification schemes is given here with reference to the Coryell plutons. The Coryell intrusives (average SiO_2 = 52%) fall on the borderline between what are commonly considered intermediate and basic rocks They are mineralogically undersaturated,

TABLE 1

Precision Estimates of McMaster XRF Data

SiO2	51.9	52.1	0.1 %
Al2O3	11.8	11.7	0.05 %
Fe2O3	8.35	8.12	0.115 %
MgO	11.36	11.62	0.13 %
CaO	7.86	7.80	0.03 %
Na2O	2.02	1.90	0.06 %
K2O	5.06	5.13	0.035 %
TiO2	0.71	0.73	0.01 %
MnO	0.14	0.13	0.005 %
P2O5	0.80	0.80	0.0 %
Rb	177	175	1 ppm
Sr	851	848	1.5 ppm
Y	26	23	1.5 ppm
Zr	181	184	1.5 ppm
Nb	10	13	1.5 ppm
Ba	1765	1840	37.5 ppm

containing magnesian olivine and augite but no quartz.

The more recent inclination is to identify each series by its trend on the AFM diagram (Nockolds and Allen, 1953). Plots of various tholeiitic, alkaline and calc-alkaline suites by Irvine and Baragar (1971) show, however, that there is sometimes considerable overlap between series. Alkaline and calc-alkaline suites generally show less iron enrichment than tholeiites (Figure 11). The Coryell intrusions follow a relatively flat curve on the AFM diagram.

Other classification schemes of lesser importance include agpaitic coefficients, colour indices, Peacock's (1931) concept of calc-alkalinity, and simple comparison with average chemical compositions of other rocks.

Ussing (1912) introduced the term agpaitic to describe nepheline syenites of the Ilimaussaq Intrusion. The agpaitic coefficient is defined as $(Na_2O + K_2O)/Al_2O_3$. All Coryell rocks have values considerably below 1 and are therefore classed as miaskitic. The colour index of these rocks is between 30 and 60, placing them in the mesocratic range. Calc-alkali and other rock types have been distinguished from alkaline rocks using Peacock's (1931) scheme whereby CaO is plotted with the alkalies versus silica. Based on this usage, the Coryell rocks plot into the "alkali-calcic" field. A simple comparison with the average chemical compositions of igneous rocks (Nockolds, 1954), places the Coryell plutons within the nepheline normative augite-biotite-olivine shonkinite through augite-biotite monzonite range.

Present Classification Schemes

The chemical classification system used for volcanic rocks can be utilized for plutonic rocks, as it facilitates a ready comparison with other rock suites discussed in the literature. Although the majority of Coryell rock types are clearly coarse-grained plutonics, the occurrence of very finegrained phases in the eastern plutons and their chemical similarity to adjoining coarse-grained phases, attests to their hypabyssal nature. In situ differentiation of these small intrusions was probably minimal therefore a

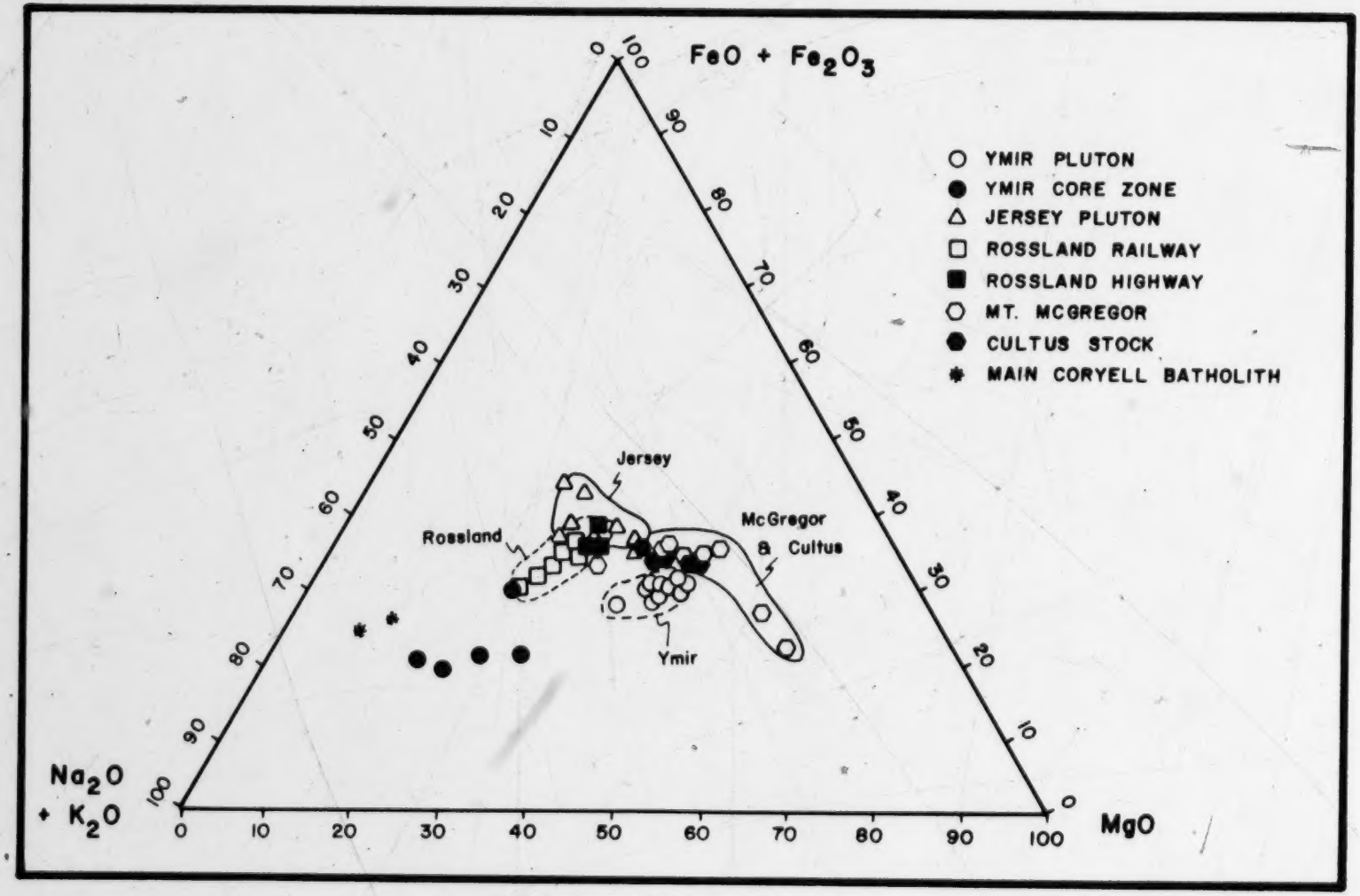

FIGURE 11. AFM diagram

comparison with similar volcanic suites can be useful in tracing out their petrogenetic histories.

A consideration of the SiO_2 versus $Na_2O + K_2O$ diagram (as compiled in Cox *et al.*, 1979) shows that the Coryell plutons plot principally into 2 main groups; the potassic equivalents of the hawaiites and mugearites, namely the trachybasalts and alkali basalts (Figure 12). A dividing line between alkalic and tholeiitic (or sub-alkaline) series has been plotted on the alkali versus silica diagram by Macdonald (1968). The Coryell suite falls completely within the alkali basalt division.

Perhaps the most useful application of the norms is in the determination of the degree of saturation of these rocks. 75% of all samples collected are nepheline normative, 20% are hypersthene normative and 5% (representing leucocratic dykes and core zones) show quartz in the norm. The concept of saturation forms the basis of many chemical classification schemes in the literature. Most alkali olivine basalts are nepheline normative, whereas tholeiitic and calc-alkalic series show normative orthopyroxene and sometimes quartz.

Irvine and Baragar (1971), after a very thorough analysis and consideration of the various proposed classification schemes, have utilized CIPW norms and pertinent geochemical parameters to produce one of the most useful chemical classification systems. Based on this system, the Coryell suite is clearly a derivative of the alkali olivine basalt series (as distinct from the tholeiitic or calc-alkaline series). Further subdivision places the entire series of Coryell intrusions into the potassic category of the alkali olivine basalts. Most Coryell rocks are classed as trachybasalts and alkali basalts although rare ankaramites and tristanites occur as well. This is in agreement with the first approximation provided by a consideration of the alkali versus silica diagram. A few late-stage, low-pressure differentiates have fallen into the tholeiitic and calc-alkaline classifications.

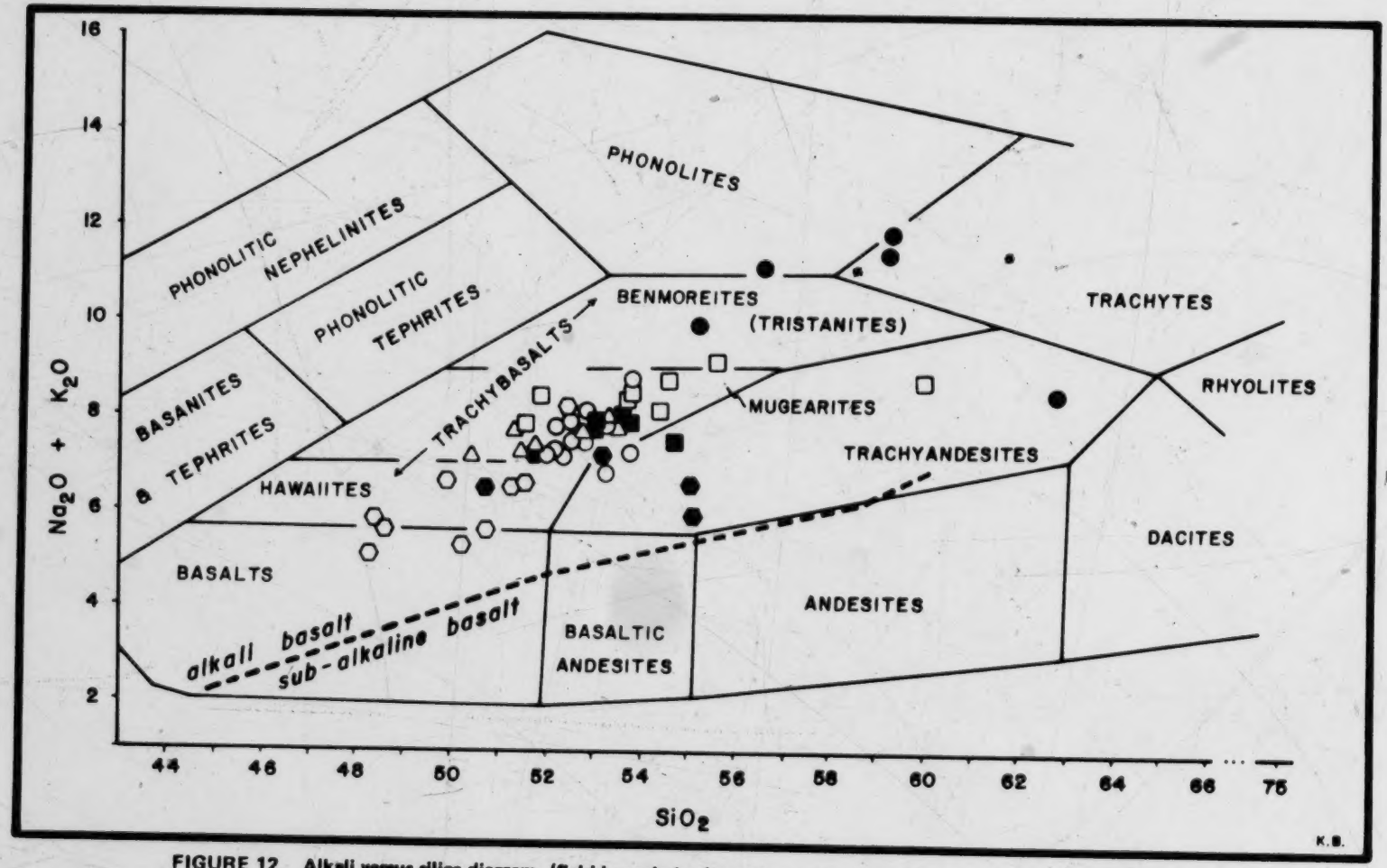

FIGURE 12. Alkali versus silica diagram. (field boundaries from Cox et al., 1979; alkali line by Macdonald (1968). See FIGURE 11 for legend.

B. Major Element Geochemistry

Mean major element values for each intrusion are presented in Table 2. Variation diagrams have been plotted for all the major elements (Figures 13–18). Owing to the strong fractionation of magnesium in the suite of Coryell rocks, it has been preferentially utilized as the abscissa on all plots.

Using geochemical, petrographic and geographic parameters, the satellitic Coryell plutons can be divided into 2 distinct clusters. The first group, hereafter referred to as Group I, consists of the 3 westernmost intrusions: Jersey, Rossland Highway and Rossland Railway. These 3 stocks are closest geographically to the main batholith. Chemically, they are depleted in magnesium and enriched in aluminum and sodium. This is reflected in their relatively olivine–poor, more plagioclase–rich mineralogy. The second group (Group II) includes the Mt. McGregor, Cultus and Ymir stocks. These far eastern intrusions are distinctly more mafic in nature and have been intruded into higher crustal levels. Mt. McGregor and Cultus are probably remnants of very shallow volcanic necks.

All major characteristics of the plutons are shown on the MgO versus Al_2O_3 plot (Figure 13). The straight–line differentiation trend is clearly demonstrated and the distinction between Group I and Group II plutons is marked. A point worthy of considering on the MgO–Al_2O_3 diagram is the location of two lamprophyric dykes with MgO values of 16.2 and 17.9%. They occupy a position representing the least amount of differentiation in almost all the variation diagrams and could possibly approximate the parental magma for these plutons. One rock sample, the Jersey shonkinite, also falls at the beginning of the differentiation trend, but microscopic examination suggests that it is totally cumulate in nature.

Another major feature to note is the strong cluster of points in the top left corner of the MgO–Al_2O_3 plot, representing the end of the differentiation sequence. These are the samples taken from the core zone of the central Ymir pluton. This core zone has been interpreted as consisting of extremely late–stage, highly fractionated portions of the Ymir pluton. It is interesting to

TABLE 2

Median Major and Minor Element Values for Each Pluton

ELEMENT	RANGE	ROSSLAND	JERSEY	YMIR	CULTUS & MCGREGOR
Al2O3	(9.1-17.8)	14.5	15.5	12.0	13.0
K2O	(3.3-8.32)	4.7	4.4	5.0	4.6
CAO	(2.85-11.43)	6.9	8.7	7.9	8.3
NA2O	(0.76-4.38)	3.3	3.0	2.1	1.9
MGO	(3.39-17.85)	6.7	7.0	10.5	10.0
SIO2	(48.6-62.9)	54.0	52.0	52.5	51.0
FE2O3	(3.17-9.46)	7.5	8.0	7.7	8.3
TIO2	(0.50-1.32)	0.8	1.2	0.7	0.75
P2O5	(0.24-1.26)	0.63	0.90	0.75	0.76
		GROUP I		GROUP II	

NOTE : ranges given do not include the main batholith, cross-cutting dykes or the Jersey cumulate.

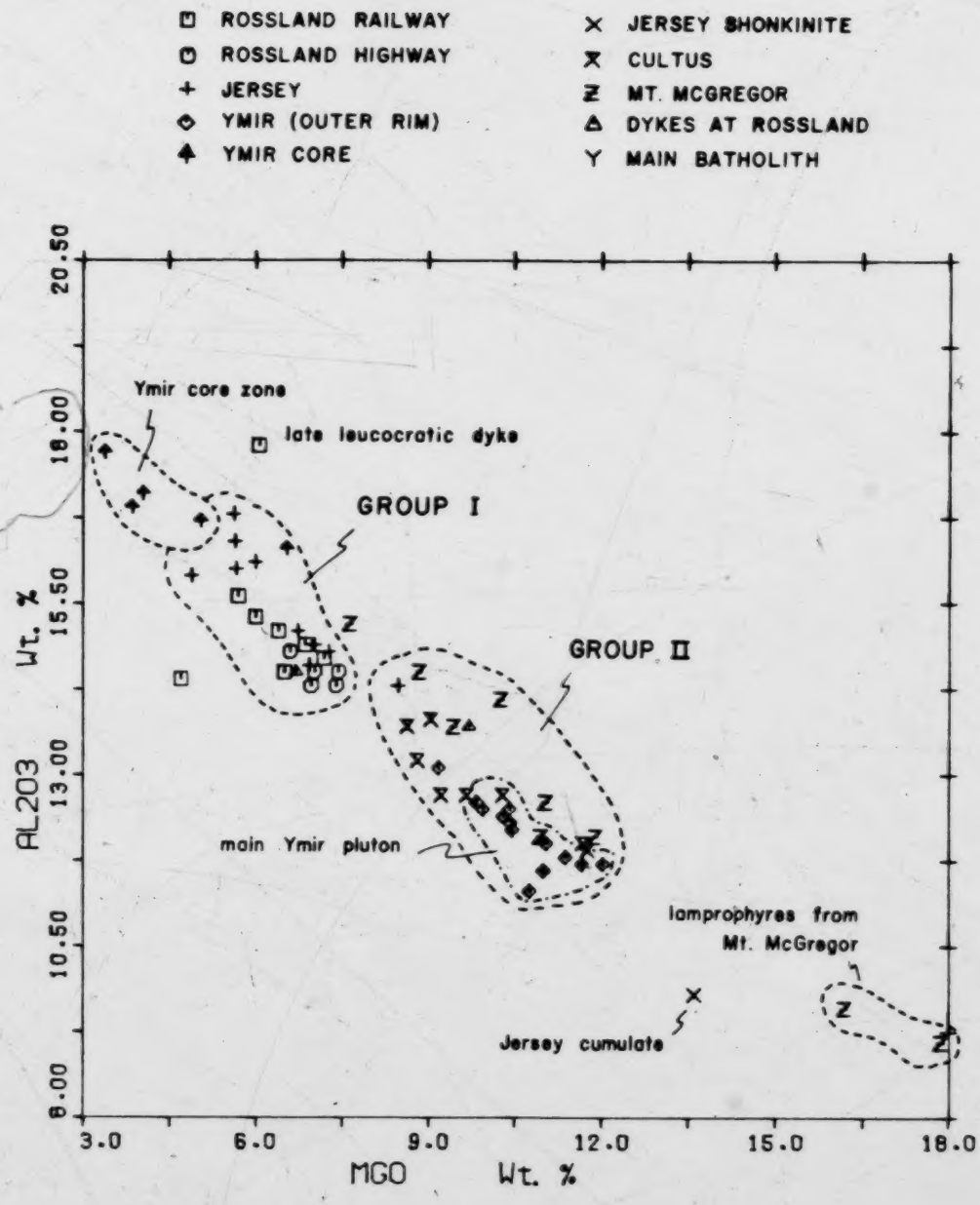

FIGURE 13. MgO versus Al_2O_3 plot

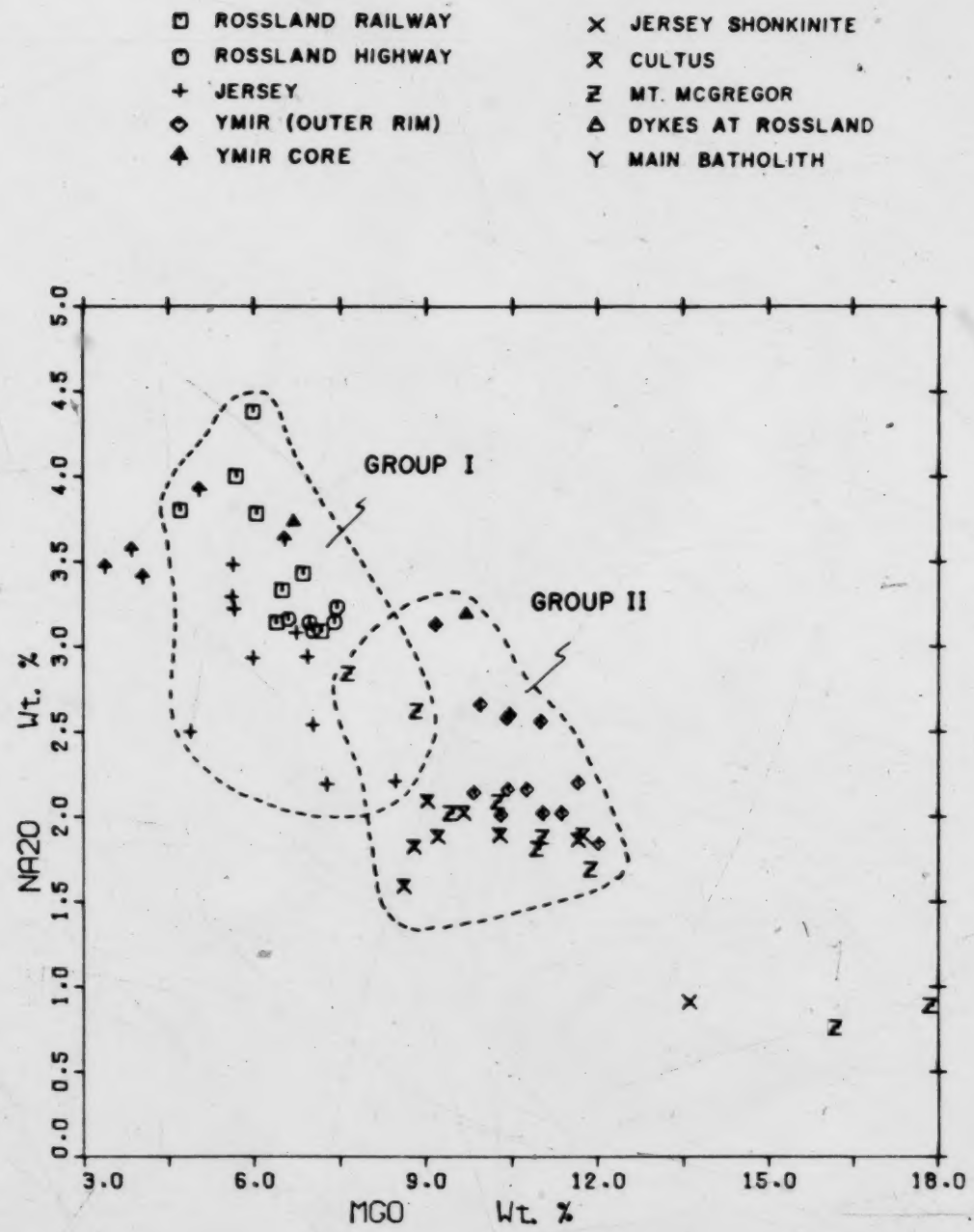

FIGURE 14. MgO versus Na_2O plot.

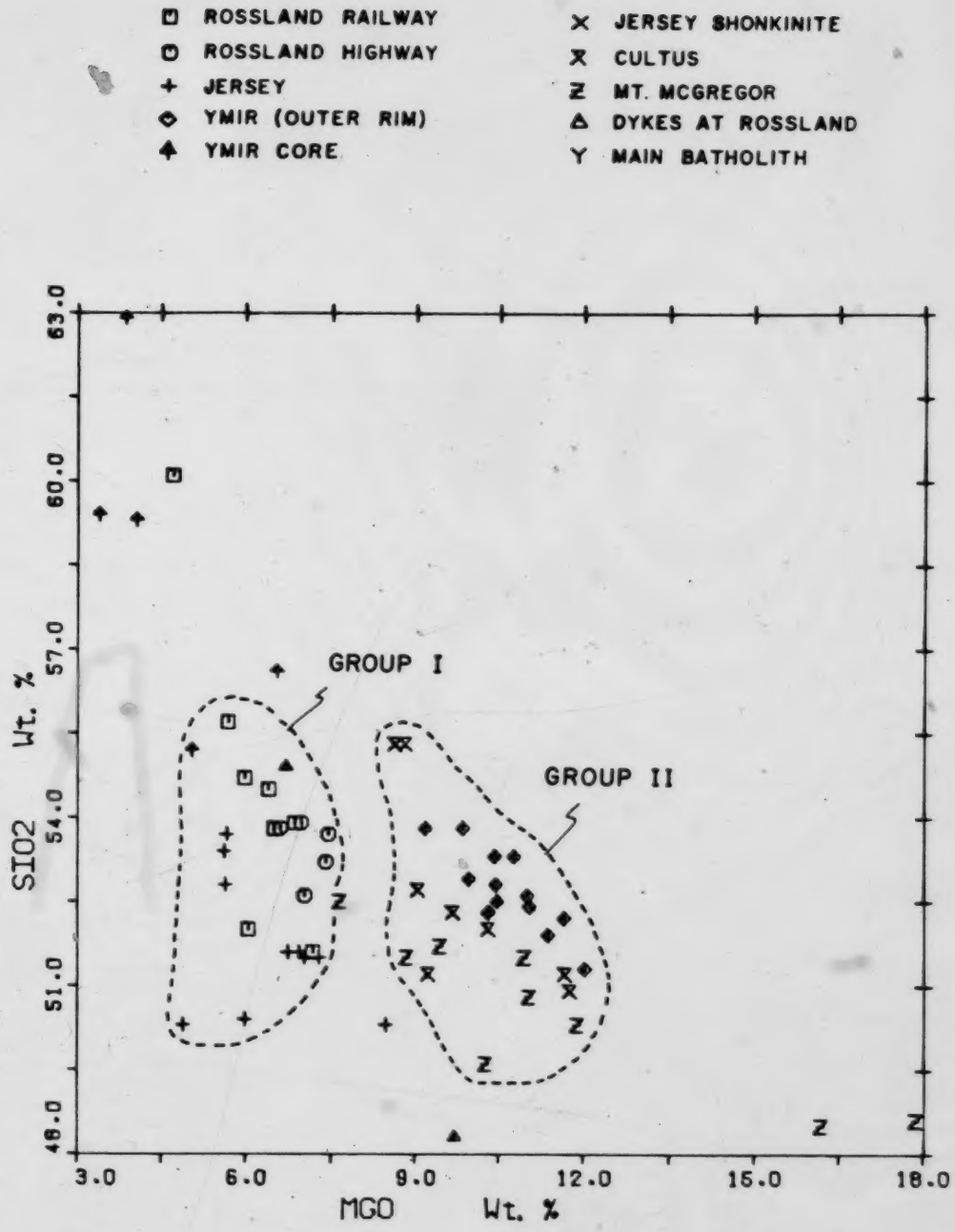

FIGURE 15. MgO versus SiO_2 plot.

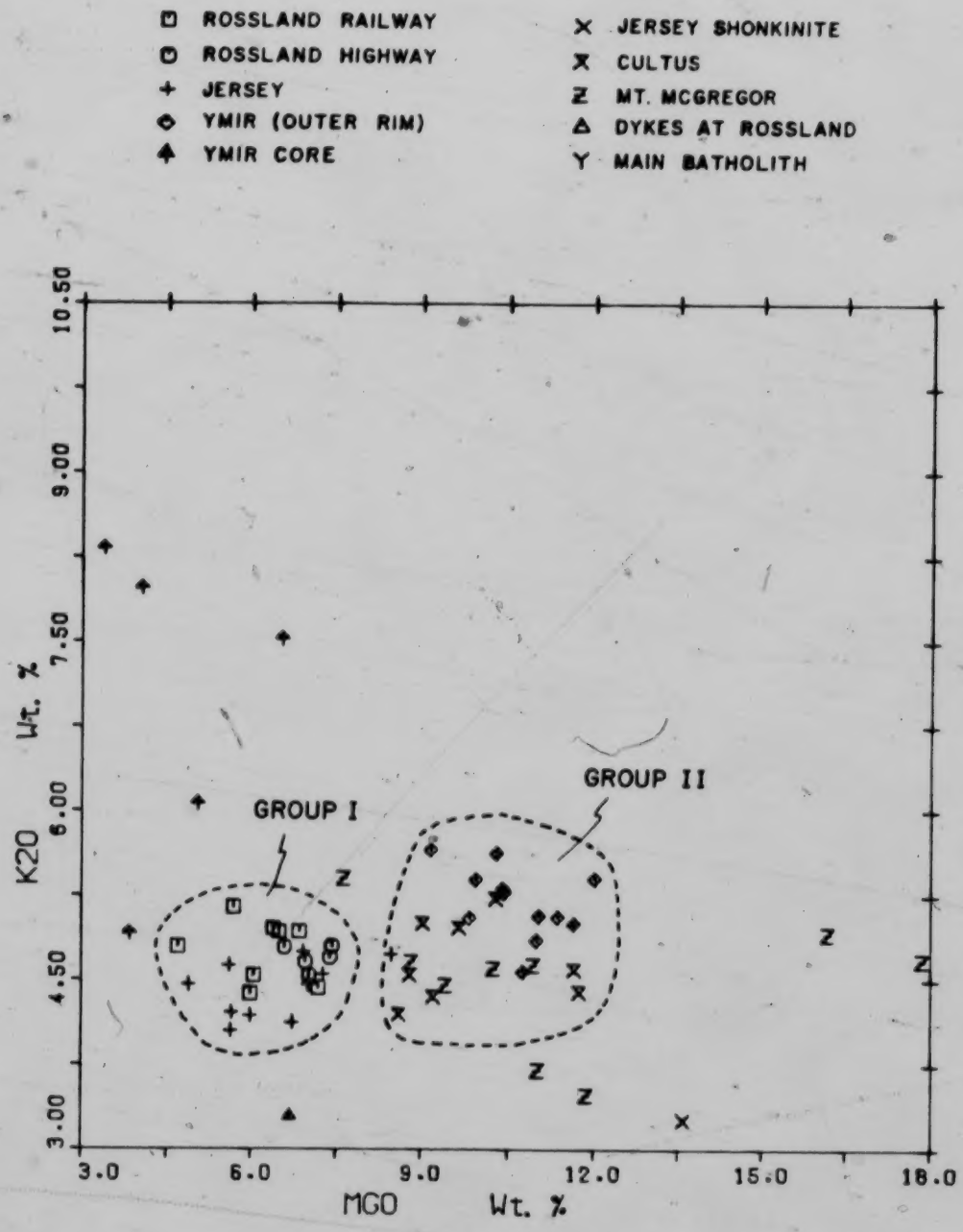

FIGURE 16. MgO versus K_2O plot.

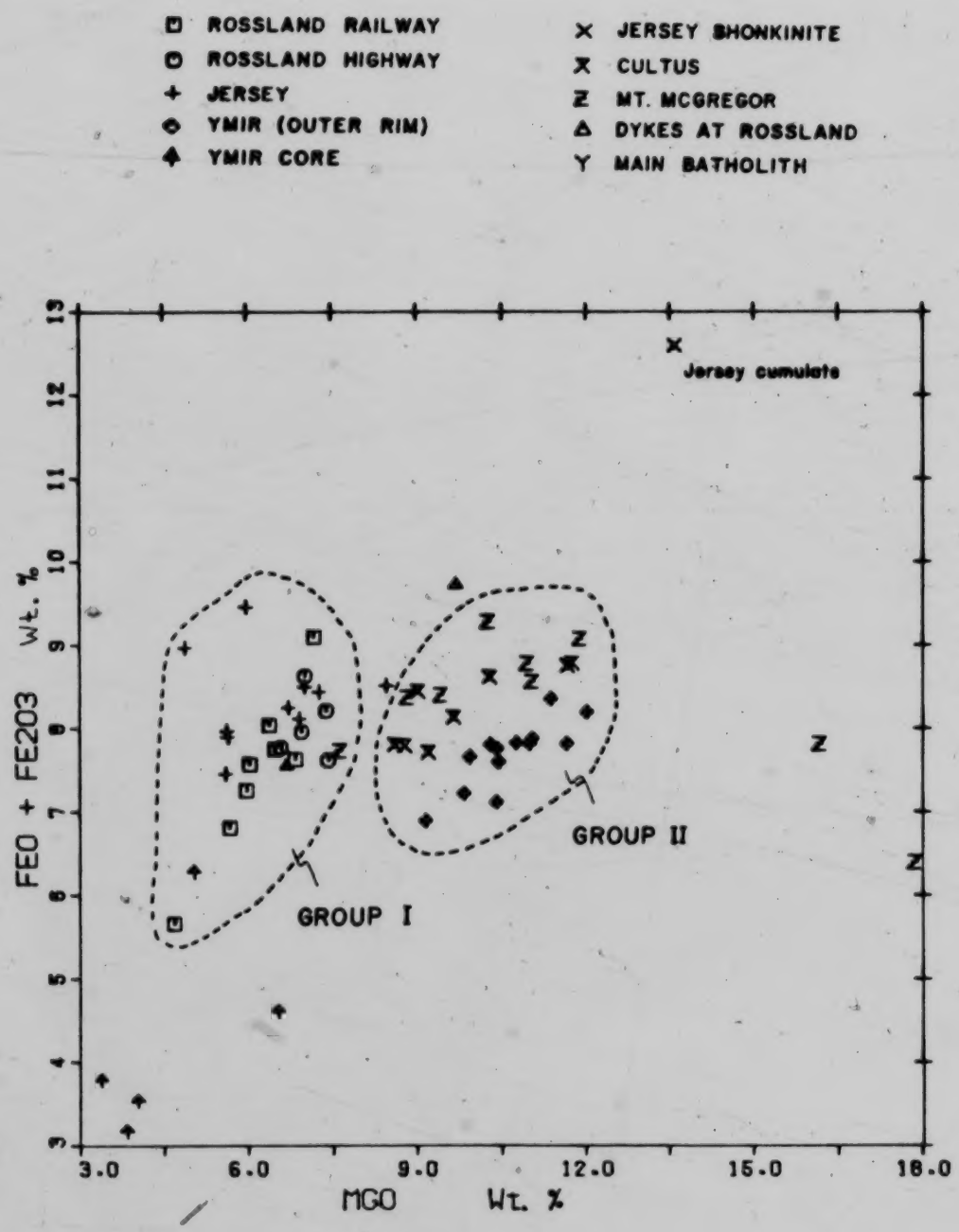

FIGURE 17. Fe_2O_3 versus MgO plot.

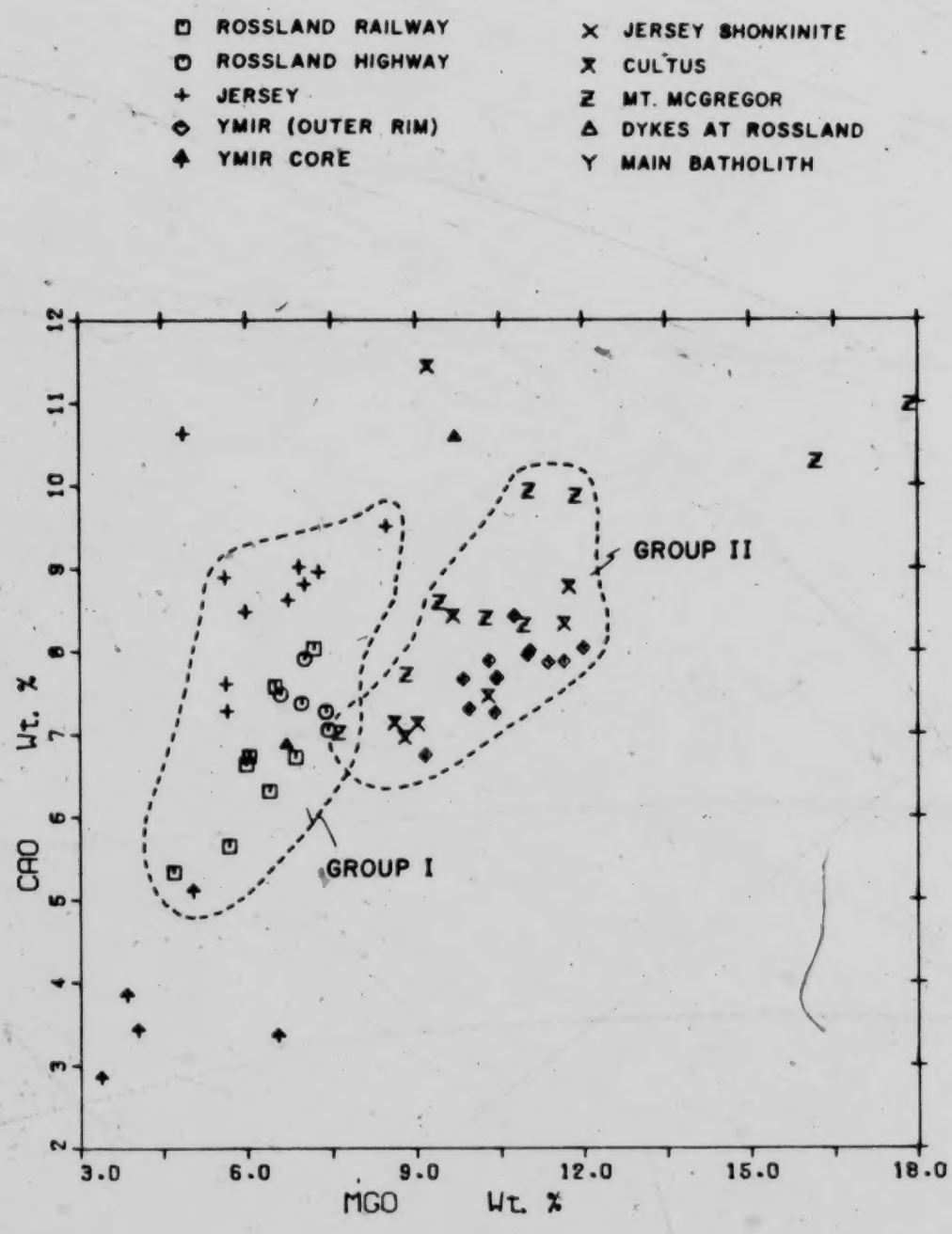

FIGURE 18. CaO versus MgO plot.

note that no continuum exists between the main pluton and this tiny core zone. This can be attributed to the operation of two different fractionation processes. The MgO depletion in the main bulk of the stock is caused by the in situ, slow settling of olivine crystals along with some clinopyroxene whereas the Ymir core zone represents a final alkali-rich, highly volatile siliceous residuum being suddenly squeezed from the intercrystalline spaces of the lower main mass. It is injected rapidly upwards carrying virtually no mafic minerals, essentially a filter-pressing effect. No continuous compositional spectrum can be expected under these conditions. The Ymir core zone shows significant SiO_2 enrichment, CaO depletion, extreme K_2O enrichment and extreme Fe_2O_3 depletion, as expected in a normal differentiation sequence.

Another sample falling off the trend is the tiny late-stage leucocratic dyke rock collected from the Rossland Railway cut. This material was injected into a fissure formed at the very edge of the intrusion.

A consideration of elemental ratios shows significant differences between the two groups of plutons. K_2O/Na_2O ratios increase progressively eastward from 1-2 for Group I to 2-3 for Group II (Figure 19). The two lamprophyric dykes on Mt. McGregor have K_2O/Na_2O ratios greater than 3. This trend is opposite to the expected trend if one considers that a higher degree of magmatic evolution usually increases K_2O/Na_2O ratios, not the opposite, as we see here. The K_2O values remain essentially constant for the entire suite and only Na_2O changes significantly, being depleted in the Group II (eastern) plutons. The major phase controlling sodium distribution is plagioclase, which is volumetrically lower in Group II and completely absent in the lamprophyres.

AFM, CNK and Differentiation Index

Based on a consideration of the other major and trace elements, the Coryell suite of rocks has a common genesis and the AFM plot clearly shows the hierarchy present (Figure 11). Inferred parental compositions are located at the mafic end of the curve (Nockolds, *et al.*, 1953). The eastern, Group II plutons appear to be the most primitive and the western, Group I intrusions, closest to the main batholith, are more highly evolved.

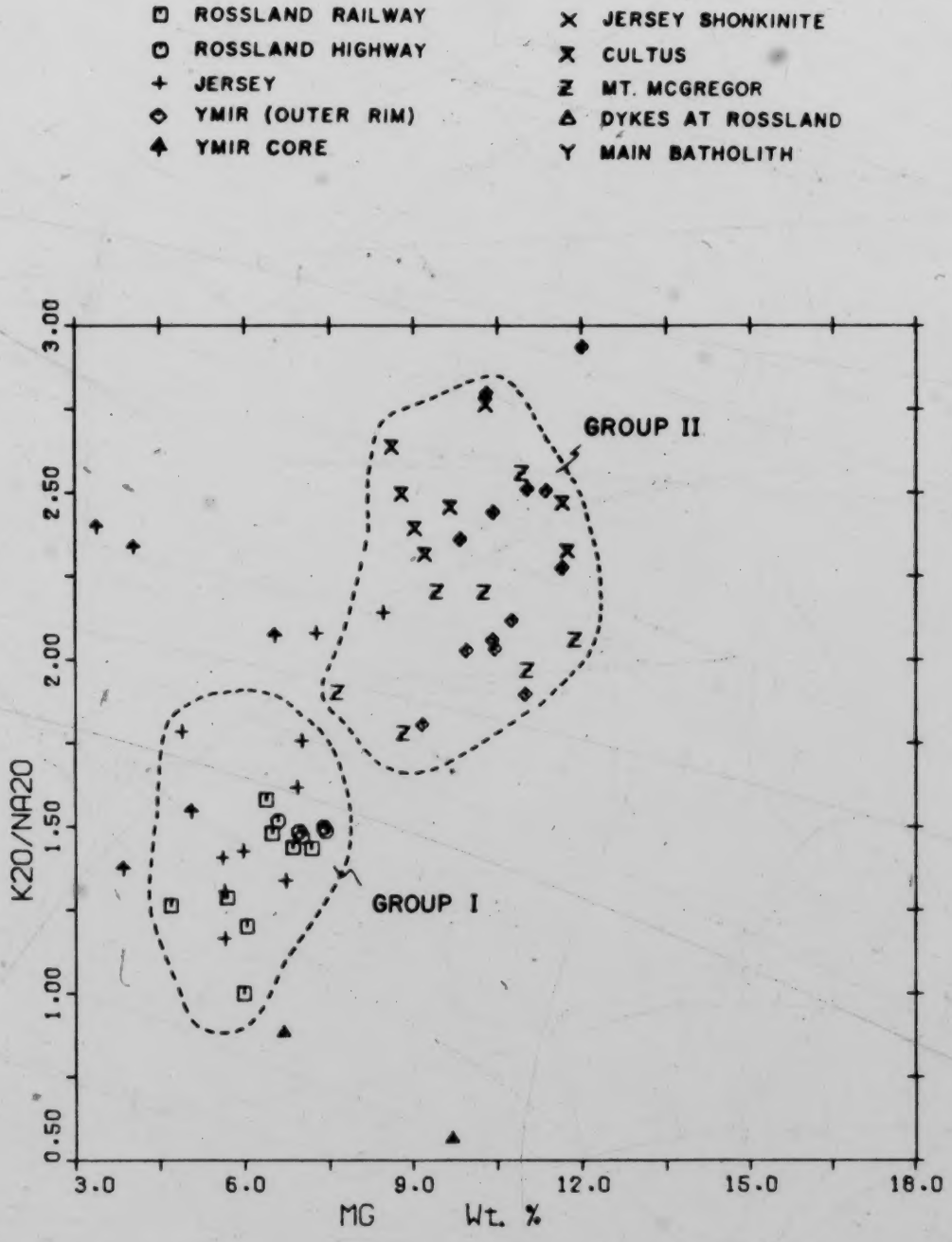

FIGURE 19. MgO versus K_2O/Na_2O plot.

Extreme evolution is shown in the main batholith samples and those from the Ymir core. The flatness of the AFM, especially the low values for the Ymir pluton, may reflect early formation and fractionation of the biotite which has been caught up inside the pyroxenes, hence depressing iron enrichment.

The CNK plot (Figure 20) also shows the Ymir pluton falling off the main upwards trend into an area of relative potassium enrichment. Although the Ymir pluton has relatively lower sodium and iron, examination of the absolute elemental abundances does not show a very substantial lowering of either iron or sodium in the pluton.

The plot showing the differentiation index (Larsen Factor) versus geographic distance from the main pluton clearly shows that the degree of evolution increases towards the main pluton (Figure 21).

C. Trace Element Geochemistry

Trace elements, especially those which are strongly partitioned between the crystal and liquid phases are much more sensitive indicators of crystal fractionation than most of the major elements, which vary over relatively limited ranges. The so-called "residual elements" (or incompatible elements) possess constant ratios with one another that mirror their source composition. Their absolute abundances are a function of the degree of partial melting but their ratios will not be significantly changed. Likewise, fractional crystallization will increase their concentration in the residual melt but, it will not change their ratio until their concentration becomes high enough that they partition into a late-stage crystalline phase or form minerals of their own.

An attempt to quantify the behaviour of these elements has been attempted by various authors (Gast, 1968; Barberi, *et al.*, 1975). Partitioning is strongly dependant on composition and temperature, and the present knowledge of partition coefficients is too limited to justify the implementation of complex models. Nevertheless, many qualitative observations can be made.

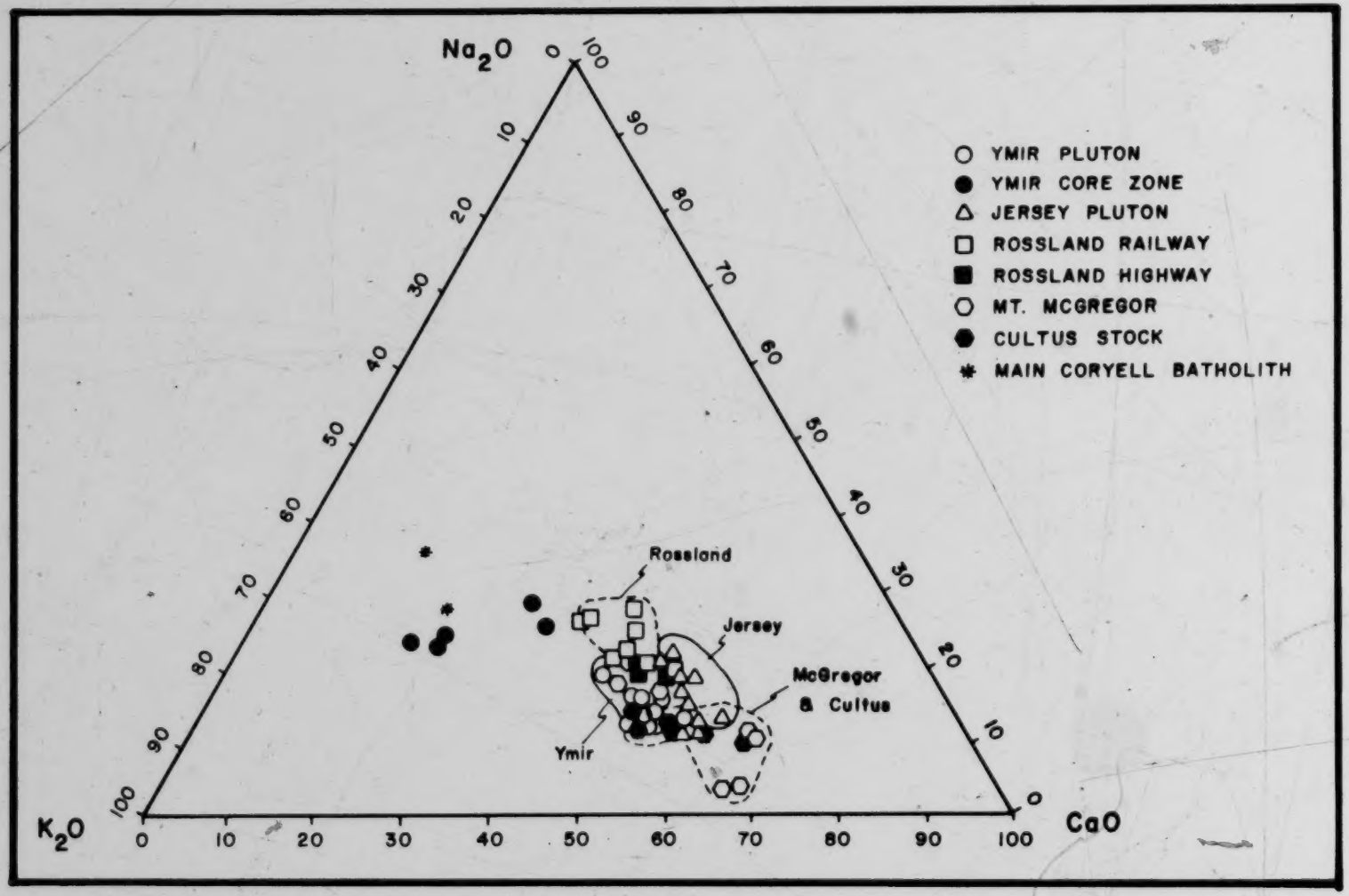

FIGURE 20. CNK diagram

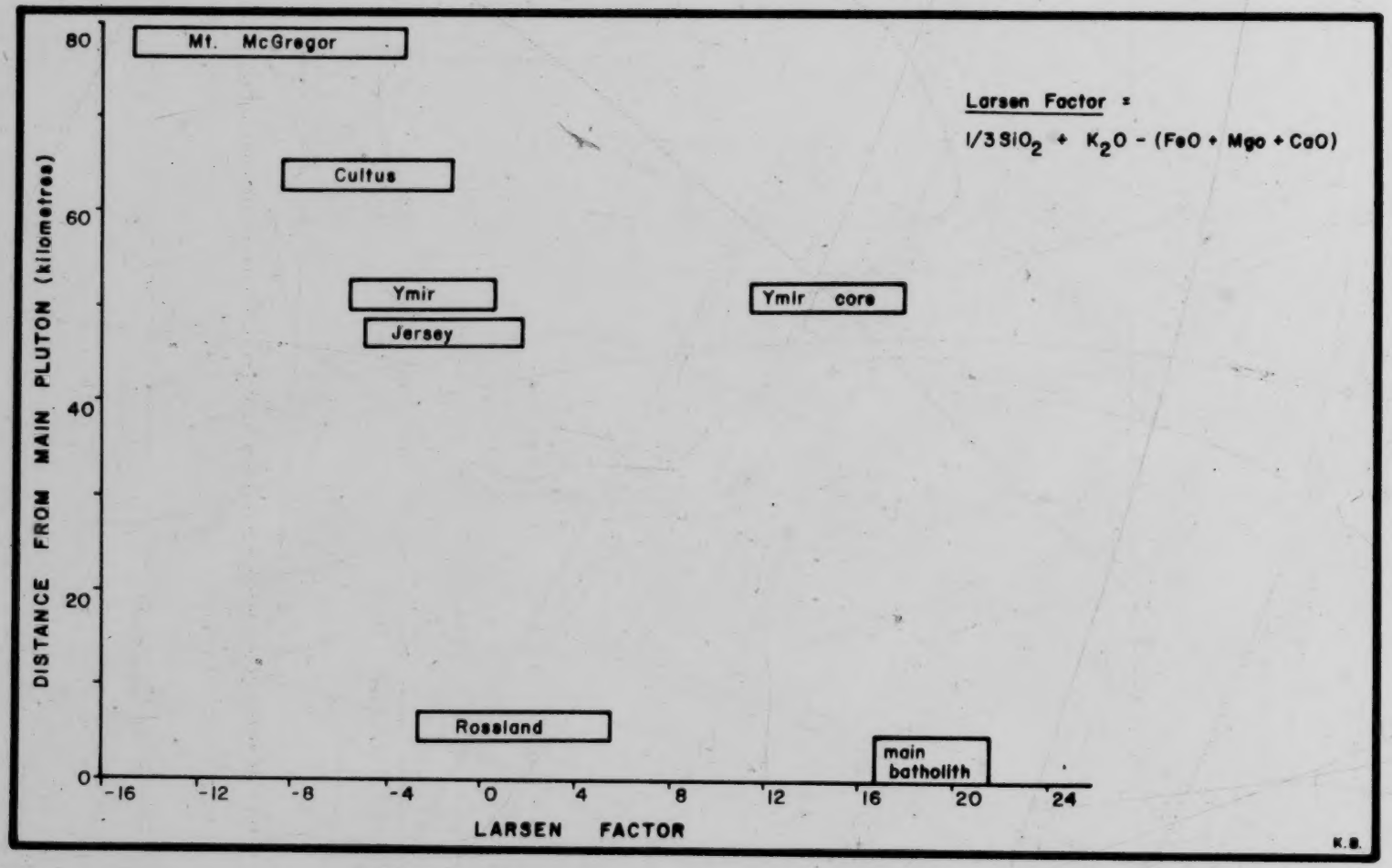

FIGURE 21. Distance versus differentiation index (Larsen Factor)

Residual Alkali Elements

A consideration of the incompatible alkali metals and alkali earths, Ba, Sr and Rb, confirms that they are all positively enriched in these alkaline Coryell intrusions.

Barium, strontium and rubidium

Barium, strontium and rubidium are by far the most anomalously enriched elements. Compared with the compilation of average abundances by Turekian and Wedepohl (1961), the strontium contents are enriched 6 times over normal syenites and 2.5 times over basaltic rocks (median = 1200). Barium is enriched 1.5 times over syenites and 8 times over basalts (median is approximately 2300). Rubidium is enriched 5 times over basaltic rocks and 1.5 times over syenites (median values = 160 ppm). These elevated concentrations are typical for alkaline magmas (Weaver *et al.*, 1962; Nash and Wilkinson, 1971; Le Maitre, 1962). 3 Ma alkali olivine basalts intruded into the Sierra Nevada batholith (Van Kooten, 1980) show a parallel enrichment of Ba and Sr, similar to the Coryell intrusions. Van Kooten hypothesizes the probability of alkali metasomatism by a K, Ba, Sr and Rb enriched fluid at depth which forms a phlogopite. Decomposition of the phlogopite en route to the surface will release these incompatible elements into the melt.

Barium and strontium, in the Coryell series, are extremely coherent, following one another throughout the entire crystallization sequence. Average Ba/Sr is 2.5, defining an approximate straight line trend (Figure 22). A dividing line can be distinguished on the barium-strontium plot separating the Group I from Group II plutons. Group I plutons are enriched in Ba and Sr relative to Group II.

Owing to its higher charge, barium is strongly partitioned into potassium minerals. From microprobe analyses, the barium is most highly concentrated in the alkali feldspars (up to 1.43%) but significant amounts are also contained within the biotites (up to 0.93%).

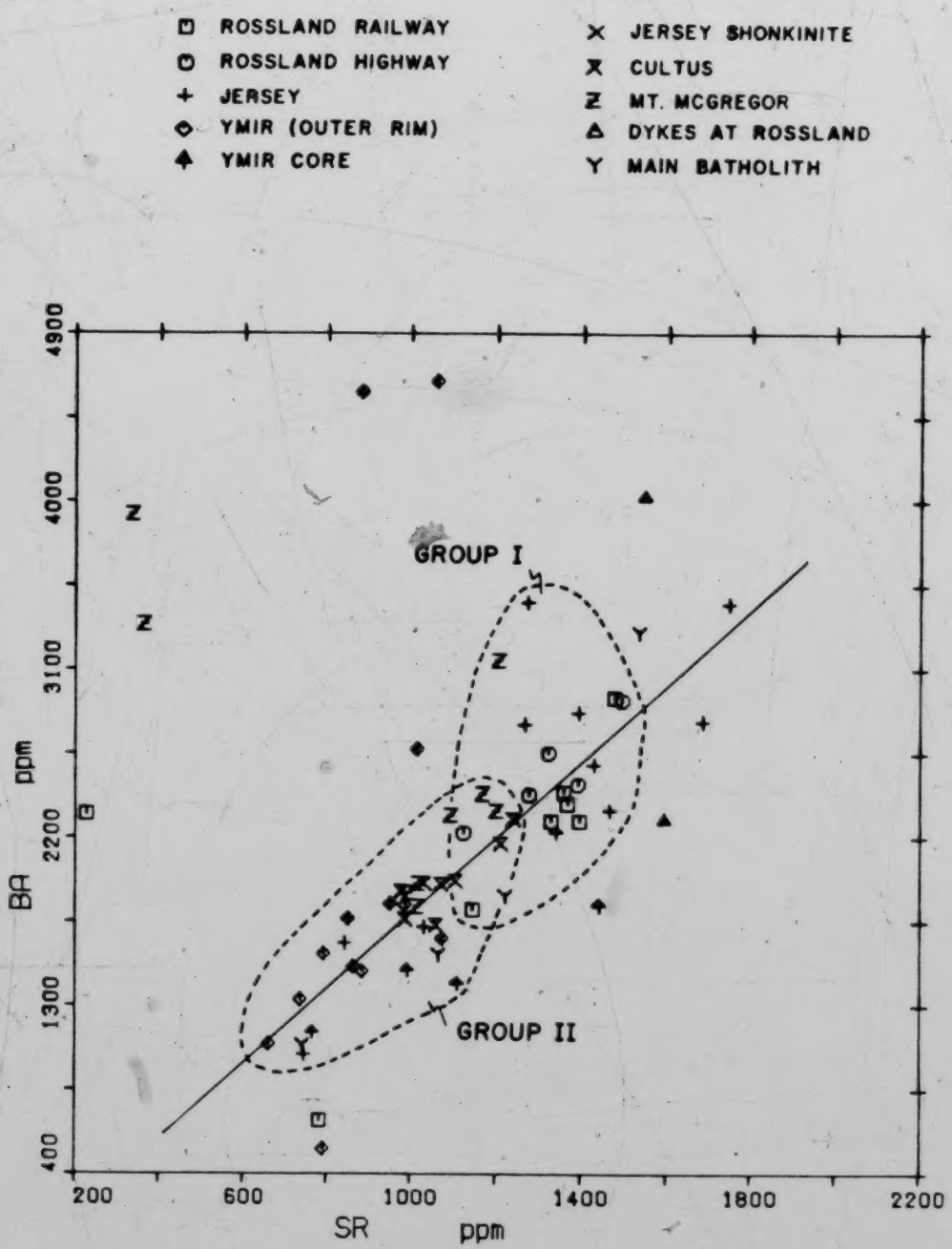

FIGURE 22. Sr versus Ba plot

Strontium will substitute first into Ca^{2+} positions in plagioclases and then into K^{+} positions in alkali feldspars due to its similar ionic radius (Barberi *et al.*, 1975). XRF analyses done for Sr on mineral separates prepared for the $^{87}Sr/^{86}Sr$ isochron of the Ymir pluton show that the strontium is concentrated in the alkali feldspars (ranges 1032-1810 ppm) with a moderate increase in the plagioclases. Apatites contain about 600 ppm Sr and the pyroxenes carry approximately 200 ppm. Barium and strontium contents do not show any change between the rim and the differentiated core zone of the Ymir pluton. It is interesting to note that late cross-cutting dykes at Cultus and Rossland Highway have extremely low Ba and Sr values. This suggests either that Ba and Sr were so completely partitioned into the alkali feldspars, leaving minute amounts for the remaining fractions, or that these dykes are totally unrelated to the Coryell event.

Plagioclase or alkali feldspar fractionation, a feature typical for pantellerites (Ferrara and Treuil, 1974), is not postulated for these rocks, owing to their anomalously high Ba and Sr contents.

An additional factor concerning the barium and strontium should be noted; the Jersey pluton shows a comparatively large degree of scatter of barium and strontium concentrations, to an extent not observed in other elements. Mobility of these elements is well documented (Pearce *et al.*, 1975; Goff, 1983) and the surprising spread in the Jersey rocks may imply the effect of late stage contamination or metasomatism in the Jersey pluton.

XRF work for the Ymir pluton on mineral separates indicates that rubidium is concentrated mainly within the alkali feldspars (590 ppm) with a marked decrease in the plagioclases (180 ppm). Biotite contains approximately 300 ppm Rb. Due to the single charge of rubidium, it will not substitute as easily as strontium into potassium sites in the feldspars (Ferrara and Treuil, 1975).

Although rubidium shows a marked coherence with potassium due to its similar size and chemical character (Taylor, 1965), K-Rb ratios tend to decrease as the degree of magmatic evolution increases (Shaw, 1968). Zone-refining processes, contamination, volatile transport, biotite accumulation, removal of hornblende and post-magmatic, late hydrothermal processes can all contribute towards a decrease in the K/Rb. Gast (1968) notes that alkali basalts tend to have a lower K/Rb value (250-900) than tholeiitic (abyssal) basalts (500-1900). The K/Rb for the Coryell suite continues to emphasize the division between the Group I and Group II plutons (See Figure 28) . McGregor, Cultus and Ymir (Group II) have the lowest K/Rb, falling mainly above the K/Rb = 275 line whereas Rossland (Group I) falls below. This lower K/Rb for the Group II plutons could be due to volatile loss. The Jersey pluton exhibits a high scatter of ratios which may be the result of local post-magmatic alteration, partly linked to the close proximity of the Jersey ore body.

Rb/Sr ratios are useful as a general indicator of the degree of magmatic differentiation (Faure, 1977). They tend to increase gradually with continued crystallization. Sr will concentrate in the early formed plagioclase and the Rb will remain in the melt. Rb/Sr ratios range between 0.06 for basaltic rocks to 1.7 for highly differentiated low-calcium granites. The Ymir pluton shows anomalously high Rb/Sr ratios (0.25) relative to the other intrusions of this Coryell series (0.15) (Figure 23).

Calcium-yttrium relationships

Yttrium is an element which is generally incorporated into calcium minerals in varying percentages (See Figure 29) . Y-Ca ratios tend to increase in the residual material during igneous differentiation processes (Lambert *et al.*, 1974). Hornblende and garnet are high Y/Ca minerals whereas augitic clinopyroxene and plagioclase have a low Y/Ca. Y-Ca ratios are higher for the Group I plutons (Rossland and Jersey). This is most likely a reflection of their elevated hornblende content. The Ymir core zone is clearly related to the main mass (or outer rim) via differentiation of

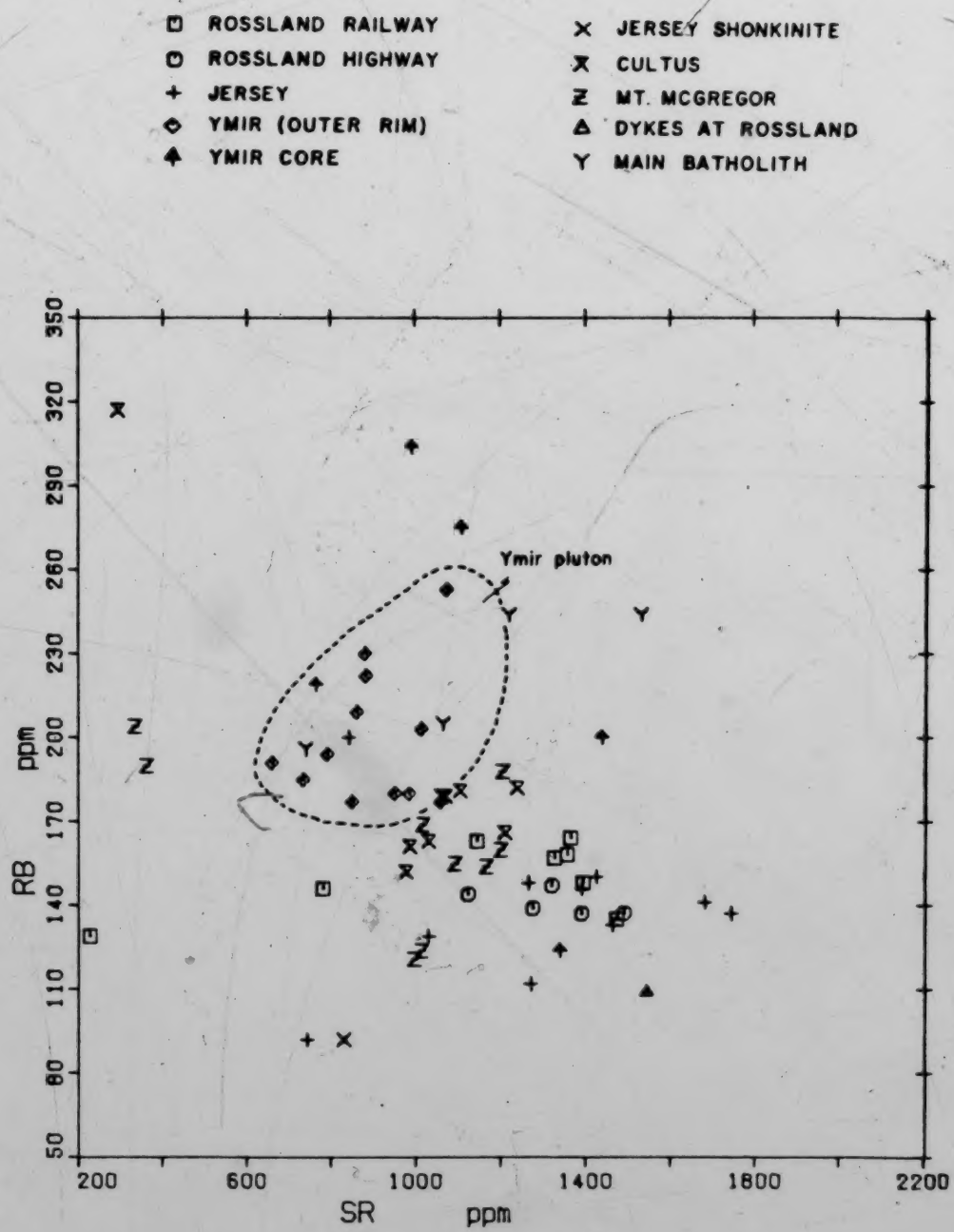

FIGURE 23. Rb versus Sr plot

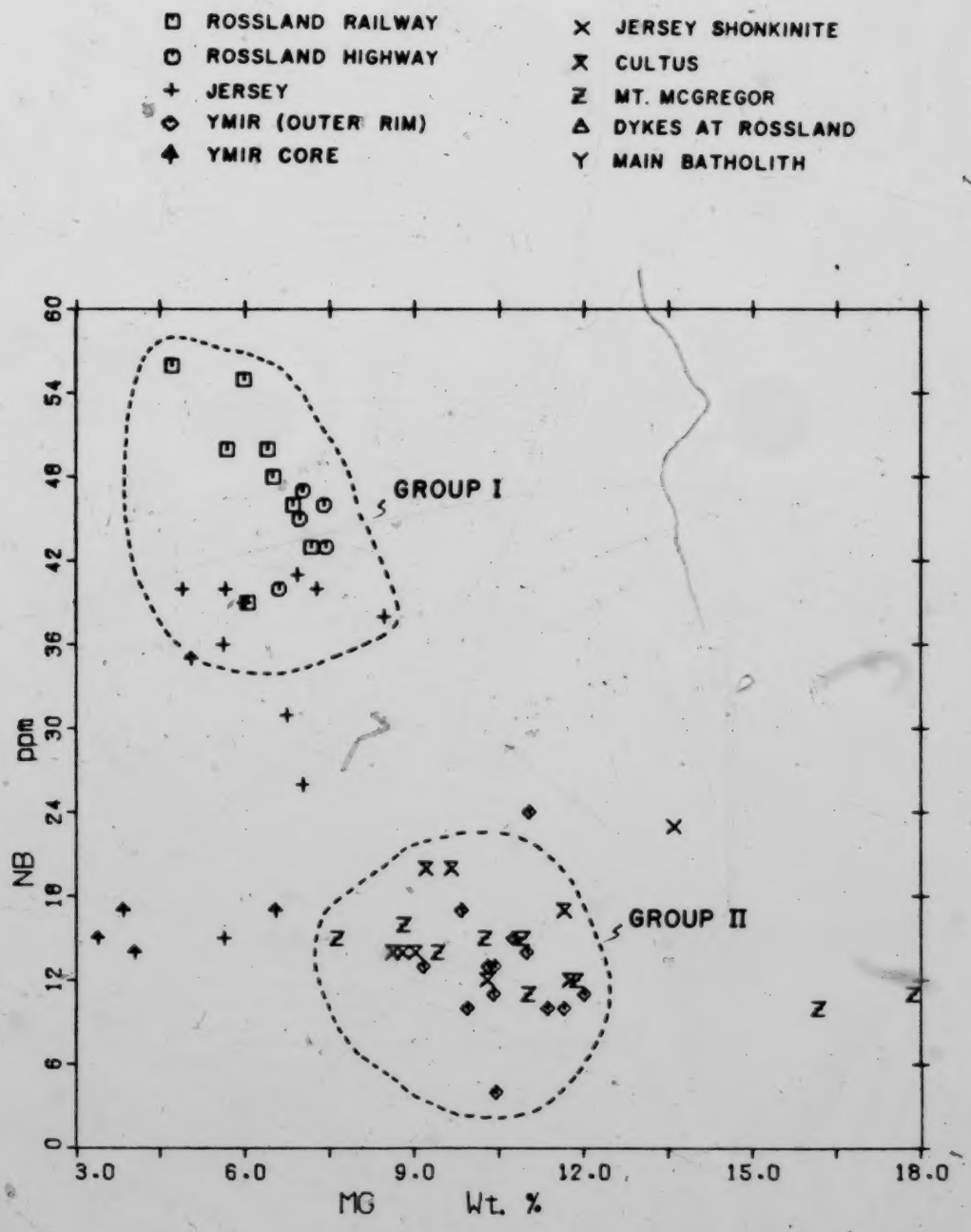

FIGURE 24. MgO versus Nb plot

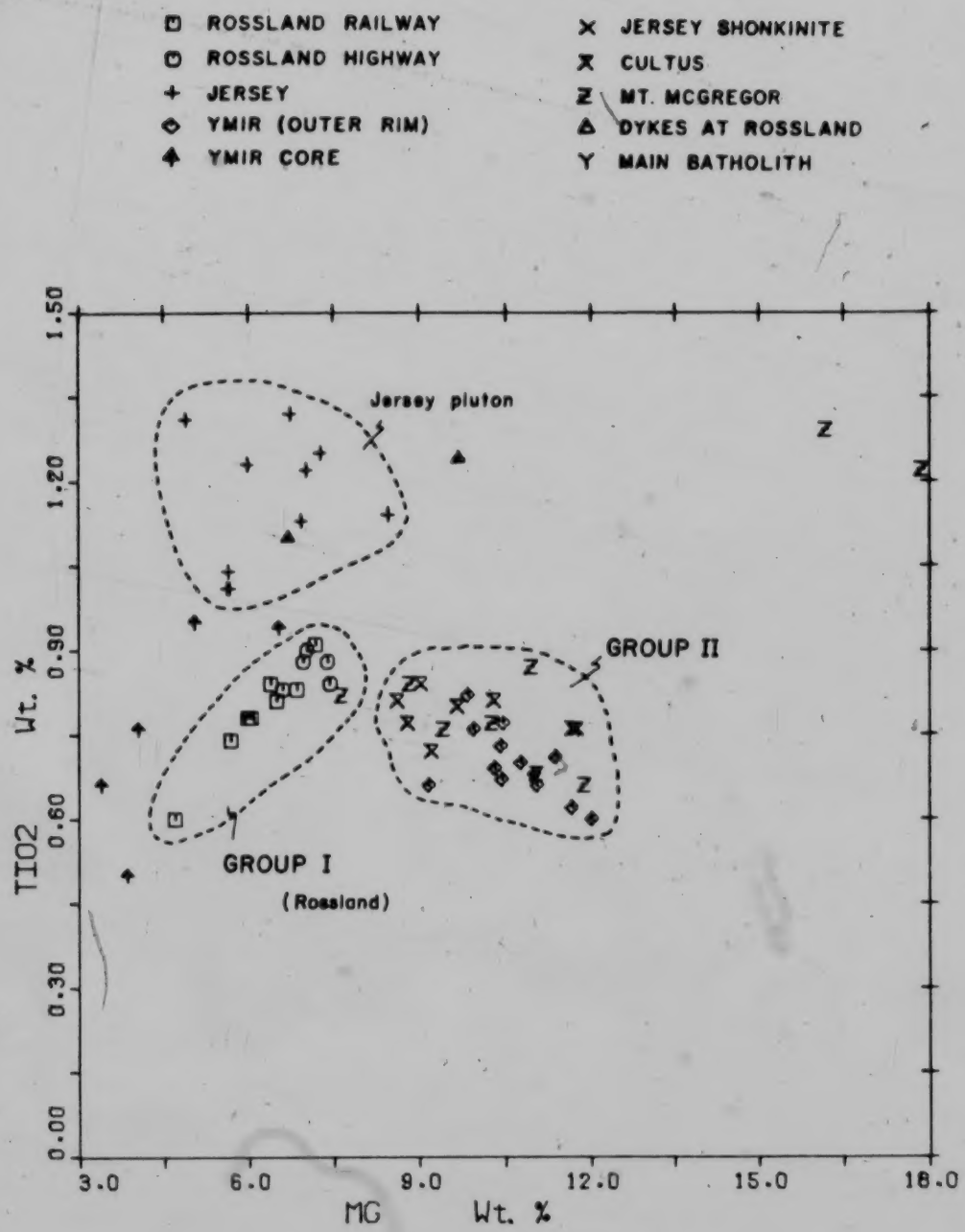

FIGURE 25. MgO versus TiO_2 plot

clinopyroxene. The Y-Ca ratio increases significantly towards the more highly evolved material. The accumulation of biotite and olivine (Y-poor phases) in the Mt. McGregor rocks may account for the anomalously low yttrium content.

Immobile Elements

Immobile elements (Nb, Zr, Y, Ti and P) are particularily stable when subjected to weathering or metamorphism, as they tend to concentrate in the refractory accessory minerals such as zircon and apatite (Goff, 1983). They are, therefore, more reliable indicators when attempting to analyze partial melting, fractionation and other effects.

A major feature concerning Nb distribution should be noted. Niobium contents (Figure 24) show a very marked increase in the three Group I plutons. This increase is not gradual and is concentrated into two distinct clusters with a 15 ppm average for the Group II plutons and a 40 ppm average for the Group I series. The degree of partial melting at the source affects the concentration of the incompatible elements but not the ratios between them (Hart and Allegre, 1980). Zr/Nb ratios should be similar to those of the parental magma. Consideration of the Zr/Nb for the Coryell's shows a distinctly bimodal distribution. Group I plutons have ratios from 3 to 5 and Group II plutons have ratios between 14 and 17.

The niobium concentration does not seem to be affected by differentiation within the plutons themselves. The differentiated Ymir core zone has identical Nb contents to the surrounding main mass and leucocratic fissure-filling dykes in the Rossland Railway pluton all have identical Nb contents to the rest of the intrusion. Even the very mafic lamprophyres (18% MgO) of the McGregor pluton have similar niobium values to the remainder of the stock. In the absence of a phase fractionating Zr relative to Nb, it can be inferred from this evidence that atleast 2 distinct magmas were involved in the formation of the Coryell rock series.

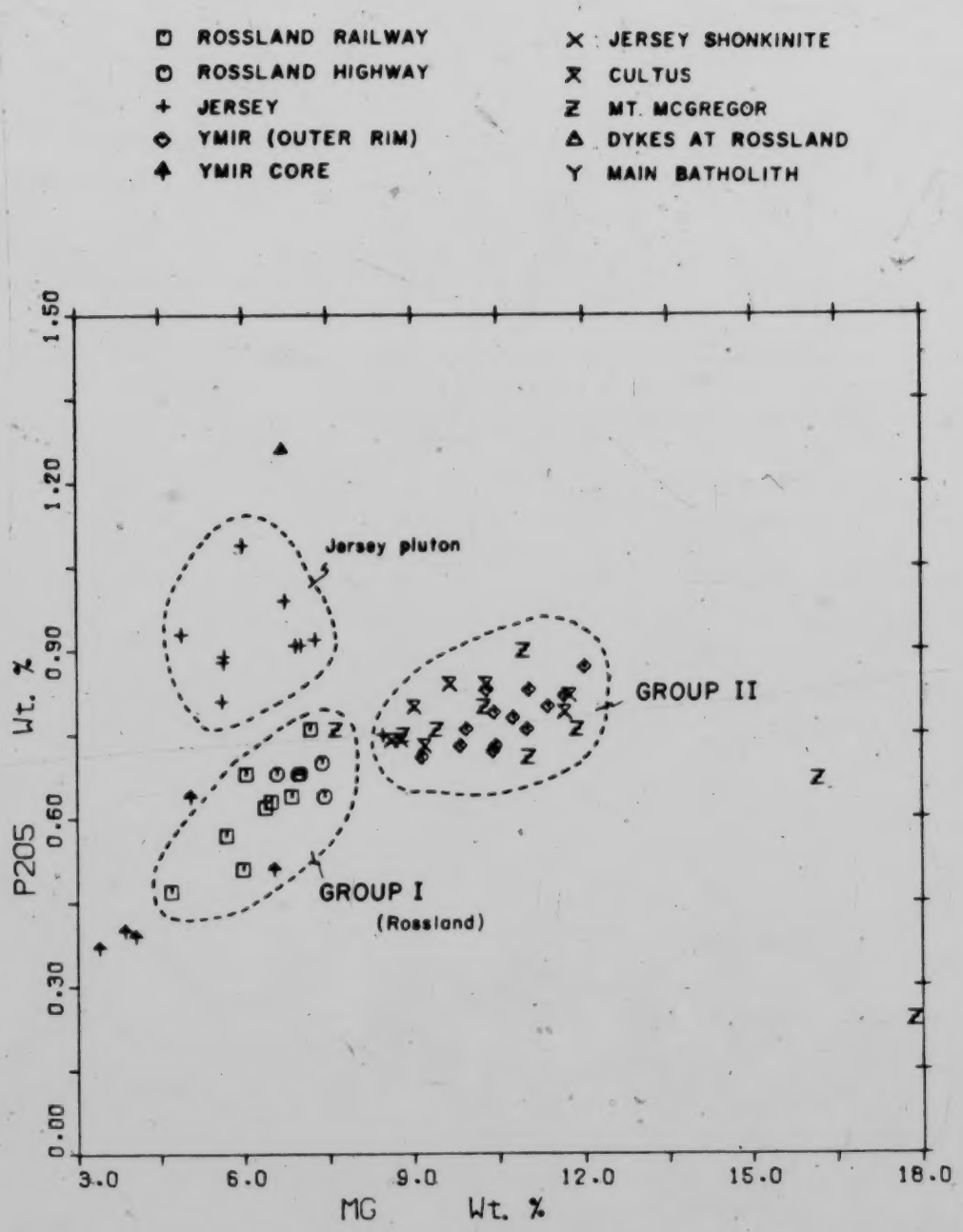

FIGURE 26. MgO versus P_2O_5 plot

It is also worth noting the anomalous immobile element concentrations present in the Jersey stock. Plots of MgO versus TiO_2, Y and P_2O_5 (Figures 25-27) show the Jersey pluton to be clearly enriched over the other intrusions. Either a heterogeneous source region or assimilation of an underlying volcanic pile could account for this. The Coryell's are characterized by anomalously low TiO_2, Y and Zr values when compared with those presented by Pearce and Cann (1973), Floyd and Winchester (1975), Winchester and Floyd (1977) and Pearce and Norry (1979). The reasons for this low TiO_2 content are varied but may be caused by early crystallization of biotite or magnetite which effectively removes a large proportion of the titanium. Evidence to support early biotite formation is provided by the abundant micaceous inclusions within the cumulate augite crystals of the Jersey shonkinite.

Uranium and Thorium

Uranium and thorium also belong to the group of incompatible elements, their large charge and size preventing their substitution into major minerals. Uranium and thorium concentrations in average syenites are 3.0 and 13.0 ppm respectively (Turekian and Wedepohl, 1961). Averages for basaltic rocks are 1.0 ppm for uranium and 3.0 ppm for thorium. Coryell rocks do not show any significant enrichments in either of these elements, possessing an average uranium content of 3.5 ppm and an average thorium content of 9.0 ppm. Late-stage dykes show U and Th enrichment while the two Mt. McGregor lamprophyres and the cumulate Jersey shonkinite have very low values.

No uranium minerals have been identified within the Coryell plutons, although it is possible that some of the uranium is complexed within the apatite, zircon and sphene. It is more probable that the uranium and thorium is adsorbed onto mineral grains. The samples within the Coryell suite exhibiting the greatest degree of hydrothermal alteration (eg.- albitization, pervasive kaolinitization, hydrous alteration products, etc.) have the lowest U/Th values. This is a leaching effect that adds credence to the hypothesis that the U and Th are principally adsorbed onto mineral surfaces.

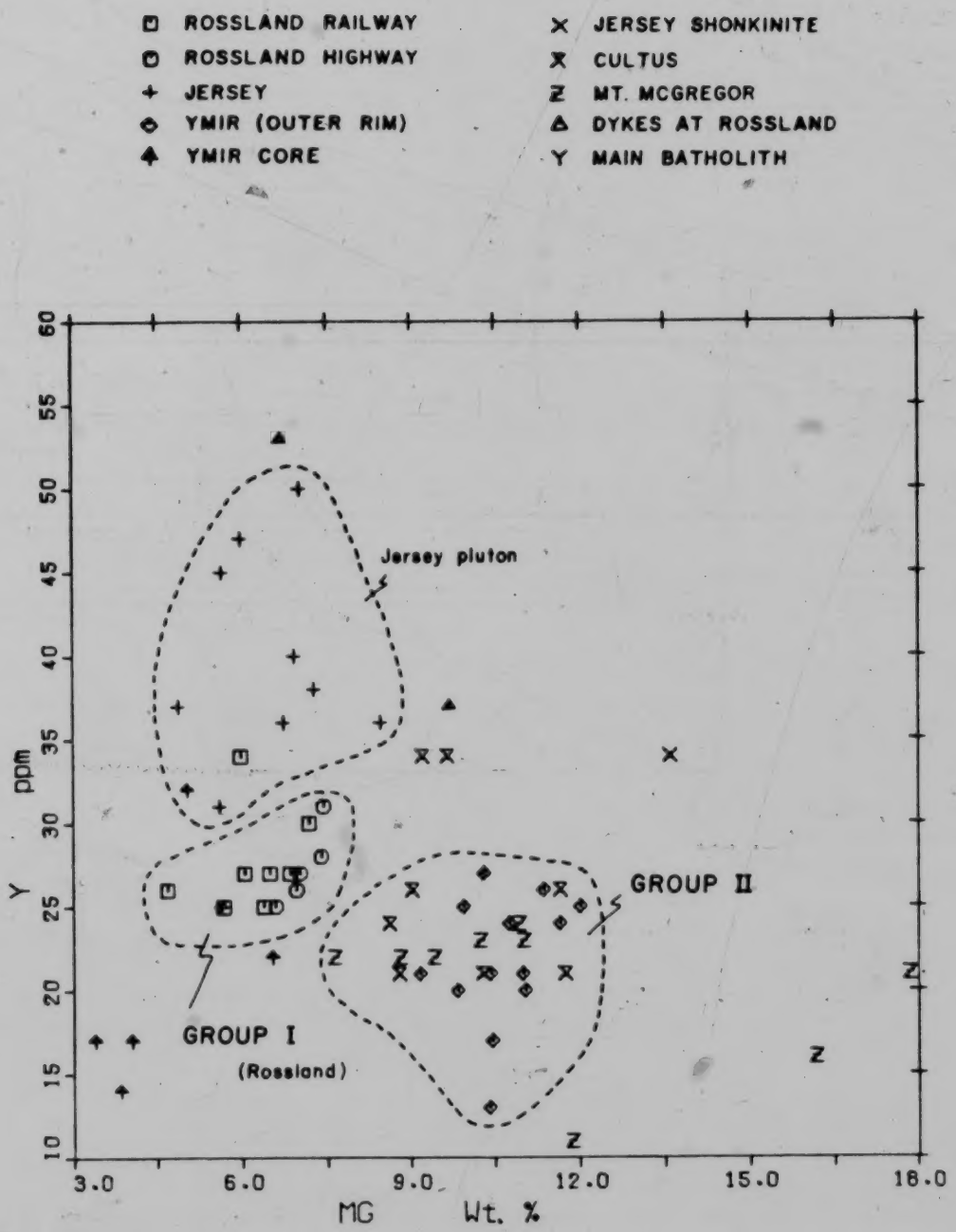

FIGURE 27. MgO versus Y plot

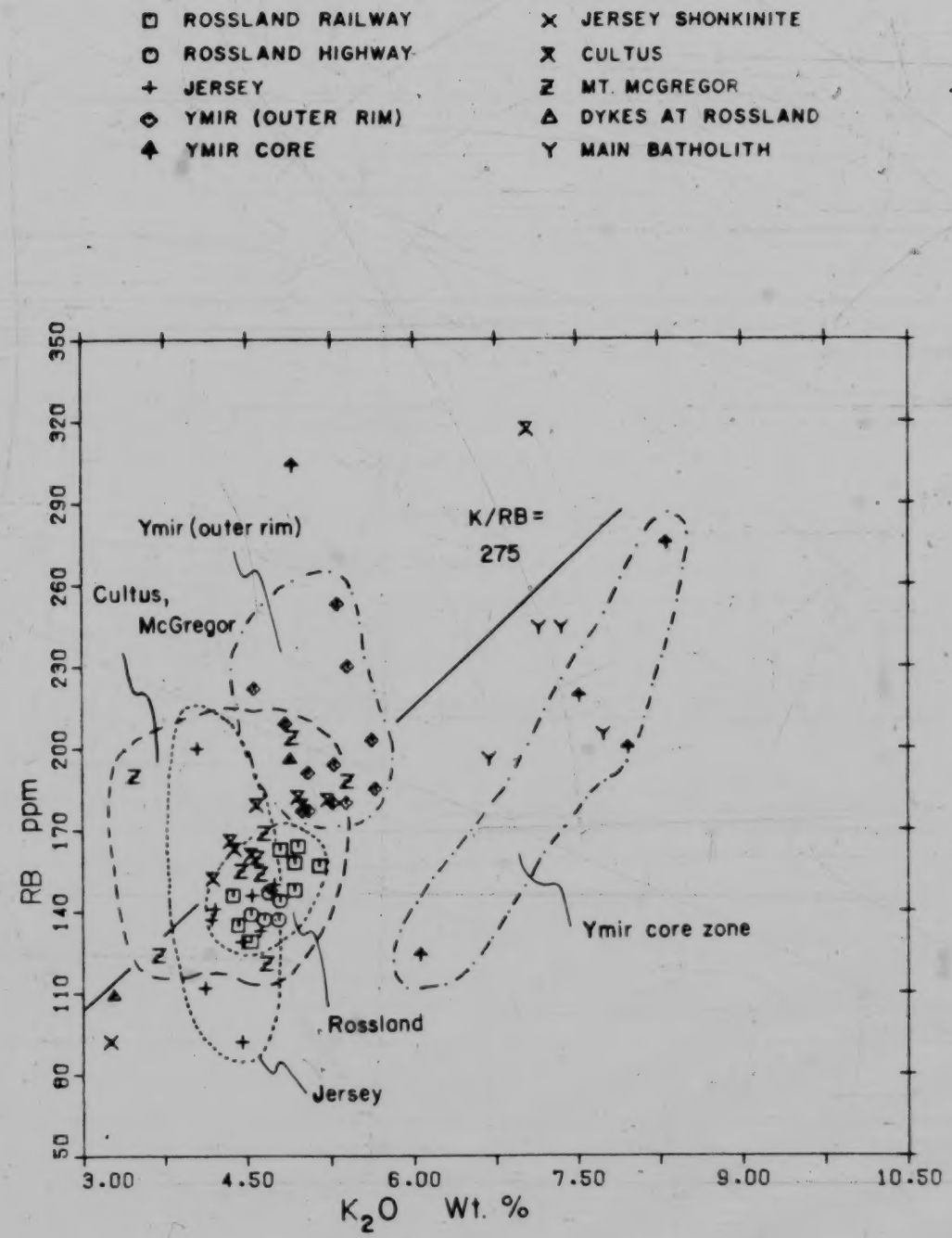

FIGURE 28. K_2O versus Rb plot

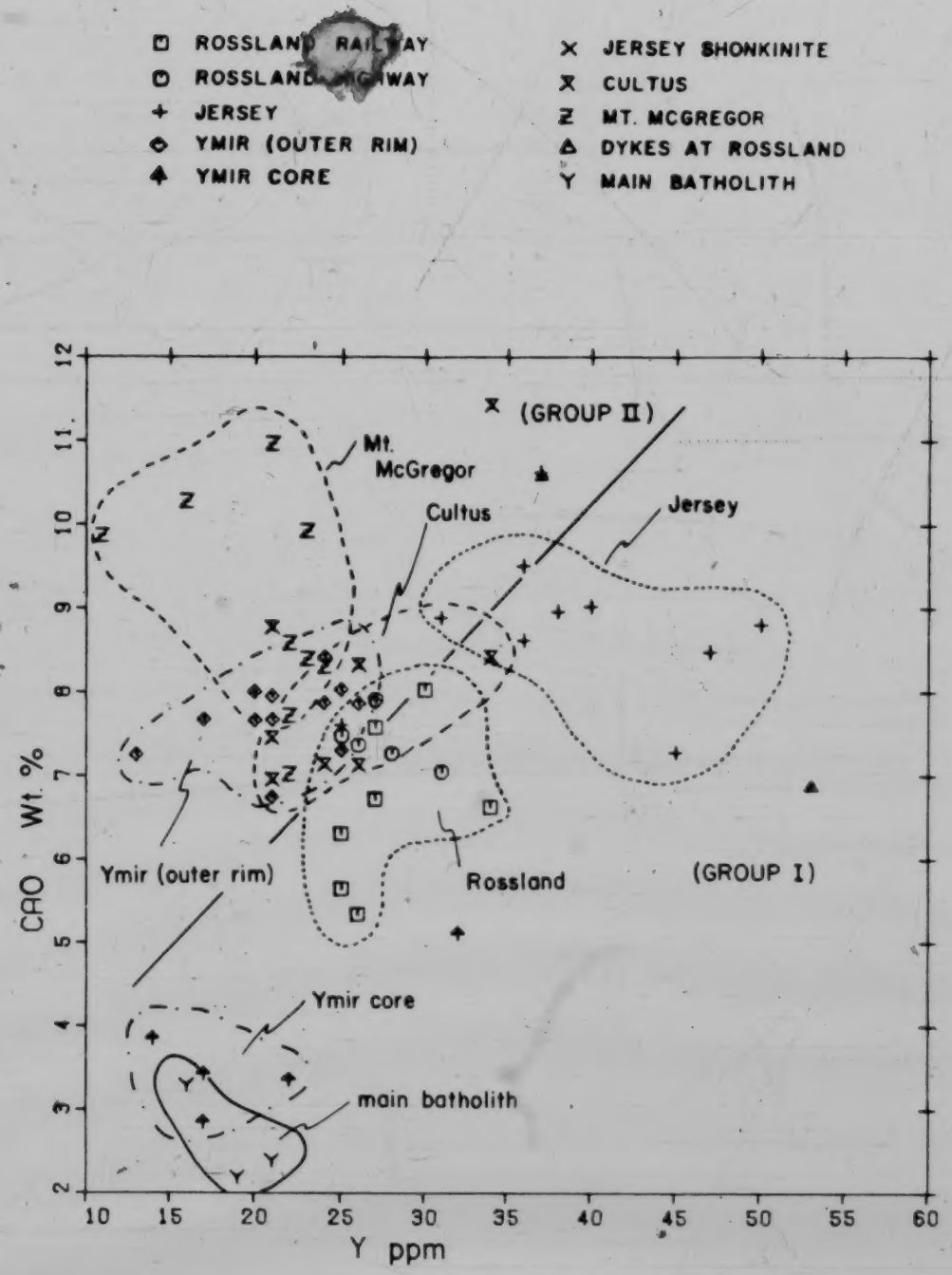

FIGURE 29. Ca O versus Y plot

Uranium and thorium classically show a marked coherence throughout a magma series (Burwash and Cavell, 1978). Correlation coefficients for uranium and thorium in the Coryell suite of rocks is 0.90 (Figure 30). Initially, these 2 elements remain together in a melt, although they become segregated in the final stages. The major process affecting the seperation of uranium from thorium in a magma is the oxidation of the U^{4+} ion to the hexavalent uranyl ion; UO_2^{2+} to U^{6+}. Thorium does not oxidize and remains in the tetravalent form. Due to their stability in water, uranyl compounds will be carried in the late stage aqueous phases.

Uranium/thorium ratios for the Coryell suite are 0.33 with very little variation from this value. There is a gradual geographic trend whereby the U/Th ratio increases in the eastern Group II plutons. A possible explanation for this trend could be related to the influence of the underlying crust. Regional examination of uranium contents (Sutherland Brown, 1980) in southeastern British Columbia show a marked increase in uranium content as one moves eastward towards the continent, especially over the Omineca Crystalline Belt. Uranium, thorium and lead are strongly concentrated within the crust and the belt within the Cordillera that is most highly evolved by crustal processes is the Omineca, hence the enrichment in the large ions. Given a hot, volatile-rich melt travelling upward through a thick pile of cratonically-derived sediments and or piercing the craton itself, we can see that it is possible to enrich uranium relative to thorium during the upward migration. The total thickness of these sediments increases towards the craton, therefore possibly providing a mechanism whereby we can account for the pattern of eastwardly increasing U/Th ratios apparent in the Coryell plutons.

Metallic Elements

Cr, Ni, Cu, Pb, Zn, Co, Mo, Hg and As have also been analyzed for these plutons. Due to the extremely high partition coefficients (ie.- concentration in the crystallizing solid phase/concentration in the melt) for Ni and Cr, they are almost immediately incorporated into solid phases, therefore providing an

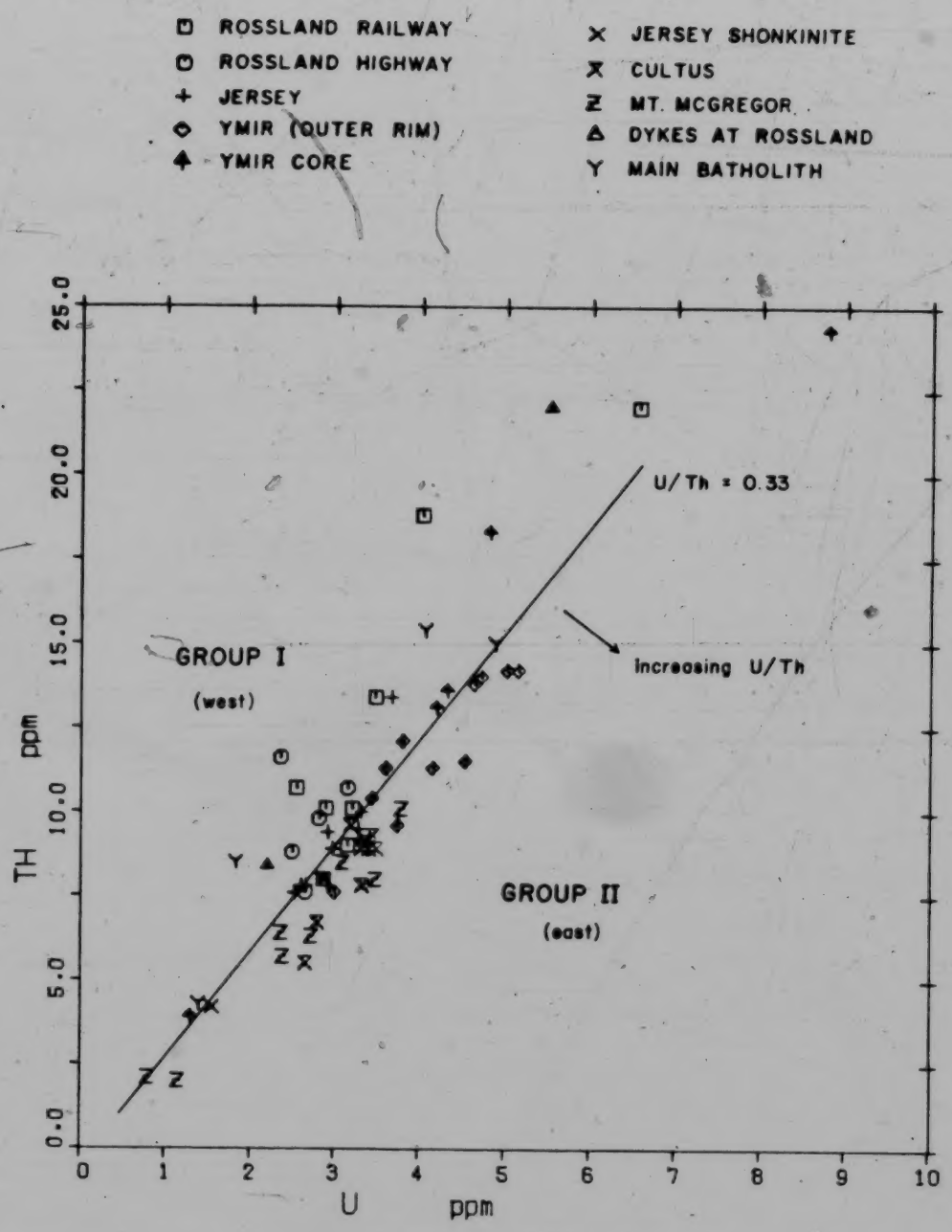

FIGURE 30. U versus Th plot

approximate method for estimating the degree of fractional crystallization. The sympathetic relationship between Ni and olivine can be seen on the Mg versus Ni plot (Figure 31). The olivine-poor, eastern Group I plutons and the Ymir core zone are strongly depleted in nickel content with an average of 37 ppm compared with an average of 80 ppm for the eastern group of more mafic plutons. Again, the distinct separation between the 2 groups is evident. Chromium will tend to concentrate in the first-formed pyroxenes and shows a good correlation with increasing magnesium. The Ymir pluton falls significantly low on the trend (Figure 32). A lamprophyric dyke and an olivine-rich syenite from the Mt. McGregor stock have the highest Ni (116, 200 ppm) and Cr (104, 104 ppm) concentrations.

Due to their low, unvarying concentrations and the insensitivity of the analyses, the Mo, As and Hg have not been considered as significant. Mean Mo concentration is 1 ppm, arsenic is 2 ppm and mercury is around 20 ppb. No trends can be identified. Cobalt and copper increase with increasing mafic content of the rocks (ie.- eastwards). Chromium and zinc do not show such a definite trend, but also increase with higher mafic content. Lead shows a positive correlation with the more leucocratic rocks, having slightly higher values in the Rossland plutons and the differentiated core zone of the Ymir pluton.

Summary

The Coryell intrusions are a suite of undersaturated rocks approximating the composition of alkali olivine basalt and its derivatives. A distinct geographic trend occurs, with the eastern intrusions being more mafic. Their higher Mg and lower Al and Na contents reflect the higher amounts of olivine and lower amounts of plagioclase. Silica, potassium, calcium and iron vary little between the two groups. These rocks are strongly enriched in potassium, barium, rubidium and strontium and show relatively low concentrations of the other immobile elements. K_2O/Na_2O and U/Th ratios increase towards these more mafic rocks, contrary to expected trends where potassium and related elements increase in the direction of more advanced fractionation. Elevated K and U values may be

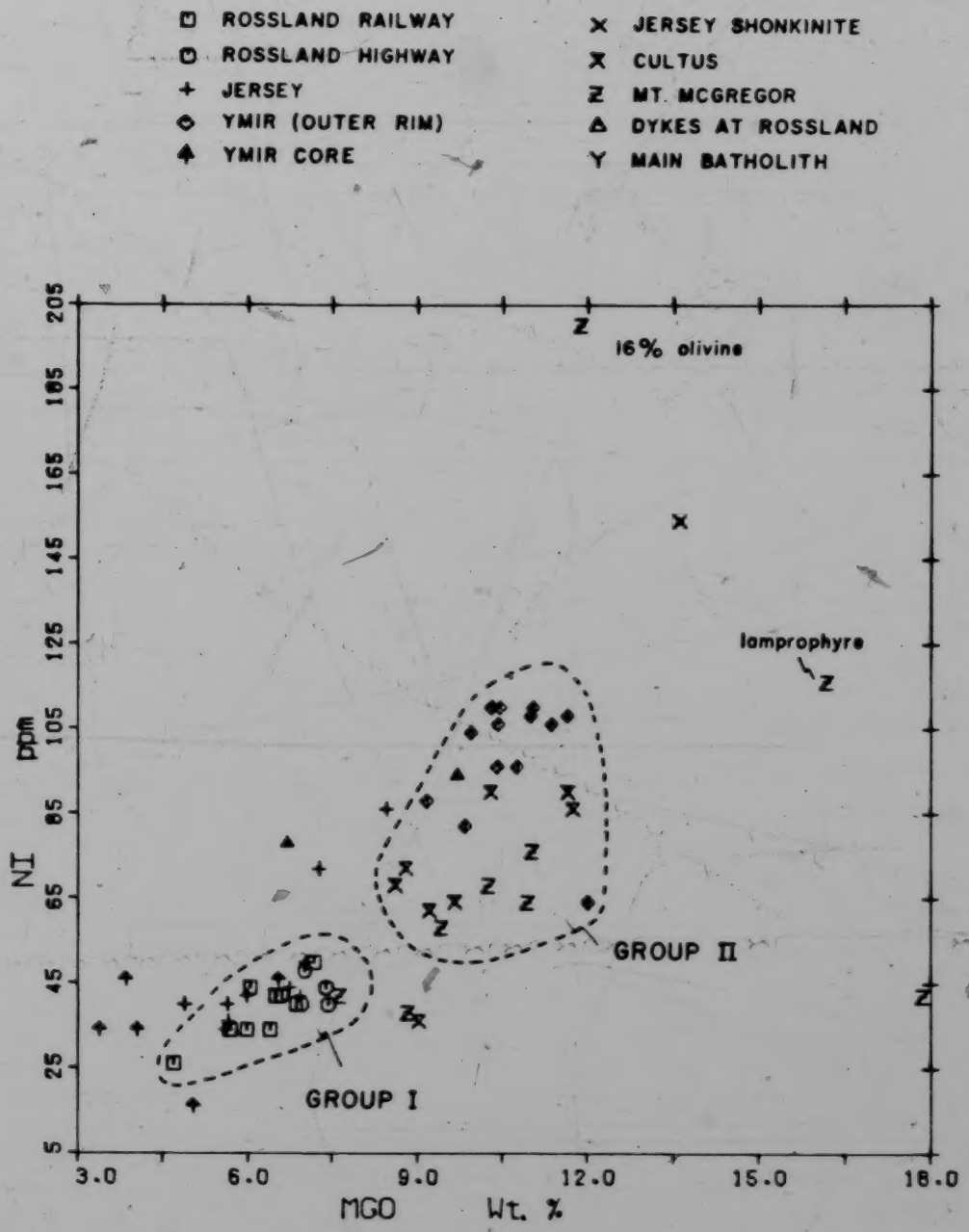

FIGURE 31. MgO versus Ni plot

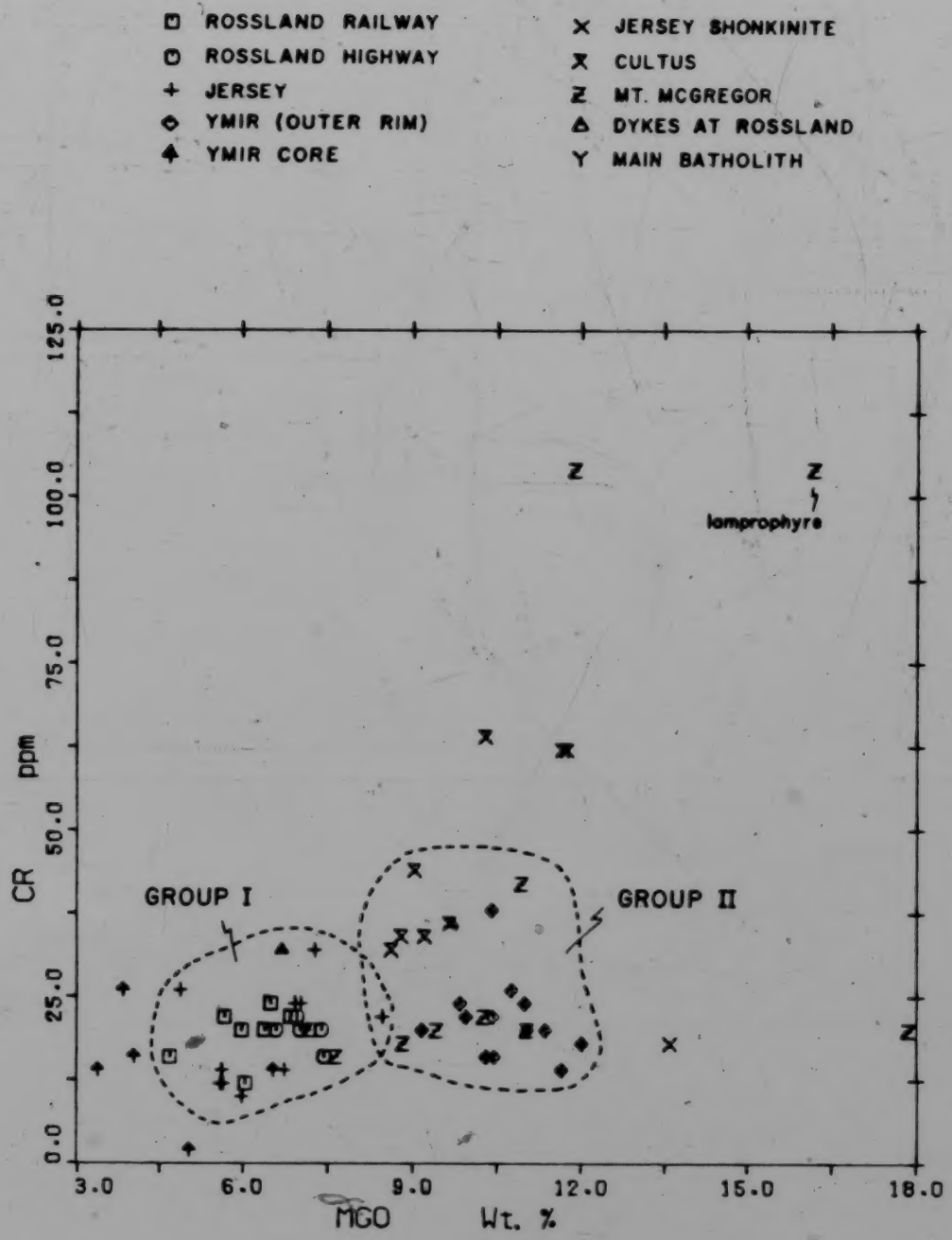

FIGURE 32. MgO versus Cr plot

evidence of contamination from the underlying crystalline basement.

Strongly depleted TiO_2 contents characterize the entire suite, possibly a reflection of early biotite and augite fractionation. Two separate clusters of plutons are noted, especially with respect to niobium and nickel concentrations.

The Jersey pluton is anomalous in several respects. It has significantly elevated TiO_2, P_2O_5 and Y concentrations, as well as significant scatter of barium and strontium values. Pervasive late metasomatism is a distinct possibility, owing to the close proximity of several ore deposits (tungsten skarn). The Ymir pluton drops consistently off the AFM and CNK magmatic trends and has the highest K_2O content of all the sampled plutons.

One of the most important results to be obtained from the geochemical analysis is the relative effects of partial melting relative to fractional crystallization in these rocks. Other factors to be considered are the possibilities of contamination, metasomatism, magma mixing, etc. The petrogenetic significance of these geochemical observations will be investigated in the following chapter.

Time of Intrusion

A $^{87}Sr/^{86}Sr$ isochron was prepared using mineral separates from a freshly blasted sample collected from the centrally-located Ymir pluton. The isotopic composition of the rubidium and strontium was determined on the mass spectrometer at the University of Alberta. The age obtained using 8 mineral separates and a whole rock sample was 50.8 ± 0.6 Ma (Table 3). The correlation coefficient was calculated to be 0.99968, confirming the reliability of this data.

Recently, a K/Ar date of 52 Ma (Archibald *et al.*, 1982) was obtained on this same plug. The $^{87}Sr/^{86}Sr$ and the K/Ar dates are the first isotopically determined ages available for the Coryell Intrusives east of the Trail area. An age of 50.8 Ma coincides with a strong geothermal event related to the Laramide Orogeny in southeastern British Columbia and the Northwestern United States (Medford, 1975; Mathews, 1981).

TABLE 3

Strontium isotope results

87Rb/86Sr	87Sr/86Sr	
0.63719	0.70742 +- 0.000016	WHOLE ROCK
0.00942	0.70700 +- 0.000026	APATITE
1.44762	0.70803 +- 0.000023	ORTHOCLASE
0.40634	0.70728 +- 0.000014	ANORTHOCLASE
0.25813	0.70728 +- 0.000034	ALBITE
0.08890	0.70690 +- 0.000028	AUGITE
14.56842	0.71747 +- 0.000048	BIOTITE 1
14.45413	0.71741 +- 0.000027	BIOTITE 2
0.62537	0.70744 +- 0.000091	OLIVINE

87Sr/86Sr initial ratio =

0.70697 +- .000061

t= 50.8 +- 0.6 Ma

Strontium Initial Ratios

From the inception of the earth onwards, Rb has tended to concentrate in the crust to a much greater degree than Sr. ^{87}Rb decays via beta particle emission to ^{87}Sr, therefore crustal areas will contain much higher ^{87}Sr values than the mantle. Whereas Rb and Sr will be fractionated from one another during normal magmatic evolution, the stable isotopes ^{86}Sr and ^{87}Sr will not. They therefore serve as an excellent indicator of the parental source region. Initial $^{87}Sr/^{86}Sr$ ratios of between 0.702 and 0.706 have generally been inferred to represent purely mantle-derived magmas and values above 0.710 are indicative of crustal rocks (Powell and Bell, 1974). Ratios in between these two values may involve some form of mixing of crustal rocks with mantle magmas.

The initial $^{87}Sr/^{86}Sr$ ratio for the Ymir pluton sample was 0.7070 (Figure 33). With such an intermediate ratio, crustal contamination is suggested. The parental magma for these rocks may have been ponded in a lower crustal region or have resided for an extended period in a zone of elevated Rb/Sr. It is also possible that the strontium was never at equilibrium upon melting. An Rb-rich phase in the mantle, such as phlogopite, may melt preferentially, forming a magma with a higher $^{87}Sr/^{86}Sr$ ratio. Magnesium and potassium contents will also be elevated, a feature characteristic of the entire suite of Coryell intrusions.

The coeval and mineralogically-related alkalic rocks of the Highwood Mts. in Montana possess $^{87}Sr/^{86}Sr$ ratios of 0.7078 (Powell and Bell, 1974). Most Mesozoic granitic rocks in southeastern British Columbia have initial ratios of between 0.706 and 0.708 (Fairbairn *et al.*, 1964). Armstrong *et al.* (1977) have delineated a $^{87}Sr/^{86}Sr$ line of 0.706 which corresponds to the edge of the cratonic basement in the western United States.

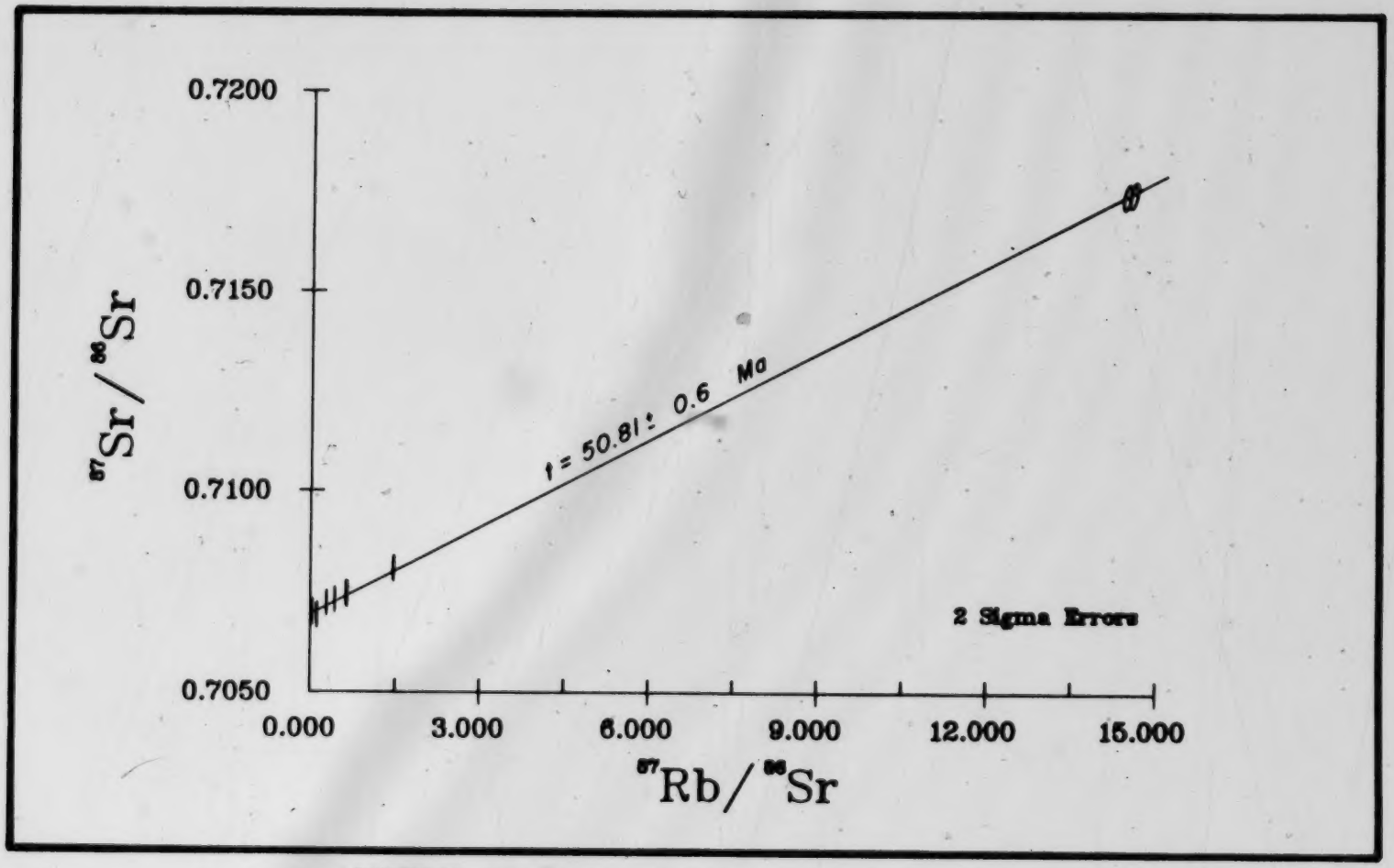

FIGURE 33. Strontium isotope isochron plot

VI. PETROGENESIS

A. Initiation of Melting

Melting of the solid mantle will require a change in pressure, temperature or composition at the source. Since all other regional evidence points to a relaxing, extensional environment during Coryell time, the preferred mechanism to explain initial magma production for these Coryell intrusives is the decompression caused by local extension. This would inevitably cause the initiation of a diapir or plume (Ross, 1981). This zone could also serve as a locus for metasomatism which would introduce CO_2, H_2O, K_2O and radioactive elements, all of these contributing to increased melting. Further extension would provide fissures through which the small bodies of buoyant magma could escape to the near-surface epizone (Buddington, 1959). Removal of this volatile-rich fraction would cause the melting to cease.

B. Petrogenetic Models

Various theories regarding the generation of the potassic-rich rocks have been proposed. Turner and Verhoogen (1960), Bell and Powell (1969) and Sorenson (1974) have reviewed the applicability of these hypotheses. Possible mechanisms have included limestone assimilation, crustal anatexis, zone refining, immiscibility, partial fusion and alkali metasomatism in the mantle. A few of these hypotheses will be briefly considered with relation to the generation of the Coryell intrusives.

Daly proposed in 1910 that limestone assimilation by a sub-alkaline magma could produce a desilicated alkaline magma. Conflicting field data, the discovery of the thermal barrier between saturated and undersaturated rocks and the existence of carbonatites tended to counter the arguments in favour of the limestone assimilation theory. The Coryell stocks at Cultus and Jersey intrude the Lower Cambrian Laib formation which contains abundant carbonate material. Evidence for the uptake of some of this carbonate is suggested by the high percentage of calcite and sphene observable in the Jersey pluton. Concomitant

with the higher CaO content of this pluton is the occurrence of higher Y, P_2O_5 and TiO_2 values. Other plutons in the Coryell suite have been intruded through widely differing country rocks and show similar major element geochemistry to the Jersey and Cultus plutons, therefore the effects of limestone assimilation are probably not a major controlling influence.

Crustal involvement has been invoked in the formation of the majority of granitic magmas. Boettcher and O'Neil (1980) point out the fact that alkali basalts in continental and ocean island environments are chemically very similar, suggesting that crustal contamination is not important in the genesis of this rock type. The existence of felsic xenoliths on both Cultus and Mt. McGregor suggests the possibility of minor crustal effects. Two factors tend to negate the probability of extensive crustal involvement:

a. if large scale granitic assimilation had taken place, the Al and Si concentration of these plutons would have increased along with the K_2O content and

b. resorption of the xenoliths is not extensive.

The effects of zone refining on trace element contents are difficult to distinguish from the effects of partial fusion. Boettcher *et al.* (1980) have suggested that wall-rock reaction cannot selectively increase K_2O and TiO_2, without altering significantly the major element chemistry. Alkaline rocks move rapidly through their conduits due to high ascent rates ,thereby reducing wall-rock reaction. Zone refining may have affected the Coryell intrusions by selectively increasing the alkali contents, but it is a difficult hypothesis to prove and is probably minor in importance.

The possibility of volatile immiscibility exists, where a late alkali-rich fraction separates from the main magma mass and migrates towards the apex of the magma chamber, producing alkaline rocks. Due to the high mafic content of the Coryell suite of rocks, this is not a likely mechanism for generation of the observed compositions. It is, however, possible that highly alkaline, volatile fractions migrated into the upper portions of the plutons. The residual element enriched fractions have probably been eroded off or vented, leaving no field evidence to support this hypothesis. The low residual element contents of these

intrusions confirms the feasibility of this idea.

C. Coryell Model

Consideration of the field relations, textures, mineralogy and geochemistry of the Coryell plutons suggests that their origin and evolution can be explained utilizing the concepts of partial fusion, crystal fractionation and alkali metasomatism at depth.

Source Composition and Partial Melting

Based on the work of Green and Ringwood (1967), Ringwood (1975) and numerous other workers, production of alkali olivine basalts (of which the Coryell intrusions are a more highly differentiated, potassium-rich member) occurs only at intermediate pressures (10 to 20 kbars) which correspond to depths of 35 to 70 km. The entire process of magma generation would be initiated by the separation of a pyrolitic diapir at 125 kilometres in the low velocity zone. As the diapir rises, the degree of partial melting increases. A magma segregating after 3-4% melting and 50 km (and around 1200° C) would be made over into an alkali olivine basalt. A high-alumina basalt would be produced at 30 km and 5-10% partial melting.

The major requirement for forming undersaturated rocks is the early separation of orthopyroxene, a high silica mineral. In a normal, low pressure (0-10 kb) environment, olivine is the stable liquidus phase, but at higher pressures (10-20 kb), the stability of orthopyroxene may supercede that of olivine and its separation can cause an undersaturated residua. Recently, Eggler (1978), Wendlandt and Mysen (1978) and Wyllie (1979) have shown the importance of CO_2 in the genesis of alkalic magmas by partial melting of the upper mantle. At pressures between 25 and 30 Kbar, the presence of CO_2 in the mantle reduces melting temperatures by about 200° C and the partial melts are alkalic.

Crustal thickness in this area of the southeastern Cordillera is postulated to lie between 30 and 50 km (Medford, 1975). The magmatic plume would

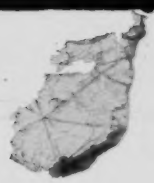

probably stop and pool at the base of the crust at 50 km. Segregation of the liquid fraction would conceivably occur at this point. According to Ringwood's (1975) model, the separating fraction would approximate an alkali olivine basalt at this depth.

Consideration of Ringwood's (1975) model alone is insufficient to explain the enhanced K_2O and other incompatible element contents of these Coryell rocks relative to tholeiites (Boettcher *et al.*, 1980). The addition of phlogopite to the mantle source area appears to be the most likely mechanism for enriching these intrusives in K_2O, MgO and the other trace elements. Phlogopite exists in ultramafic nodules (Wendlandt *et al.*, 1980), and hydrous minerals such as titanium-rich phlogopites and amphiboles have also been identified (Lloyd and Bailey, 1975). Metasomatized mantle lherzolites are sometimes found in alkali basalt flows (Menzies and Murthy, 1980). Phlogopite occurs liberally as inclusions in the clinopyroxenes of the Coryell rocks, adding credence to the hypothesis of a mica-rich mantle source. Phlogopite would act as a repository for incompatible elements such as Ba, Sr, Rb, K and volatile components such as H_2O and CO_2. Its high Rb content would also facilitate the elevation of the initial $^{87}Sr/^{86}Sr$ ratios. En route to the surface, the phlogopite becomes unstable, providing the elements for formation of the abundant alkali feldspars and biotites of the near-surface intrusions. At shallow depths, olivine will appear on the liquidus and begin to fractionate out of the melt, producing the final products of the satellitic Coryell plutons.

Through work on the system K_2O-MgO-CaO-Al_2O_3-SiO_2-H_2O, Boettcher *et al.* (1975) described the beginning of mantle melting with the reaction:

orthopyroxene + clinopyroxene + mica ± vapour $\rightleftharpoons$ olivine + garnet + ultrapotassic liquid.

At this point, a discussion of the lamprophyres associated with the Coryell intrusions becomes important. The lamprophyres on Mt. McGregor consist almost solely of pyroxene and mica, with absolutely no evidence of olivine or olivine

replacements. Based on their extremely elevated MgO contents (17%), the trace element characteristics which appear to define the beginning of a fractionation sequence, and the elevated Ni and Cr values, it has previously been suggested in this thesis that the lamprophyres may be a parental magma. It is postulated here that the lamprophyres represent the left side of the above reaction, a pyroxene-mica primary melt, which due to its rapid expulsion has not undergone the transition to olivine and garnet. Additional evidence in support of the hypothesis in favour of phlogopite involvement, is the occurrence of abundant inclusions of mica within clinopyroxenes of the Jersey cumulate fractions (constituting up to 30% of the mineral).

Low Pressure Fractional Crystallization

Field evidence for low-pressure crystal fractionation is shown by the strong basification at the contact zones of the main batholith (Daly, 1912). The overwhelming chemical similarity of these zones with the satellitic intrusions attests to the strong influence of fractional crystallization in the formation of these rocks. Separation of early-formed mafic components would be an extremely effective process in the main batholith, owing to its large volume and far slower cooling rates compared with the small satellitic stocks. The classic example of this phenomenon is provided by the Shonkin Sag laccolith of the Highwood Mts. in Montana (Hurlburt, 1939; Osborne and Roberts, 1931; Weed and Pirsson, 1895; Nash and Wilkinson, 1970). The shonkinites and syenites of this layered intrusion are almost identical chemically to the rocks of the Coryell intrusives and were intruded at approximately the same time period at the end of the Laramide Orogeny. The leucocratic, quartz-normative core zone of the Ymir pluton is also ample evidence for the existence of pervasive low-pressure fractional crystallization in the smaller, more basic intrusions.

VII. SUMMARY AND CONCLUSIONS

The lower-Eocene (50.8 Ma) Coryell intrusions represent the most alkaline magmatic event in this region of southern British Columbia. The numerous satellitic plutons range in composition from leucocratic syenites to olivine-augite melasyenites. Chemically, they are members of the potassic alkali basalt series.

From a regional examination, the tectonic environment at this time was extensional in nature. The relaxing crust may have provided a favourable locus for the upwelling of a mantle plume centred beneath the large central Coryell batholith. High heat flows in this region exist to the present day (Leroux, 1981). The eastern satellites and coeval western volcanics intruded the flanks of the thermal dome. Rapid erosion of this elevated central area has exposed the main batholith.

The evolutionary path of these rocks can be traced through numerous lines of evidence. The occurrence of two distinct groups of intrusions attests to the heterogeneity of the mantle source region. The source composition is postulated to be an alkali-enriched mica peridotite. Evidence for the existence of this parental magma is provided by the mica-pyroxene lamprophyre dykes which are genetically related to the Coryell suite. The elevated $^{87}Sr/^{86}Sr$ ratio of 0.7070 could easily be caused by the melting of Rb-rich phlogopite in the upper mantle. Strongly enriched Ba, Sr, Rb and K values of these plutons attests to their derivation from a small degree of partial melting (less than 5%) of the metasomatized mantle.

Continued evolution involved strong crystal fractionation of the mafic components and the possibility of both deep crustal and shallow crustal influences is indicated. Early fractionation of the phlogopite phase is suggested by the flat (Fe_2O_3-poor) AFM curve of these intrusions and the anomalously low TiO_2 contents. Though difficult to prove, involvement of the cratonic and shallow crustal rocks may prove significant. U/Th and K_2O/Na_2O contents increase eastwards towards an area of thickened crust. The high $^{87}Sr/^{86}Sr$ ratios, which

are characteristic of the zone to the east of the Intermontane Belt, may be influenced by the underlying craton in addition to the existence of a high $^{87}Sr/^{86}Sr$ phase in the mantle. Granitic xenoliths and the elevated calcium contents of a pluton (Jersey) which has clearly intruded carbonate-rich sediments, suggests that minor crustal contamination has occurred. Late stage crystal fractionation of forsteritic olivine and Ca-clinopyroxene components is a strong modifier of the final mineralogical compositions. Strong basification of contact zones, the existence of pure pyroxene cumulates, the highly differentiated granitic core zone of the Ymir pluton and the elevated mafic contents of the smaller, shallower eastern intrusions, confirm the significance of shallow differentiation.

Final modifications to the chemistry and mineralogy of these plutons involve the venting of volatile-rich fractions and post-consolidation hydrothermal effects. The eastern group of plutons are characterized by depleted residual element contents, a fine-grained mineralogy, and the almost total absence of alteration compared to the western group. This is interpreted as evidence of venting of the eastern plutons, allowing a rapid escape of incompatible element-enriched gaseous components. Post-solidification hydrothermal remobilization of large-ion lithophile elements is the final factor affecting these plutons. The extremely wide scatter of Ba and Sr values in the Jersey Pluton is suggestive of fluid migration. The close proximity to a major tungsten skarn deposit (Emerald mine) may imply that the timing of ore formation was Tertiary and associated with the Coryell event rather than the Jurassic Nelson intrusion.

The relationship of the satellitic intrusions to the main batholith is uncertain. They were most definitely formed around the same time period but are not necessarily derivatives of the same magma chamber. The marked differences in trace element contents between the Group I and Group II plutons implies that two totally separate mantle source areas may be responsible for their formation.

Additional strontium isotope data, oxygen isotope work, REE analyses and microprobe analyses of the various mineral phases would improve greatly the

understanding of these intrusions.

A strontium isotope isochron constructed for each pluton would give an indication of the timing of these intrusions relative to their geographic location. The degree of crustal contamination and its areal variability could be ascertained using both strontium and oxygen isotopes. Oxygen isotopes obtained from the sediments surrounding each pluton would indicate the extent of the fluid interchange.

Rare earth analyses could be used to contruct more precise melting models for the Coryell suite of rocks and microprobe analyses on co-existing mineral phases would give an indication of crystallization temperatures and the extent of magma mixing prior to emplacement. A more accurate plotting of fractionation diagrams would also be facilitated.

REFERENCES

Archibald, D. A., Glover, J. K., Price, R. A., and Farrar, E. 1982. Geochronology and tectonic implications of magmatism and metamorphism; southern Kootenay Arc and neighbouring regions, southeastern B.C. : Part I; Jurassic to Mid-Cretaceous. Canadian Journal of Earth Sciences (in press).

Armstrong, R. L., Taubeneck, W. H., and Hales, P. O. 1977. Rb-Sr and K-Ar geochronometry of Mesozoic granitic rocks and their Sr isotopic composition, Oregon, Washington and Idaho. Geological Society of America Bulletin, 88, pp. 387-411.

Baadsgaard, H., Folinsbee, R. E., and Lipson, J. 1961. Potassium-argon dates of biotites from Cordilleran granites. Geological Society of America Bulletin, 72, pp. 689-702.

Bailey, D. K. 1964. Crustal warping - a possible tectonic control of alkaline magmatism. Journal of Geophysical Research, 69, pp. 1103-1111.

Barberi, F., Ferrara, G., Santacroce, R., Treuil, M., and Varet, J. 1975. A transitional basalt-pantellerite sequence of fractional crystallization, the Boina Centre (Afar Rift, Ethiopia). Journal of Petrology, 16, pp. 22-56.

Bell, K., and Powell, J. L. 1974. Strontium isotopic studies of alkalic rocks: the potassium-rich lavas of the Birunga and Toro-Ankole regions, East and Central Equatorial Africa. Journal of Petrology, 10, pp. 536-572.

Boettcher, A. L., and O'Neil, J. R. 1980. Stable isotope, chemical, and petrographic studies of high-pressure amphiboles and micas: evidence for metasomatism in the mantle source regions of alkali basalts and kimberlites. American Journal of Science, 280-A, pp. 594-621.

Brown, R. L. 1978. Structural evolution of the southeast Canadian Cordillera: a new hypothesis. Tectonophysics, 48, pp. 133-151.

Buddington, A. F. 1959. Granite emplacement with special reference to North America. Geological Society of America Bulletin, 70, pp. 671-747.

Burwash, R. A., and Cavell, P. A. 1978. U-Th enrichment in alkali olivine basalt magma - Simpson Island Dyke, Northwest Territories, Canada. Contributions to Mineralogy and Petrology, 66, pp. 243-250.

Carmichael, I. S. E., Turner, F. J., and Verhoogen, J. 1974. Igneous Petrology. McGraw-Hill, New York. 739 p.

Daly, R. A. 1912. North American Cordillera, Forty-Ninth Parallel. Geological Survey of Canada, Memoir 38. 546 p.

Dawson, G. M. 1889. Report on a portion of the West Kootenai District, B. C. Geological Survey of Canada Annual Report.

Dickinson, W. R., and Snyder, W. S. 1978. Plate tectonics of the Laramide orogeny. Geological Society of America, Memoir 151, pp. 355-366.

Drysdale, C. W. 1915. Geology and ore deposits of Rossland, British Columbia. Geological Survey of Canada, Memoir 77. 317 p.

Drysdale, C. W. 1917. Ymir mining camp, British Columbia. Geological Survey of Canada, Memoir 94. 185 p.

Eggler, D. H. 1978. The effect of CO_2 upon partial melting of peridotite in the system Na_2O-CaO-Al_2O_3-MgO-SiO_2-CO_2 to 35 kilobars with an analysis of the melting in a peridotite-H_2O-CO_2 system. American Journal of Science, 278, pp. 305-343.

Fairbairn, H. W., Hurley, P. M., and Pinson, W. H. 1964. Initial $^{87}Sr/^{86}Sr$ and possible sources of granitic rocks in southern British Columbia. Journal of Geophysical Research, 69, pp. 4889-4893.

Faure, G. 1977. Principles of Isotope Geology. New York, Wiley. 464 p.

Ferrara, G., and Treuil, M. 1974. Petrological implications of trace element and Sr isotope distributions in basalt-pantellerite series. Bulletin Volcanologique, 88, pp. 548-574.

Floyd, P. A., and Winchester, J. A. 1975. Magma type and tectonic setting discrimination using immobile elements. Earth and Planetary Science Letters, 27, pp. 211-218.

Fyles, J. T., Harakal, J. E., and White, W. H. 1973. The age of sulphide mineralization at Rossland, British Columbia. Economic Geology, 68, pp. 23-33.

Gabrielse, H., and Reesor, J. E. 1974. The nature and setting of granitic plutons in the central and eastern parts of the Canadian Cordillera. Pacific Geology, 8, pp. 109-138.

Gast, P. W. 1968. Trace element fractionation and the origin of tholeiitic and alkaline magma types. Geochimica et Cosmochimica Acta, 32, pp. 1057-1086.

Goff, S. 1983. The mobility of major and trace elements in altered volcanics. Unpublished manuscript.

Hart, S. R. and Allegre, C. J. 1980. Trace-element constraints on magma genesis. *In* Physics of Magmatic Processes, *Edited by* R. B. Hargraves. Princeton University Press, New York, pp. 121-159.

Hurlburt, C. S. 1939. Igneous rocks of the Highwood Mountains, Montana. Geological Society of America Bulletin, 50, pp. 1043-1112.

Irvine, T. N., and Baragar, W. R. A. 1971. A guide to the chemical classification of the common volcanic rocks. Canadian Journal of Earth Sciences, 8, pp. 523-548.

Keith, S. B. 1982. Paleoconvergence rates determined from $K_2O/SiO2$ ratios in magmatic rocks and their application to Cretaceous and Tertiary tectonic patterns in Southwestern North America. Geological Society of America Bulletin, 93, pp. 524-534.

Lambert, R.St St. J., and Holland, J. G. 1974. Yttrium geochemistry applied to petrogenesis utilizing calciumyttrium relationships in minerals and rocks. Geochimica et Cosmochimica Acta, 88, pp. 1393-1414.

Le Maitre, R. W. 1962. Petrology of volcanic rocks, Gough Island, South Atlantic. Geological Society of America Bulletin, 73, pp. 1309-1340.

Leroux, J. 1980. Geothermal potential of the Coryell Intrusions, Granby River area, British Columbia; *In* Current Research, Part B, Geological Survey of Canada Paper 80-1B, pp. 213-215.

Little, H. W. 1960. Nelson Map-area, west half, British Columbia. Geological Survey of Canada, Memoir 308. 205 p.

Little, H. W. 1982. Geology of the Rossland-Trail map-area, British Columbia. Geological Survey of Canada, Paper 79-26. 38 p.

Lloyd, F. E., and Bailey, D. K. 1975. Light element metasomatism of the continental mantle: the evidence and the consequences. Physics and Chemistry of the Earth, 9, pp. 389-416.

MacDonald, G. A., and Katsura, T. 1964. Chemical composition of Hawaiian lavas. Journal of Petrology, 5, pp. 82-133.

MacDonald, G. A. 1968. Composition and origin of Hawaiian lavas. Geological Society of America, Memoir 116, pp. 477-522.

Mathews, W. H. 1953. Geology of the Sheep Creek Camp. British Columbia Department of Mines, Bulletin 31.

Mathews, W. H. 1964. Potassium-argon determinations of Cenozoic volcanic rocks from British Columbia. Geological Society of America Bulletin, 75, pp. 465-468.

Mathews, W. H. 1981. Early Cenozoic resetting of potassium-argon dates and geothermal history of north Okanagan area, British Columbia. Canadian Journal of Earth Sciences, 18, pp. 1310-1319.

McAllister, A. L. 1950. The Geology of the Ymir Map-area, British Columbia. Unpubl. PhD. Thesis, McGill University, Montreal.

Medford, G. A. 1975. K-Ar and fission track geochronology of an Eocene thermal event in the Kettle River (West half) map area, Southern British Columbia. Canadian Journal of Earth Sciences, 12, pp. 836-843.

Menzies, M., and Murthy, V. R. 1980. Mantle metasomatism as a precursor to the genesis of alkaline magmas isotopic evidence. American Journal of Science, 280-A, pp. 622-638.

Monger, J. W. H. 1967. Early Tertiary stratified rocks, Greenwood map-area, British Columbia. Geological Survey of Canada, Paper 67-42. 39 p.

Monger, J. W. H., Price, R. A., and Tempelman-Kluit, D. J. 1982. Tectonic accretion and the origin of the two major metamorphic and plutonic welts in the Canadian Cordillera. Geology, 10, pp. 70-75.

Nash, W. P., and Wilkinson, J. F. G. 1971. Shonkin Sag Laccolith, Montana. II. Bulk Rock Geochemistry. Contributions to Mineralogy and Petrology, 33, pp. 162-170.

Nockolds, S. R. 1954. Average chemical compositions of some igneous rocks. Geological Society of America Bulletin, 65, pp. 1007-1032.

Nockolds, S. R., and Allen, R. 1953. The geochemistry of some igneous rock series. Geochimica et Cosmochimica Acta, 4, pp. 105-142.

Osborne, F. F., and Roberts, E. J. 1931. Differentiation in the Shonkin Sag Laccolith, Montana. American Journal of Science, 22, pp. 331-353.

Padgham, W. A. 1955. The structure and petrology of the Salmon River monzonite. Unpubl. B. A. Sc thesis, University of British Columbia. 24 p.

Peacock, M. A. 1931. Classification of igneous rock series. Journal of Geology, 39, pp. 54-67.

Pearce, J. A., and Cann, J. R. 1973. Tectonic setting of basic volcanic rocks determined using trace element analyses. Earth and Planetary Science Letters, 19, pp. 290-300.

Pearce, J. A., and Norry, M. J. 1979. Petrogenetic implication of Ti, Zr, Y, and Nb variations in volcanic rocks. Contributions to Mineralogy and Petrology, 69, pp. 33-47.

Price, R. A., and Mountjoy, E. W. 1970. Geologic structure of the Canadian Rocky Mountains between Bow and Athabasca Rivers - A progress report. *In* Structure of the Southern Canadian Cordillera. *Edited by* J. O. Wheeler. Geological Society of Canada Special Paper, 6, pp. 7-25.

Price, R. A. 1980. The Cordilleran overthrust belt in southern Canada. Canadian Society of Petroleum Geologists Reservoir, 7, No. 8, pp. 1-2.

Price, R. A. 1981. The Cordilleran foreland thrust and fold belt in the southern Canadian Rocky Mountains, *In* Thrust and Nappe Tectonics. *Edited by* N. J. Price and K. McClay. Geological Society of London, Special Publication 9, pp. 427-448.

Rice, H. M. A. 1941. Nelson Map-area, east half. Geological Survey of Canada, Memoir 228. 86 p.

Ringwood, A. E. 1962. Present status of the chondritic earth model. *In* Researches in Meteorites. Edited by C. B. Moore. Wiley, New York, pp. 198-216.

Ringwood, A. E. 1974. The petrological evolution of island arc systems. Geological Society of London Journal, 130, pp. 183-204.

Ringwood, A. E. 1975. Compostion and Petrology of the Earth's Mantle. McGraw-Hill, Inc., New York, N.Y. 618 p.

Ross, J. V. 1981. A geodynamic model for some structures within and adjacent to the Okanagan Valley, Southern British Columbia. Canadian Journal of Earth Sciences, 18, pp. 1581-1598.

Shand, S. J. 1943. Eruptive Rocks. Wiley, New York. 488 p.

Shaw, D. M. 1968. A review of K-Rb fractionation trends by covariance analysis. Geochimica et Cosmochimica Acta, 32, pp. 573-601.

Smith, D. G. W. and Gold, C. M. 1979. :EDATAII: A FortranIV computer program for processing wavelengths and/or energy-dispersive electron microprobe analyses. Microbeam Analyses Society Proceedings. 14th Annual Conference, San Antonio, 1979. Edited by D. E. Newbury, pp. 273-278.

Sorenson, H. *Ed.* 1974. The Alkaline Rocks. John Wiley and Sons, London. 622 p.

Stacey, R. A. 1973. Gravity anomalies, crustal structure, and plate tectonics in the Canadian Cordillera. Canadian Journal of Earth Sciences, 10, pp. 615-627.

Streckeisen, A. 1973. Plutonic rocks: classification and nomenclature recommended by the IUGS Subcommission on the Systematics of Igneous

Rocks. Geotimes, pp. 26-30.

Streckeisen, A. 1979. Classification and nomenclature of volcanic rocks, lamprophyres, carbonatites, and melilitic rocks: recommendations and suggestions of the IUGS Subcommission on the Systematics of Igneous Rocks. Geology, 7, pp. 331-335.

Sutherland Brown, A. 1980. Metallogeny by numbers. Geoscience Canada, 7, pp. 95-102.

Taylor, S. R. 1965. The application of trace element data to problems in petrology. Physics and Chemistry of the Earth, 6, pp. 133-204.

Turekian, K. K., and Wedepohl, K. H. 1961. Distribution of the elements in some major units of the earth's crust. Geological Society of America Bulletin, 72, pp. 175-192.

Ussing, N. V. 1912. Geology of the country around Julianhaab, Greenland. Medd. om Gronland, 38, pp. 1-376.

Van Kooten, G. K. 1980. Mineralogy, petrology, and geochemistry of an ultrapotassic basaltic suite, central Sierra Nevada, California, U.S.A. Journal of Petrology, 21, pp. 651-684.

Weaver, S. D., Sceal, J. S. C., and Gibson, I. L. 1972. Trace-element data relevant to the origin of trachytic and pantelleritic lavas in the East African rift system. Contributions to Mineralogy and Petrology, 36, pp. 181-194.

Weed, W. H., and Pirsson, V. 1895. Highwood Mountains of Montana. Geological Society of America Bulletin, 6, pp. 389-422.

Wendlandt, R. F., and Eggler, D. H. 1980a. The origins of potassic magmas: 1. melting relations in the systems $KAlSiO_4$-$MgSiO_4$-SiO_2 and $KAlSiO_4$-MgO-SiO_2-CO_2 to 30 kilobars. American Journal of Science, 280, pp. 345-420.

Wendlandt, R. F., and Eggler, D. H. 1980b. The origins of potassic magmas: 2. Stability of phlogopite in natural spinel lherzolite and in the system $KAlSiO_4$-MgO-SiO_2-H_2O-CO_2 at high pressures and high tempertures. American Journal of Science, 280, pp. 421-458.

Wendlandt, R. F. and Mysen, B. O. 1978. Melting phase relations of natural peridotite and CO_2 as a function of degree of partial melting at 15 and 30 kilobars. Carnegie Institute of Washington Yearbook, 77, pp. 756-761.

Wheeler, J. O., and Gabrielse, H. 1972. The Cordilleran structural province. *In* Variations in Tectonic Styles. *Edited by* R. A. Price and R. J. W. Douglas. Geological Association of Canada, Special Paper, 11, pp. 2-81.

Winchester, J. A., and Floyd, P. A. 1977. Geochemical discrimination of different magma series and their differentiation products using immobile elements. Chemical Geology, 20, pp. 325-343.

Wyllie, P. J. 1979. Magmas and volatile components. American Mineralogist, 64, pp. 469-500.

Yoder, H. S., and Tilley, C. E. 1962. Origin of basalt magmas: An experimental study of natural and synthetic rock systems. Journal of Petrology, 3, pp. 342-532.

APPENDIX I. GEOCHEMICAL ANALYSES

ROSSLAND RAILWAY (10617)

SAMPLE	1	2	3	4	5A	6	8	5A
SIO2	51.6	54.7	53.8	52	53.9	55.7	54.5	60.1
AL2O3	14.7	15.3	14.5	17.8	14.9	15.6	15.9	14.4
FE2O3	9.10	7.26	7.75	7.57	7.63	6.81	8.04	5.66
MGO	7.18	5.98	6.49	6.04	6.85	5.68	6.39	4.70
CAO	8.03	6.63	7.58	6.73	6.72	5.65	6.31	5.34
NA2O	3.09	4.38	3.33	3.78	3.43	4.00	3.14	3.80
K2O	4.43	4.38	4.93	4.54	4.93	5.15	4.96	4.80
TIO2	0.91	0.78	0.81	0.78	0.83	0.74	0.84	0.60
MNO	0.12	0.14	0.11	0.12	0.13	0.11	0.10	0.10
P2O5	0.76	0.51	0.63	0.68	0.64	0.57	0.62	0.47
RB	135	146	148	129	158	157	164	163
SR	1474	783	1393	228	1358	1328	1366	1147
Y	30	34	27	27	27	25	25	26
ZR	158	335	181	161	140	188	182	192
NB	43	55	48	39	46	50	50	56
BA	2948	685	2288	2328	2442	2289	2382	1817
U	3.16	6.55	3.21	2.87	2.54	2.89	3.47	4.02
TH	9	22	10.1	8	10.7	10.1	13.4	18.8
CR	20	20	24	12	22	22	20	16
CO	34	58	26	30	32	34	28	30
NI	50	34	42	44	40	34	34	26
CU	50	374	50	48	16	48	38	10
ZN	58	58	66	64	58	52	52	46
AS	2	3	1	1	1	1	1	1
MO	1	1	1	1	1	1	1	1
HG	10	20	10	10	20	20	10	40
PB	4	8	6	2	6	6	10	8

EO ROSSLAND HIGHWAY (10621)

SAMPLE	5-1	7	8	9	2	5	3	6
SIO2	53.7	52.6	53.8	53.2	53.9	54.9	48.3	75
AL2O3	14.5	14.5	14.8	14.3	14.3	14.5	13.7	13.4
FE2O3	7.62	8.63	7.77	8.21	7.96	7.55	9.72	1.88
MGO	7.43	7.02	6.59	7.39	6.96	6.69	9.69	0.51
CAO	7.05	7.91	7.48	7.27	7.37	6.87	10.58	0.19
NA2O	3.23	3.09	3.16	3.14	3.14	3.73	3.19	4.01
K2O	4.80	4.54	4.79	4.70	4.66	3.29	1.80	4.89
TIO2	0.84	0.90	0.83	0.88	0.88	1.10	1.24	0.07
MNO	0.13	0.14	0.13	0.13	0.14	0.13	0.17	0.04
P2O5	0.64	0.68	0.68	0.70	0.68	1.26	1.62	0.01
RB	144	139	137	147	137	109	41	196
SR	1125	1276	1492	1321	1390	1544	1592	113
Y	31	27	25	28	26	53	37	26
ZR	159	112	168	180	165	245	191	152
NB	43	47	40	46	45	80	75	114
BA	2224	2429	2931	2654	2484	4023	2293	194
U	2.35	2.49	2.81	3.15	2.65	5.51	2.19	10.95
TH	11.6	8.8	9.8	10.7	7.6	22	8.4	53
CR	16	20	20	20	22	32	36	2
CO	28	30	24	32	26	30	34	58
NI	40	48	42	44	40	78	94	2
CU	40	52	44	50	48	34	54	1
ZN	48	60	56	54	52	88	72	32
AS	2	2	1	2	2	3	2	2
MO	1	1	1	1	1	1	2	1
HG	10	10	10	10	10	10	10	10
PB	4	2	4	2	6	44	6	24

JERSEY (10564)

SAMPLE	1	2	3	4	5
SIO2	51.6	50.3	50.3	52.8	51.5
AL2O3	14.6	14.3	15.9	16.4	14.8
FE2O3	8.12	8.51	8.97	7.97	8.44
MGO	6.93	8.46	4.89	5.64	7.27
CAO	9.02	9.51	10.63	7.61	8.96
NA2O	2.94	2.21	2.50	3.48	2.19
K2O	4.75	4.73	4.46	4.05	4.55
TIO2	1.13	1.14	1.31	1.04	1.25
MNO	0.12	0.12	0.14	0.16	0.13
P2O5	0.91	0.75	0.93	0.88	0.92
RB	150	148	129	200	146
SR	1427	1266	1033	844	1391
Y	40	36	37	25	38
ZR	157	146	150	221	160
NB	41	38	40	15	40
BA	2591	2804	1722	1636	2868
U	2.91	2.66	2.6	3.67	2.97
TH	7.8	7.8	7.8	13.4	8.9
CR	24	22	26	14	32
CO	24	28	22	24	30
NI	42	86	40	40	72
CU	46	50	1	44	36
ZN	62	62	102	70	62
AS	1	1	1	2	1
MO	1	1	1	1	1
HG	20	20	10	20	10
PB	4	1	1	1	1

SAMPLE	6	8	9	10	11	20
SIO2	51.5	51.6	50.4	53.7	53.4	43.6
AL2O3	14.9	15.1	16.1	16	16.8	9.8
FE2O3	8.50	8.25	9.46	7.90	7.46	12.59
MGO	7.02	6.73	5.98	5.65	5.61	13.59
CAO	8.81	8.62	8.48	7.28	8.89	12.19
NA2O	2.54	3.08	2.93	3.22	3.29	0.91
K2O	4.46	4.12	4.18	4.21	4.63	3.26
TIO2	1.22	1.32	1.23	1.01	1.01	1.73
MNO	0.11	0.15	0.11	0.13	0.12	0.15
P2O5	0.91	0.99	1.09	0.89	0.81	2.19
RB	92	112	137	141	133	92
SR	746	1272	1746	1684	1465	833
Y	50	36	47	45	31	34
ZR	188	214	159	140	180	100
NB	26	31	39	40	36	23
BA	1038	3458	3451	2821	2346	5040
U	2.52	3.32	3.3	3.28	2.92	1.55
TH	7.6	10	9.2	9.5	9.4	4.2
CR	24	14	10	12	12	18
CO	24	30	26	30	22	44
NI	50	44	42	36	34	154
CU	56	44	54	44	34	200
ZN	22	62	68	66	64	72
AS	2	3	3	1	1	2
MO	1	1	1	1	3	1
HG	10	20	20	20	10	20
PB	6	1	1	6	4	4

YMIR (10563)

SAMPLE	2	3	4	5	8	9
SIO2	51.3	52.2	52.3	51.9	52.4	52.9
AL2O3	11.7	11.7	12.4	11.8	12	12.5
FE2O3	8.19	7.81	7.80	8.35	7.87	7.65
MGO	12.01	11.65	10.30	11.36	11.03	9.94
CAO	8.03	7.87	7.88	7.86	8.00	7.30
NA2O	1.84	2.20	2.01	2.02	2.02	2.66
K2O	5.40	5.00	5.62	5.06	5.07	5.39
TIO2	0.60	0.62	0.69	0.71	0.66	0.76
MNO	0.12	0.14	0.14	0.14	0.13	0.14
P2O5	0.87	0.82	0.83	0.80	0.83	0.76
RB	230	177	203	177	404	180
SR	882	1061	1015	851	791	986
Y	25	24	27	26	20	25
ZR	191	173	211	181	405	185
NB	11	10	13	10	24	10
BA	4582	4643	2673	1765	532	1838
U	3.33	3	3.74	3.44	3.41	3.8
TH	9.1	7.6	9.6	10.4	9.2	12.1
CR	18	14	16	20	20	22
CO	52	40	58	42	52	36
NI	64	108	110	106	110	104
CU	46	58	56	58	66	58
ZN	62	64	60	62	68	62
AS	2	39	1	1	1	1
MO	1	1	1	1	1	1
HG	10	10	10	10	10	20
PB	1	1	4	1	2	1

SAMPLE	10	11	12	13	18
SIO2	52.6	53.8	53.3	53.8	53.3
AL2O3	11.6	13.1	11.3	12.6	12.5
FE2O3	7.81	6.89	7.82	7.22	7.11
MGO	10.99	9.16	10.75	9.83	10.40
CAO	7.95	6.74	8.42	7.66	7.25
NA2O	2.56	3.13	2.16	2.14	2.58
K2O	4.85	5.65	4.57	5.05	5.31
TIO2	0.68	0.66	0.70	0.82	0.73
MNO	0.14	0.12	0.13	0.13	0.11
P2O5	0.76	0.71	0.78	0.73	0.72
RB	209	185	222	191	253
SR	863	736	885	661	1075
Y	21	21	24	20	13
ZR	196	197	232	216	78
NB	14	13	15	17	11
BA	1508	1332	1483	1093	1662
U	4.15	4.72	4.64	5.15	5.02
TH	11.3	14	13.8	14.2	14.2
CR	24	20	26	24	38
CO	32	23	32	30	54
NI	108	88	96	82	96
CU	58	58	72	56	50
ZN	60	58	54	46	60
AS	1	1	1	1	12
MO	1	1	1	1	1
HG	80	20	20	10	10
PB	1	1	4	1	6

SAMPLE	20	23	7	14	15	16	17
SIO2	52.5	52.8	55.2	56.6	59.4	62.9	59.3
AL2O3	12.2	12.3	16.7	16.3	17.7	16.9	17.1
FE2O3	7.59	7.75	6.28	4.61	3.78	3.17	3.53
MGO	10.45	10.42	5.05	6.54	3.39	3.85	4.05
CAO	7.67	7.67	5.11	3.36	2.85	3.85	3.43
NA2O	2.60	2.16	3.92	3.63	3.47	3.57	3.41
K2O	5.28	5.27	6.06	7.52	8.32	4.91	7.97
TIO2	0.77	0.67	0.95	0.94	0.66	0.50	0.76
MNO	0.12	0.13	0.09	0.06	0.05	0.03	0.03
P2O5	0.73	0.79	0.64	0.51	0.37	0.40	0.39
RB	194	180	124	219	275	304	200
SR	793	953	1340	766	1110	993	1440
Y	17	21	32	22	17	14	17
ZR	202	196	168	225	222	216	139
NB	4	13	35	17	15	17	14
BA	1576	1846	2227	1155	1416	1488	1834
U	3.6	4.53	8.78	4.32	4.81	4.19	1.3
TH	11.3	11.5	24.3	13.6	18.3	13.1	3.9
CR	16	22	2	14	14	26	16
CO	34	34	20	22	18	56	16
NI	110	106	16	46	34	46	34
CU	76	56	82	54	38	4	34
ZN	64	58	46	40	36	36	28
AS	1	1	1	1	2	1	1
MO	1	1	1	1	1	1	1
HG	10	10	20	10	10	10	50
PB	2	1	16	14	6	4	1

CULTUS (10620)

SAMPLE	4	5	6	7	8
SIO2	51.2	52.7	55.3	50.9	52.3
AL2O3	12	13.8	13.7	11.9	12.7
FE2O3	8.75	8.44	7.80	8.78	8.13
MGO	11.65	9.02	8.61	11.74	9.65
CAO	8.32	7.12	7.13	8.77	8.42
NA2O	1.86	2.09	1.59	1.89	2.02
K2O	4.59	5.00	4.19	4.39	4.96
TIO2	0.76	0.84	0.81	0.76	0.80
MNO	0.13	0.11	0.12	0.13	0.13
P2O5	0.79	0.80	0.74	0.82	0.84
RB	179	179	152	163	182
SR	1061	1072	978	1032	1239
Y	26	26	24	21	34
ZR	172	219	206	158	194
NB	17	14	14	12	20
BA	1730	1949	1910	1954	2297
U	2.86	2.79	3.40	2.65	3.31
TH	8	6.7	8.9	5.5	8.9
CR	62	44	32	62	36
CO	34	40	32	48	28
NI	90	36	68	86	64
CU	46	54	40	48	52
ZN	56	64	58	60	54
AS	3	2	1	1	2
MO	2	1	2	1	1
HG	10	10	10	10	10
PB	1	1	2	1	4

SAMPLE	1	2	3	DYKE
SIO2	52	51.2	55.3	68.7
AL2O3	12.7	12.7	13.2	16.5
FE2O3	8.61	7.71	7.79	2.87
MGO	10.28	9.20	8.78	0.62
CAO	7.45	11.43	6.95	0.43
NA2O	1.89	1.88	1.82	3.72
K2O	5.22	4.35	4.54	7.04
TIO2	0.81	0.72	0.77	0.11
MNO	0.14	0.10	0.12	0.01
P2O5	0.84	0.73	0.74	0.08
RB	181	166	161	317
SR	1106	1210	987	294
Y	21	34	21	2
ZR	188	172	198	427
NB	12	20	14	28
BA	1966	2168	1762	277
U	3.32	3.49	3.19	7.91
TH	7.8	8.9	9.6	29.1
CR	64	34	34	4
CO	36	26	34	22
NI	90	62	72	8
CU	26	46	74	12
ZN	70	46	58	24
AS	2	2	1	2
MO	1	2	1	1
HG	10	10	10	10
PB	1	1	2	4

MCGREGOR (10619)

SAMPLE	1	2	4	5	6
SIO2	48.6	50.3	50.8	49.6	48.5
AL203	9.1	12.1	12.6	14.1	9.6
FE203	6.39	9.07	8.56	9.28	7.81
MGO	17.85	11.87	11.02	10.25	16.17
CAO	10.97	9.87	9.93	8.40	10.28
NA2O	0.89	1.69	1.88	2.09	0.76
K2O	4.68	3.48	3.70	4.60	4.91
TIO2	1.22	0.66	0.68	0.77	1.29
MNO	0.07	0.14	0.13	0.14	0.10
P2O5	0.24	0.76	0.71	0.80	0.67
RB	121	190	124	160	204
SR	997	363	1015	1200	336
Y	21	11	23	23	16
ZR	127	53	148	182	49
NB	11	12	11	15	10
BA	1907	3343	1830	2343	3929
U	2.36	0.80	2.72	3.47	1.15
TH	6.4	2.1	6.3	8	2
CR	20	104	20	22	104
CO	20	34	32	48	42
NI	42	200	76	68	116
CU	38	82	46	80	66
ZN	62	32	48	52	48
AS	1	1	2	2	1
MO	1	1	1	1	1
HG	10	20	10	30	50
PB	1	1	1	1	1

SAMPLE	7	8	10	12
SIO2	51.7	51.5	51.5	52.5
AL2O3	13.7	12.1	14.5	15.2
FE2O3	8.40	8.78	8.37	7.73
MGO	9.42	10.93	8.82	7.63
CAO	8.59	8.31	7.72	7.02
NA2O	2.02	1.81	2.62	2.84
K2O	4.45	4.63	4.66	5.40
TIO2	0.76	0.87	0.84	0.82
MNO	0.13	0.16	0.16	0.11
P2O5	0.76	0.90	0.75	0.76
RB	155	154	169	188
SR	1094	1168	1018	1205
Y	22	24	22	22
ZR	153	148	170	177
NB	14	15	16	15
BA	2320	2433	1955	3148
U	3.09	2.38	3.44	3.78
TH	8.5	5.7	9.3	10.1
CR	20	42	18	16
CO	44	36	26	30
NI	58	64	38	42
CU	32	50	38	94
ZN	54	54	58	48
AS	2	1	2	2
MO	1	1	1	1
HG	10	20	20	10
PB	1	1	6	1

MAIN BATHOLITH

SAMPLE	U	K	N	O
SIO2	61.8	60.6	61.9	58.6
AL203	18.5	19.5	18.1	19
FE203	3.75	4.19	4.19	4.46
MGO	1.13	0.27	1.40	1.89
CAO	1.87	2.39	2.19	3.29
NA2O	4.39	5.50	4.76	3.90
K2O	7.74	7.15	6.69	7.36
TIO2	0.54	0.31	0.47	0.92
MNO	0.06	0.14	0.10	0.05
P2O5	0.23	0.02	0.21	0.47
RB	205	244	196	244
SR	1066	1221	742	1532
Y	19	21	19	16
ZR	244	253	396	142
NB	40	57	39	32
BA	1571	1885	1085	3295
U	4.05	4.88	1.82	1.39
TH	15.4	15	8.5	4.3
CR	1	2	14	6
CO	42	19	16	20
NI	2	2	6	10
CU	4	6	8	14
ZN	46	76	36	44
AS	1	1	1	1
MO	1	1	1	1
HG	30	10	10	20
PB	6	4	6	1

APPENDIX II. NORMATIVE CALCULATIONS

ROSSLAND RAILWAY (10617)

SAMPLE	1	2	3	4
Q	0	0	0	0
OR	26.2	25.9	29.2	26.8
AB	18.4	27.7	21.6	21.1
AN	\13.1	9.1	10.1	18.2
NE	4.2	5.1	3.6	5.9
DI	12	11.5	13.3	6
HE	5.5	5	5.7	2.7
EN	0	0	0	0
FS	0	0	0	0
FO	8.6	6.7	7	8.6
FA	5	3.7	3.8	4.9
MT	3.3	2.6	2.8	2.7
IL	1.7	1.5	1.5	1.5
AP	1.8	1.2	1.5	1.6
D.I.	48.9	58.7	54.3	53.8
COL. I.	36.2	31	34.1	26.4
NAME	TRACHYBAS POTASSIC	TRACHYBAS POTASSIC	TRACHYBAS POTASSIC	TRACHYBAS POTASSIC

SAMPLE	5A	5B	6	8
Q	3.2	0	0	0
OR	28.4	29.2	30.5	29.1
AB	32.2	23.8	29.5	26.4
AN	8	10.7	9.4	14.5
NE	0	2.9	2.4	0
DI	8.7	10.7	8.4	7
HE	3.8	4.3	3.6	3.1
EN	7.7	0	0	.5
FS	3.8	0	0	.2
FO	0	8.5	7.2	8.5
FA	0	4.3	3.9	4.8
MT	2.1	2.8	2.5	2.9
IL	1.1	1.6	1.4	1.6
AP	1.1	1.5	1.3	1.4
D.I.	63.7	55.8	62.3	55.5
COL. I.	27.2	32	27	28.6
NAME	CALC-ALK HIGH AL	TRACHYBAS POTASSIC	TRACHYBAS POTASSIC	TRACHYBASA POTASSIC

ROSSLAND HIGHWAY (10621)

SAMPLE	5-1	6	7	8
Q	0	30.8	0	0
C	0	1.2	0	0
OR	28.4	29	26.9	28.3
AB	23.1	33.9	20.4	23.4
AN	10.9	.9	12.3	12
NE	2.3	0	3.1	1.8
DI	11.7	0	12.6	11.7
HE	4.3	0	5.6	5
EN	0	1.3	0	0
FS	0	2.2	0	0
FO	9.2	0	8.1	7.7
FA	4.2	0	4.6	4.1
MT	2.8	.7	3.1	2.8
IL	1.6	.1	1.7	1.6
AP	1.5	0	1.6	1.6
D.I.	53.8	93.7	50.4	53.5
COL. I.	33.8	4.2	35.8	32.9
NAME	TRACHYBAS POTASSIC	CALC-ALK RHYOLITE	TRACHYBAS POTASSIC	TRACHYBAS POTASSIC

SAMPLE	9	2	5	3
Q	0	0	0	0
C	0	0	0	0
OR	27.8	27.6	19.5	10.6
AB	22.5	24.7	31.5	22.5
AN	11	11.1	13.1	17.7
NE	2.2	1	0	2.4
DI	11.8	12	7.4	14.4
HE	4.7	4.9	2.8	5
EN	0	0	10.4	0
FS	0	0	4.6	0
FO	9.1	8.2	1.9	12.2
FA	4.6	4.3	.9	5.4
MT	3	2.9	2.7	3.5
IL	1.7	1.7	2.1	2.4
AP	1.6	1.6	2.9	3.8
D.I.	52.5	53.3	51	35.6
COL. I.	34.8	34	33	42.9
NAME	TRACHYBAS POTASSIC	TRACHYBAS POTASSIC	CALC-ALK HIGH ALUM ANDESITE AVERAGE	ALKALI BA POTASSIC

JERSEY (10564)

SAMPLE	1	2	3	4
Q	0	0	0	0
OR	28	28	26.4	24
AB	14.9	9.5	12.2	26.9
AN	12.6	15.1	19	17.2
NE	5.4	5	4.8	1.4
DI	15.1	16.2	14	8.1
HE	6	5.6	8.6	4
EN	0	0	0	0
FS	0	0	0	0
FO	7.2	9.4	4	7.2
FA	3.6	4.1	3.1	4.5
MT	2.9	3.1	3.2	2.9
IL	2.1	2.2	2.5	2
AP	2.1	1.7	2.2	2
D.I.	48.3	42.5	43.4	52.2
COL. I.	37	40.7	35.5	28.6
NAME	TRACHYBAS POTASSIC	ALKALI BA POTASSIC	ALKALI BA POTASSIC	TRACHYBAS POTASSIC

SAMPLE	5	6	8	9
Q	0	0	0	0
OR	26.9	26.4	24.4	24.7
AB	18	18.4	21.1	19.3
AN	17.1	16.1	15.2	18.4
NE	.3	1.7	2.7	3
DI	12.4	12.5	12.1	8.7
HE	4.8	5.1	4.9	4.7
EN	0	0	0	0
FS	0	0	0	0
FO	8.7	8.2	7.8	7.6
FA	4.2	4.2	4	5.2
MT	3.1	3.1	3	3.4
IL	2.4	2.3	2.5	2.3
AP	2.1	2.1	2.3	2.5
D.I.	45.2	46.5	48.2	47
COL. I.	35.6	35.4	34.3	32
NAME	ALKALI BA POTASSIC	ALKALI BA POTASSIC	TRACHYBAS POTASSIC	ALKALI BA POTASSIC

SAMPLE	10	11	20
Q	0	0	0
OR	24.9	26.8	19.3
AB	27.2	19.2	.2
AN	16.8	17	13
NE	0	4.4	4.1
DI	7.4	11.7	20.2
HE	3.6	5.3	6.3
EN	2.9	0	0
FS	1.6	0	0
FO	5.4	5.8	17.1
FA	3.3	3.3	6.8
MT	2.9	2.7	4.6
IL	1.9	1.9	3.3
AP	2.1	1.8	5.1
D.I.	52.2	50.4	23.6
COL. I.	29	30.7	58.4
NAME	THOLEIITI ANDESITE AVERAGE	TRACHYBAS POTASSIC	ANKARAMIT POTASSIC

YMIR (10563)

SAMPLE	2	3	4	5
Q	0	0	0	0
OR	32	29.6	33.3	29.9
AB	9.1	14.2	12.1	13.7
AN	7.7	7.3	8.2	8.2
NE	3.5	2.4	2.7	1.8
DI	16.8	16.8	16	16.1
HE	4.3	4.2	4.5	4.4
EN	0	0	0	0
FS	0	0	0	0
FO	15.5	14.9	12.8	14.6
FA	5	4.7	4.5	5
MT	3	2.8	2.8	3
IL	1.1	1.2	1.3	1.3
AP	2	1.9	1.9	1.9
D.I.	44.5	46.1	48	45.5
COL. I.	45.8	44.7	41.9	44.5
NAME	ALKALI BA POTASSIC	TRACHYBAS POTASSIC	ALKALI BA POTASSIC	ALKALI BA POTASSIC

SAMPLE	8	9	10	11
Q	0	0	0	0
OR	30	31.9	28.7	33.4
AB	15	15.4	15.7	16.9
AN	8.7	6.2	5.8	5
NE	1.1	3.8	3.2	5.2
DI	16.2	15.6	18.1	14.9
HE	4.3	4.4	4.8	4.1
EN	0	0	0	0
FS	0	0	0	0
FO	14	12.3	13.3	11.1
FA	4.7	4.4	4.4	3.9
MT	2.9	2.8	2.8	2.5
IL	1.6	1.4	1.3	1.3
AP	1.9	1.8	1.8	1.6
D.I.	46.1	51.2	47.6	55.5
COL. I.	43.3	40.9	44.8	37.8
NAME	ALKALI BA POTASSIC	TRACHYBAS POTASSIC	TRACHYBAS POTASSIC	TRACHYBAS POTASSIC

SAMPLE	12	13	18	20
Q	0	0	0	0
OR	27	29.9	31.4	31.3
AB	18.3	18.1	16.8	13.6
AN	7.6	9.8	6.8	6
NE	0	0	2.7	4.6
DI	18.3	14.8	15.7	17.3
HE	4.9	3.9	3.8	4.5
EN	1.7	3.2	0	0
FS	.5	1	0	0
FO	11.6	10.1	13.1	12.6
FA	3.9	3.3	4	4.2
MT	2.8	2.6	2.6	2.7
IL	1.3	1.6	1.4	1.5
AP	1.8	1.7	1.7	1.7
D.I.	45.3	48	50.9	49.4
COL. I.	45.2	40.5	40.6	42.9
NAME	CALC-ALK HIGH ALUM ANDESITE K-RICH	CALC-ALK HIGH ALUM BASALT K-RICH	TRACHYBAS POTASSIC	TRACHYBAS POTASSIC

SAMPLE	23	7	14	15
Q	0	0	0	0
OR	31.2	35.8	44.5	49.2
AB	15.8	24.7	21.8	28
AN	8.3	10	5.9	8.1
NE	1.3	4.6	4.8	.8
DI	15.4	6.4	4.8	2.1
HE	4.3	2.6	1	.8
EN	0	0	0	0
FS	0	0	0	0
FO	13.2	6.7	9.8	5.2
FA	4.6	3.5	2.6	2.3
MT	2.8	2.3	1.7	1.4
IL	1.3	1.8	1.8	1.3
AP	1.8	1.5	1.2	.9
D.I.	48.3	65.1	71.1	78
COL. I.	41.5	23.3	21.8	13
NAME	TRACHYBAS POTASSIC	TRACHYBAS POTASSIC	TRISTANIT POTASSIC	TRISTANIT POTASSIC

SAMPLE	16	17
Q	9.3	0
OR	29	47.2
AB	30.2	28.2
AN	15.6	7.8
NE	0	.3
DI	.6	4.3
HE	.2	1.1
EN	9.3	0
FS	2.9	0
FO	0	5.7
FA	0	1.8
MT	1.1	1.3
IL	.9	1.4
AP	.9	.9
D.I.	68.5	75.7
COL. I.	15	15.6

NAME CALC-ALK TRISTANIT
HIGH-ALUM POTASSIC
ANDESITE
AVERAGE

CULTUS (10620)

SAMPLE	4	5	6	7
Q	0	0	3.1	0
OR	27.1	29.6	24.8	25.9
AB	13.9	17.7	13.5	13.1
AN	10.8	13.5	17.9	11
NE	1	0	0	1.6
DI	15.8	10	7.7	17
HE	4.4	3.4	2.5	4.7
EN	0	3.8	17.9	0
FS	0	1.5	6.7	0
FO	15.2	9.8	0	14.9
FA	5.3	4.2	0	5.2
MT	3.2	3.1	2.8	3.2
IL	1.4	1.6	1.5	1.4
AP	1.8	1.9	1.7	1.9
D.I.	42	47.3	41.3	40.6
COL. I.	45.3	37.3	39.1	46.5
NAME	ALKALI BA POTASSIC	CALC-ALK HIGH ALUM BASALT K-POOR	THOLEIITI K-POOR	ALKALI BA POTASSIC

SAMPLE	8	1	2	3
Q	0	0	0	1
OR	29.4	30.9	25.7	26.9
AB	16	15.9	8.6	15.4
AN	10.9	10.7	13.4	14.4
NE	.6	.07	4	0
DI	15.6	12.7	23.7	9.2
HE	4.8	3.9	7.2	3
EN	0	0	0	17.6
FS	0	0	0	6.5
FO	11.8	13.8	8.4	0
FA	4.6	5.4	3.2	0
MT	2.9	3.1	2.8	2.8
IL	1.5	1.5	1.4	1.5
AP	2	2	1.7	1.7
D.I.	46	46.8	38.3	43.3
COL. I.	41.2	40.4	46.7	40.6
NAME	ALKALI BA POTASSIC	ALKALI BA POTASSIC	ALKALI BA POTASSIC	THOLEIITI K-POOR

MT. MCGREGOR (10619)

SAMPLE	1	2	4	5	6
Q	0	0	0	0	0
OR	11.4	20.6	21.9	27.2	22.2
AB	0	14.3	14.4	9.9	0
AN	7.1	15.2	15	15.5	8.3
LC	12.8	0	0	0	5.3
NE	4.1	0	.8	4.2	3.5
DI	32.5	17.9	18.4	12.6	26.2
HE	3.6	5.3	5.3	4.3	4.1
EN	0	.3	0	0	0
FS	0	.1	0	0	0
FO	20.6	14.7	13.3	13.8	19.7
FA	2.9	5.5	4.9	5.9	3.9
MT	2.3	3.1	3.1	3.3	2.8
IL	2.3	1.3	1.3	1.5	2.4
AP	.6	1.8	1.6	1.9	1.6
D.I.	28.2	34.9	37.1	41.3	31
COL. I.	64.2	48.2	46.2	41.3	59.2
NAME	ANKARAMIT POTASSIC	THOLEIITI K-POOR	ALKALI BA POTASSIC	ALKALI BA POTASSIC	ANKARAMITE POTASSIC

SAMPLE	7	8	10	12
Q	0	0	0	0
OR	26.3	27.4	27.6	31.9
AB	17.1	15.3	16.8	17
AN	15.2	11.2	14	12.8
LC	0	0	0	0
NE	0	0	2.9	3.8
DI	13.6	14.9	11.6	10.1
HE	4.5	4.4	4	3.7
EN	.1	.9	0	0
FS	.04	.3	0	0
FO	12	13.6	11.6	10
FA	5	5	5.1	4.6
MT	3	3.2	3	2.8
IL	1.4	1.7	1.6	1.6
AP	1.8	2.1	1.7	1.8
D.I.	43.4	42.7	47.3	52.7
COL. I.	39.6	44	37	32.8
NAME	THOLEIITI K-POOR	CALC-ALK HIGH ALUM BASALT K-RICH	ALKALI BA POTASSIC	TRACHYBAS POTASSIC

APPENDIX III. MODAL ANALYSES

ROSSLAND RAILWAY (10617)

SAMPLE	1	2	3	4	5
KSPAR	36	33	44	47	32
PLAGIOCLASE	15	14	11	22	8
QUARTZ	–	–	–	–	–
BIOTITE	24	28	18	20	14
OLIVINE	3	TR	2	1	2
AUGITE	23	22	24	5	41
MAGNETITE	TR	2	TR	2	1
APATITE	TR	TR	1	1	2
OTHER	–	CC TR	–	–	SP TR

SAMPLE	6	8
KSPAR	42	56
PLAGIOCLASE	15	15
QUARTZ	–	–
BIOTITE	15	11
OLIVINE	1	1
AUGITE	26	17
MAGNETITE	TR	TR
APATITE	TR	TR
OTHER	–	–

ROSSLAND HIGHWAY (10621)

SAMPLE	1	5A	5B	7	8
KSPAR	37	34	38	30	38
PLAGIOCLASE	11	16	16	14	17
QUARTZ	1	TR	–	TR	–
BIOTITE	22	16	15	19	17
OLIVINE	2	2	1	TR	2
AUGITE	26	32	29	35	27
MAGNETITE	1	TR	–	TR	TR
APATITE	TR	TR	TR	1	TR
OTHER	–	–	–	–	CC TR

SAMPLE	9	2
KSPAR	45	37
PLAGIOCLASE	14	11
QUARTZ	–	TR
BIOTITE	15	20
OLIVINE	3	4
AUGITE	20	27
MAGNETITE	TR	–
APATITE	TR	1
OTHER	–	–

YMIR (10563)

SAMPLE	2	3	4A	5	7
KSPAR	37	49	47	43	84
PLAGIOCLASE	2	5	5	4	TR
QUARTZ	–	–	–	–	–
BIOTITE	12	12	10	10	15
OLIVINE	19	17	16	9	–
AUGITE	29	18	21	25	TR
MAGNETITE	–	–	1	–	–
APATITE	1	1	TR	TR	TR
OTHER	–	–	–	–	SP TR

SAMPLE	8	9	10	11	12
KSPAR	48	48	52	49	40
PLAGIOCLASE	4	5	3	3	3
QUARTZ	–	–	–	–	–
BIOTITE	12	14	14	17	13
OLIVINE	14	10	11	6	16
AUGITE	22	23	17	21	25
MAGNETITE	–	TR	–	–	–
APATITE	1	1	TR	1	1
OTHER	–	CC TR	–	–	–

SAMPLE	13	14	15	16	17
KSPAR	47	63	74	34	69
PLAGIOCLASE	7	8	4	20	7
QUARTZ	–	–	–	28	3
BIOTITE	17	17	10	16	12
OLIVINE	7	4	5	–	1
AUGITE	21	5	4	–	6
MAGNETITE	–	–	–	–	–
APATITE	1	1	1	TR	1
OTHER	–	–	–	–	–

SAMPLE	18	19	20	23
KSPAR	40	59	45	56
PLAGIOCLASE	3	4	5	5
QUARTZ	–	–	–	–
BIOTITE	23	5	10	8
OLIVINE	8	9	12	11
AUGITE	22	23	26	20
MAGNETITE	TR	–	–	–
APATITE	1	TR	TR	1
OTHER HBL	3	–	–	–

JERSEY (10564)

SAMPLE	1	2	4	6	7
KSPAR	60	50	40	13	16
PLAGIOCLASE	3	2	23	TR	4
QUARTZ	–	–	–	–	–
BIOTITE	16	17	23	11	18
OLIVINE	–	5	1	–	4
AUGITE	16	21	11	74	59
MAGNETITE	2	2	TR	TR	TR
APATITE	1	TR	1	1	TR
OTHER	CC 2	CC 5	CC TR	–	–

SAMPLE	8	9	10	11
KSPAR	35	35	40	47
PLAGIOCLASE	19	17	14	27
QUARTZ	–	1	–	TR
BIOTITE	22	27	22	14
OLIVINE	3	1	1	–
AUGITE	22	19	22	10
MAGNETITE	TR	TR	1	TR
APATITE	TR	TR	1	TR
OTHER	–	–	–	CC TR

CULTUS (10620)

SAMPLE	1	3	5	6	7
KSPAR	74	42	35	56	35
PLAGIOCLASE	"	2	10	"	10
QUARTZ	"	–	–	–	–
BIOTITE	26	20	15	21	14
OLIVINE	"	8	5	8	5
AUGITE	"	24	32	14	31
MAGNETITE	"	1	2	1	2
APATITE	–	TR	TR	TR	TR
OTHER	–	–	–	–	–

MT. MCGREGOR (10619)

SAMPLE	1	2	4	5	6
KSPAR	24	6	22	39	11
PLAGIOCLASE	8	–	"	"	TR
QUARTZ	–	–	–	–	–
BIOTITE	12	43	21	15	44
OLIVINE	16	2	14	7	–
AUGITE	40	48	42	36	46
MAGNETITE	TR	TR	TR	5	TR
APATITE	TR	TR	TR	–	2
OTHER	–	– HBL	TR	– SP	TR

SAMPLE	7	8	12
KSPAR	33	43	41
PLAGIOCLASE	12	3	"
QUARTZ	–	–	–
BIOTITE	15	18	19
OLIVINE	10	6	13
AUGITE	30	27	27
MAGNETITE	TR	TR	TR
APATITE	TR	–	TR
OTHER	– HYP	4	–

APPENDIX IV. MICROPROBE ANALYSES

Mineral analyses were run on the ARL-EMX microprobe fitted with an ORTEC Si (Li) detector. A fully quantitative energy dispersive method was used. Methods used for background shaping and scaling, overlap corrections and adjustments for instrumental drift have been described by Smith and Gold, 1979.

The counting time was 400 seconds, operating voltage was 15.000 ± 0.001 KV, the beam current used was 280 ± 1 nA and the probe current was 30 nA.

Mineral standards used were:

1) Fe, Ti - Odergaarden Ilmenite (CCNM0152)
2) Na - Albite (CCNM0029)
3) Mg - Periclase (CCNM0238)
4) K, Si, Al - Sanidine (CCNM0279)
5) Ca - Wakefield Diopside (CCNM0087)

Energy dispersive analyses were processed by the computer program EDATAII.

SAMPLE NO.	B315	B315	B315	B411
MINERAL	PLAG,9	PLAG RR,9	AUG,10	KSPAR,12
H	-	-	-	-
NA	5.96	8.83	0.78	4.34
MG	0.27	0.21	15.01	0.23
AL	25.99	23.24	3.44	20.06
SI	55.24	64.49	53.16	66.32
CL	0.20	0.09	0.00	0.00
K	2.61	0.77	0.31	10.36
CA	4.54	4.23	12.09	0.80
TI	0.10	0.00	0.12	0.11
V	0.00	0.00	0.00	0.10
CR	0.08	0.00	0.22	0.00
MN	0.00	0.00	0.38	0.00
FE	0.40	0.22	13.20	0.21
NI	0.08	0.00	0.08	0.00
CO	0.00	0.00	0.00	0.00
CU	0.08	0.00	0.15	0.00
ZN	0.12	0.00	0.09	0.00
ZR	0.32	0.08	0.00	0.07
PB	0.00	0.00	0.00	0.00
BA	0.00	0.00	0.11	0.32

SAMPLE NO.	B411	B411	B411	B411	B411
MINERAL	PLAG,13	AUG OT,14	AUG IN,15	BI INC,16	BI BIG,17
H	-	-	-	1.69	2.08
NA	5.45	0.80	0.71	0.84	0.83
MG	0.17	13.17	14.36	13.66	11.67
AL	28.72	2.16	4.33	14.88	14.85
SI	55.91	53.09	51.03	36.80	36.17
CL	0.00	0.00	0.00	0.08	0.28
K	0.45	0.00	0.08	8.85	8.78
CA	10.52	20.96	21.56	0.35	0.16
TI	0.00	0.20	1.20	4.95	4.59
V	0.00	0.00	0.00	0.00	0.00
CR	0.00	0.09	0.10	0.00	0.00
MN	0.00	0.49	0.18	0.23	0.19
FE	0.37	10.81	8.13	16.57	19.42
NI	0.00	0.00	0.00	0.08	0.00
CO	0.00	0.00	0.00	0.00	0.00
CU	0.00	0.00	0.00	0.12	0.06
ZN	0.00	0.09	0.11	0.00	0.00
ZR	0.00	0.00	0.08	0.19	0.00
PB	0.00	0.00	0.00	0.13	0.00
BA	0.00	0.00	0.00	0.63	0.98

SAMPLE NO.	B309	B309	B309	B309
MINERAL	BIO INC,1	AUG CTR,2	OLI INC,3	KSP,4
H	2.53	-	-	-
NA	0.69	0.72	0.55	4.17
MG	24.12	17.79	33.08	0.13
AL	14.64	2.30	0.37	20.47
SI	41.91	54.45	39.55	64.18
CL	0.07	0.00	0.00	0.00
K	9.56	0.00	0.08	9.37
CA	0.49	21.57	0.21	1.09
TI	0.72	0.25	0.00	0.21
V	0.00	0.00	0.00	0.00
CR	0.14	0.29	0.00	0.00
MN	0.00	0.12	0.60	0.00
FE	5.16	4.80	28.06	0.14
NI	0.00	0.00	0.17	0.00
CO	0.00	0.00	0.00	0.00
CU	0.00	0.00	0.14	0.00
ZN	0.00	0.00	0.00	0.00
ZR	0.00	0.00	0.00	0.00
PB	0.00	0.00	0.00	0.00
BA	0.00	0.07	0.07	1.46

SAMPLE NO.	B309	B309	B315	B315
MINERAL	PLAG,5	BIO MN,6	BIO,7	KSPAR,8
H	-	4.28	3.45	-
NA	3.46	0.82	0.71	4.44
MG	0.16	15.21	12.62	0.22
AL	30.48	13.90	13.65	19.98
SI	54.73	37.37	37.02	66.07
CL	0.00	0.07	0.12	0.07
K	0.38	8.83	8.92	10.22
CA	12.14	0.00	0.08	0.91
TI	0.00	7.40	6.58	0.22
V	0.00	0.00	0.00	0.00
CR	0.08	0.00	0.00	0.00
MN	0.00	0.08	0.17	0.00
FE	0.23	11.87	16.72	0.19
NI	0.00	0.11	0.00	0.06
CO	0.00	0.00	0.00	0.00
CU	0.00	0.00	0.00	0.00
ZN	0.09	0.09	0.00	0.00
ZR	0.00	0.00	0.00	0.08
PB	0.00	0.00	0.00	0.11
BA	0.00	0.00	0.00	0.00